About OMICS Group

OMICS Group International is an amalgamation of Open Access publications and worldwide international science conferences and events. Established in the year 2007 with the sole aim of making the information on Sciences and technology 'Open Access', OMICS Group publishes 400 online open access scholarly journals in all aspects of Science, Engineering, Management and Technology journals. OMICS Group has been instrumental in taking the knowledge on Science & technology to the doorsteps of ordinary men and women. Research Scholars, Students, Libraries, Educational Institutions, Research centers and the industry are main stakeholders that benefitted greatly from this knowledge dissemination. OMICS Group also organizes 300 International conferences annually across the globe, where knowledge transfer takes place through debates, round table discussions, poster presentations, workshops, symposia and exhibitions.

About OMICS Group Conferences

OMICS Group International is a pioneer and leading science event organizer, which publishes around 400 open access journals and conducts over 300 Medical, Clinical, Engineering, Life Sciences, Pharma scientific conferences all over the globe annually with the support of more than 1000 scientific associations and 30,000 editorial board members and 3.5 million followers to its credit.

OMICS Group has organized 500 conferences, workshops and national symposiums across the major cities including San Francisco, Las Vegas, San Antonio, Omaha, Orlando, Raleigh, Santa Clara, Chicago, Philadelphia, Baltimore, United Kingdom, Valencia, Dubai, Beijing, Hyderabad, Bengaluru and Mumbai.

Mech-Aero Conference, Oct. 5, 2015

Development of Efficient Patterned Vertical Axis Wind Turbine Farms

Shaaban Abdallah
abdallsa@mail.uc.edu

Department of Aerospace Engineering and Engineering Mechanics
University of Cincinnati, Cincinnati, Oh 45221

UNIVERSITY OF Cincinnati

Outlines

- Introduction
- Motivation and Problem Definition
- Contribution to Knowledge
- Strategy for Problem Solution
- Results
- Conclusion

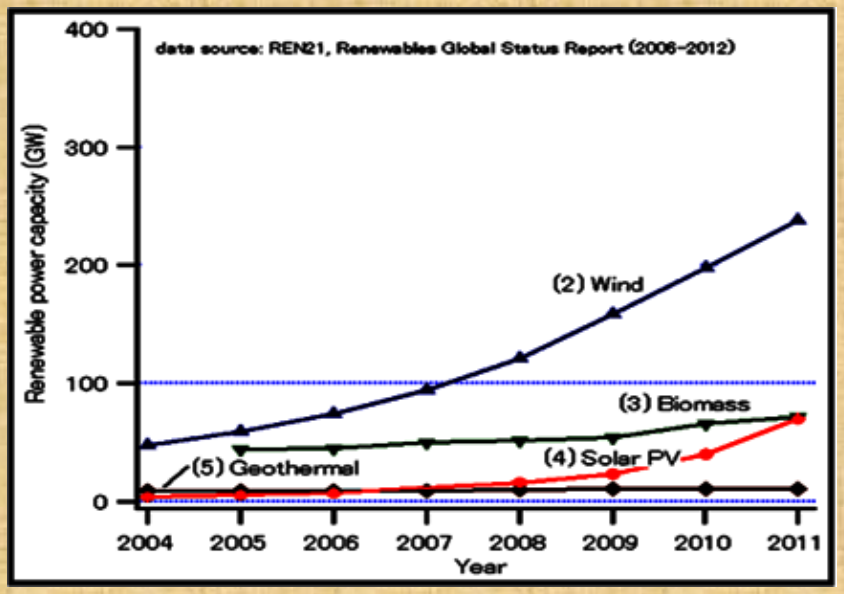
Global Wind Energy Capacity

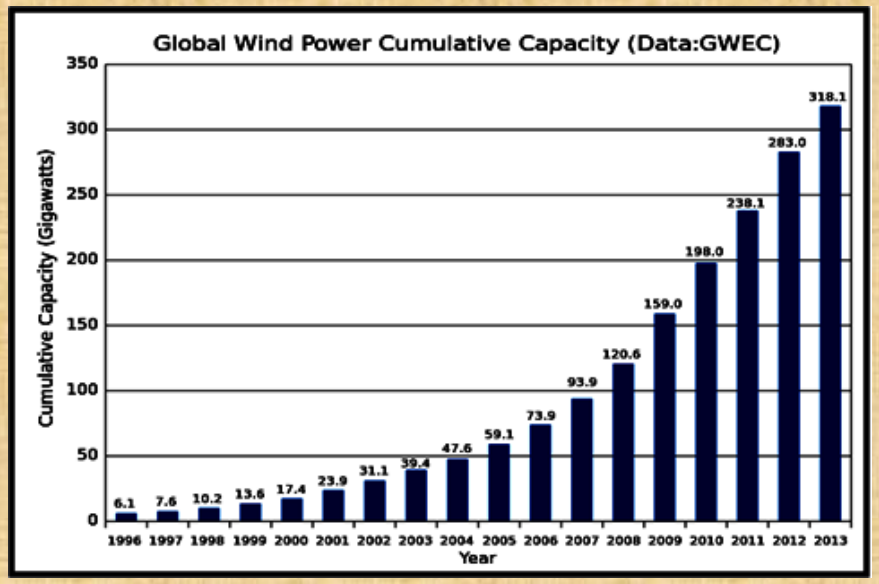
- **“**Of all the forces of nature, I should think the wind contains the largest amount of motive power "

  “ Abraham Lincoln (1860)”

- The Wind energy has the fastest growing renewable power capacity

  “ Renewables Global Report (2006-2012)”





- The total worldwide wind capacity installed was 360 GW at the end of 2014, this provided 4% of the global electricity demand

  “ World Wind Energy Association 2014 half year report (August 2014)”

Types of Wind Turbines:

Horizontal Axis Wind Turbines



Single Blade:

- Tower shadow effects
- Counter weights
- Less stability



Two Blades:

- less stability
- Low strength to wind shocks



Three Blades:

- Higher strength to wind storms.
- Less effect of tower shadow.
- Produces high output

Vertical Axis Wind Turbines



Darrieus



H-Rotor



Savonius

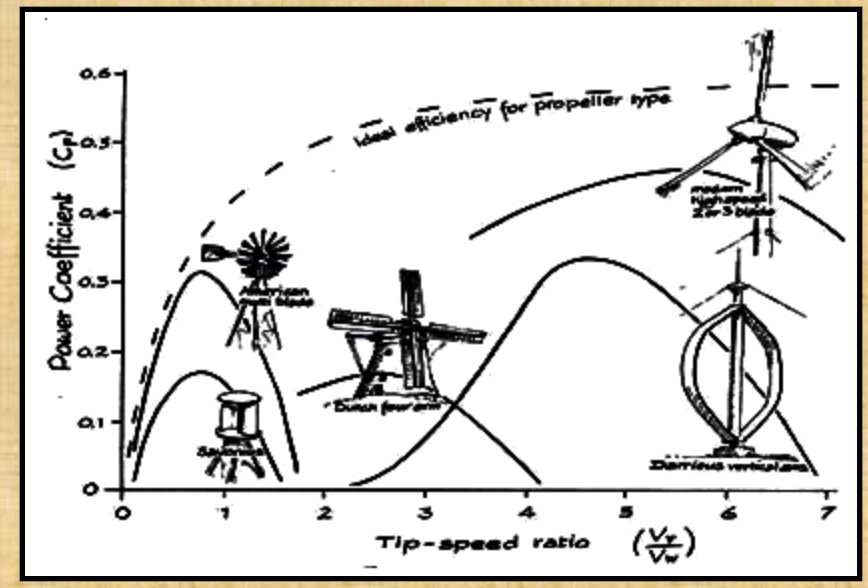






Horizontal Axis Wind Turbines (HAWTs) Farms:

- An isolated HAWT has the highest **power coefficient Cp (0.4–0.45) defined as the extracted power compared to the available power**



- **74%** of the wind **manufacturers** invest in **HAWTs** while only **18%** adopt the Vertical Axis Wind Turbines (**VAWTs**)

- Almost, all the **existing** wind turbine **farms** consists of **HAWTs**

- In **close proximity** to neighboring turbines, HAWTs suffer from a **reduced power coefficient** cause by the effect of the wake of upstream turbines

Wake interactions limit Conventional Horizontal Axis Wind Turbine Farm performance



Wind Farm Power Density:

- The **power density (P.D.)** of a wind farm is defined as the **total power** it can generate **per unit land** area it **occupies**

$$P.D = \frac{\text{Power Output of Farm}}{\text{Area of Farm}}$$

Vertical Axis Wind Turbine Farms

Vertical axis wind turbines (VAWTs) are proposed as an **alternative** to the more commonly used horizontal axis wind turbines (HAWTs) due to the potential increase in **power density** that is possible with VAWTs.

Experimental researches at **CalTech** found that the power density of **H-rotor** VAWT farms can be increased up to **10x HAWT farms** by **optimizing the placement** of the turbines that enables them to **extract energy** from adjacent turbines **wakes**

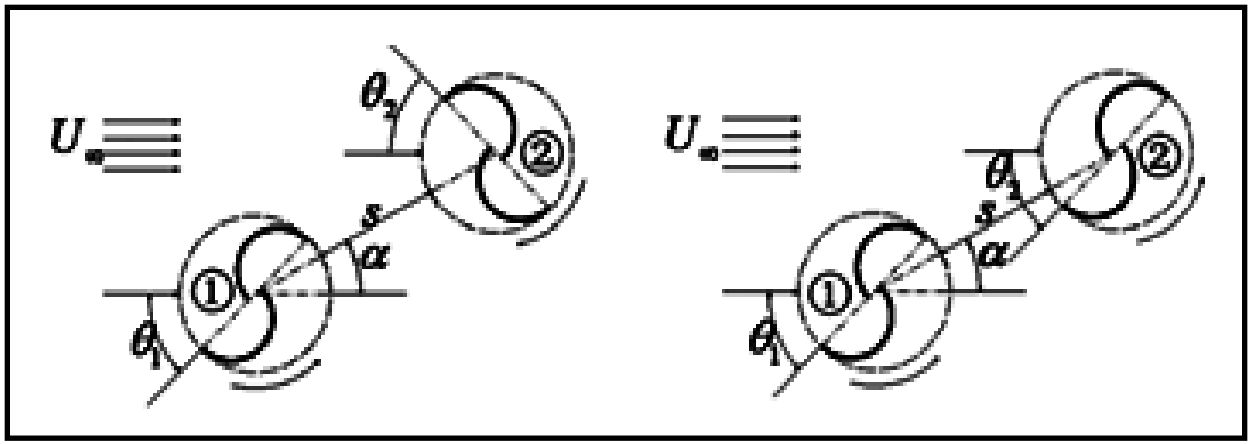


John O. Dabiri, " Potential order-of-magnitude enhancement of wind farm power density via counter-rotating vertical-axis wind turbine arrays," Journal Of Renewable And Sustainable Energy 3: 043104 (2011)

A Numerical study on two dimensional Savonius turbine clusters, showed that a mutual enhancement between closely arranged turbines occurs as a function of :

- **Relative direction of rotation.**
- **Gap Distance between rotors (S).**
- **Relative phase angle between the rotors:**

$$\varphi = \theta 1 - \theta 2$$



Xiaojing Sun, Daihai Luo, Diangui Huang and Guoqing Wu,"Numerical study on coupling effects among multiple Savonius turbines," Journal of Renewable and Sustainable Energy 4: 053107 (2012)

Motivation and Problem Definition

Motivation:

Previous studies showed that **VAWTs in close separation** distances mutually **enhance** their **power coefficients** resulting in **higher power output** for **individual** turbines and **higher power density** if arranged in a **wind farm**

Problem (1):

All the **previous** studies **did not extended the results** for efficient layouts of VAWTs to develop **larger efficient farms** that generate the highest possible power output keeping a high power density

Problem (2):

Using **non isolated turbines** in a farm will make the **prediction of a farm performance** to become a complicated job as each turbine will have a **different performance**

Contribution to Knowledge

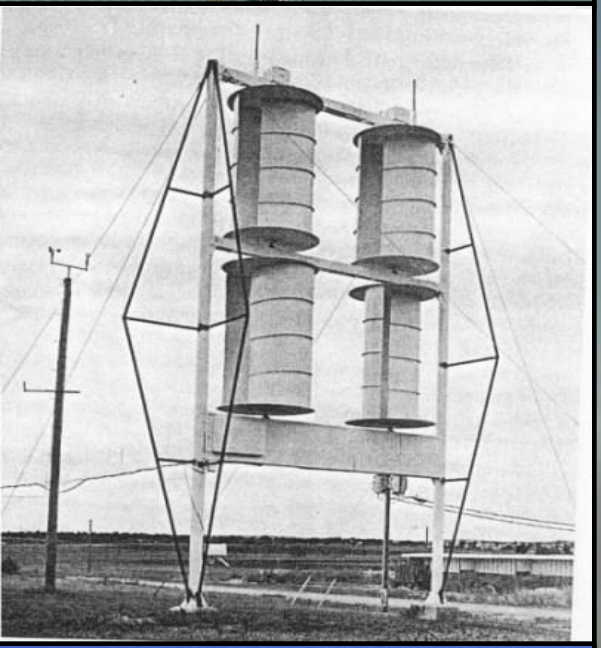
Solution (1):

This study introduces the idea of the efficient VAWT **cluster as a building unit** for an **efficient VAWT** farm that generates the **highest** possible **power** using the mutual enhancement between individual turbines and has a **high power density** compared to isolated counter-part

Solution (2):

Using the efficient cluster as a building unit for the **development of efficient and patterned VAWT farms** which have the **same geometric topology** of the **cluster** provides the capability of **predicting the performance** of a farm having a geometric progression of the efficient cluster.









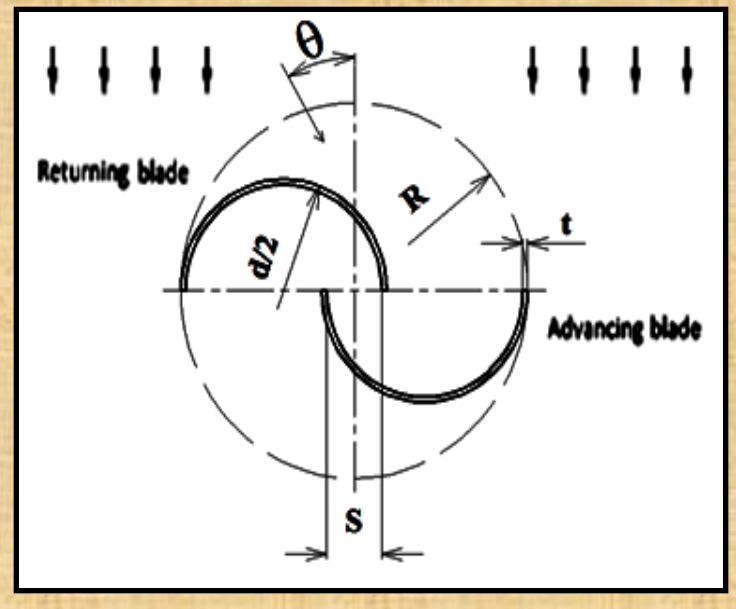
Case Study (I)

Savonius Wind Turbine

Savonius Wind Turbine

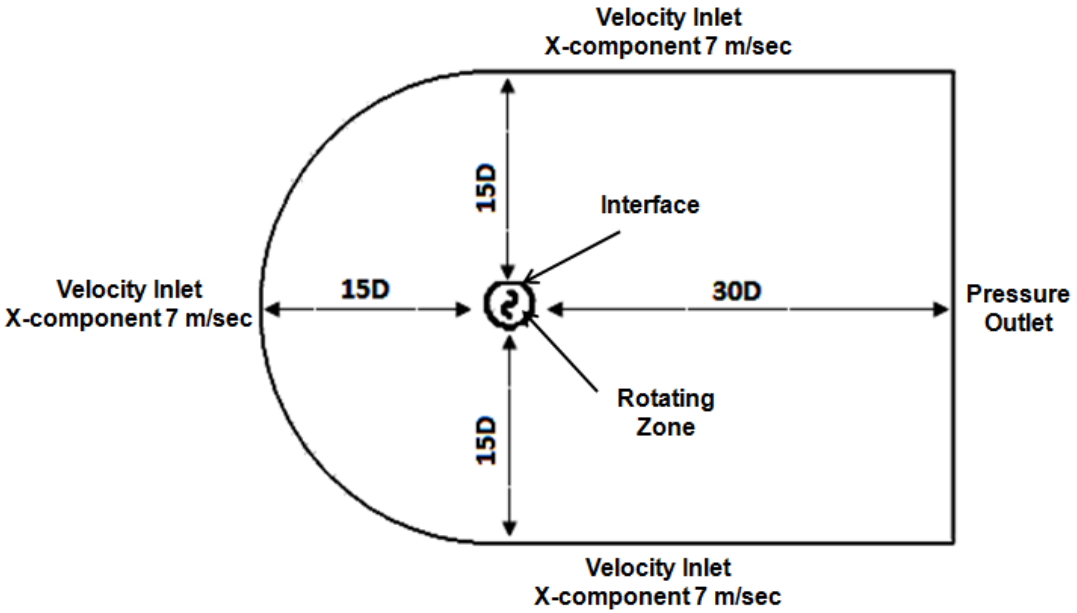
- The Savonius wind turbine was invented 1929
- It is has a Simple Construction
- It is a drag-type device
- Consists of two or three buckets
- It has self starting capability
- Low noise levels due to operation at low tips speed ratio
- Savonius turbines have low efficiencies 15-20%

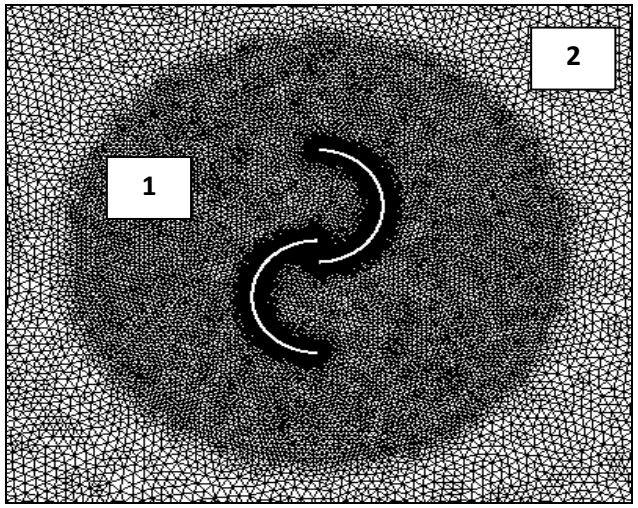




A. Shigetomi, Y. Murai, Y. Tasaka, Y. Takeda, "Interactive flow field around two Savonius turbines," Renewable Energy 36: 536-545, (2011)

Computational Domain:

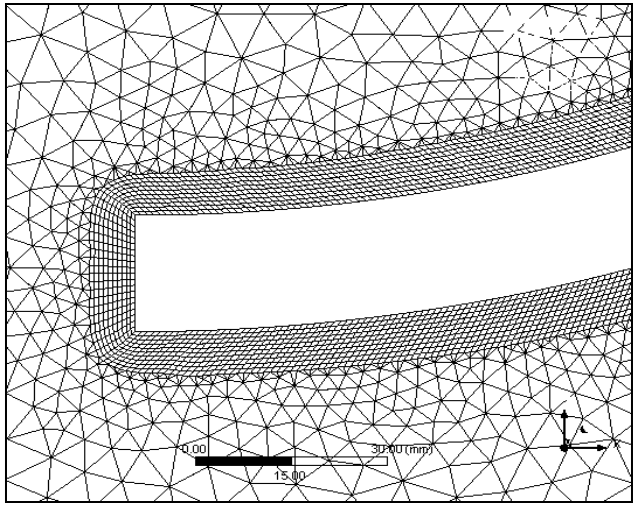




Grid Generation:

The grid structure consists of a non conformal mesh with **unstructured triangular elements** generated using ANSYS meshing.

An inflation of 10 levels of quad. cells is imposed to account for the boundary layer with a maximum thickness of 1 mm to achieve a y+ < 1 as required by the transition SST turbulence model [36, 37].



Numerical Model Validation:

Three models has been checked:

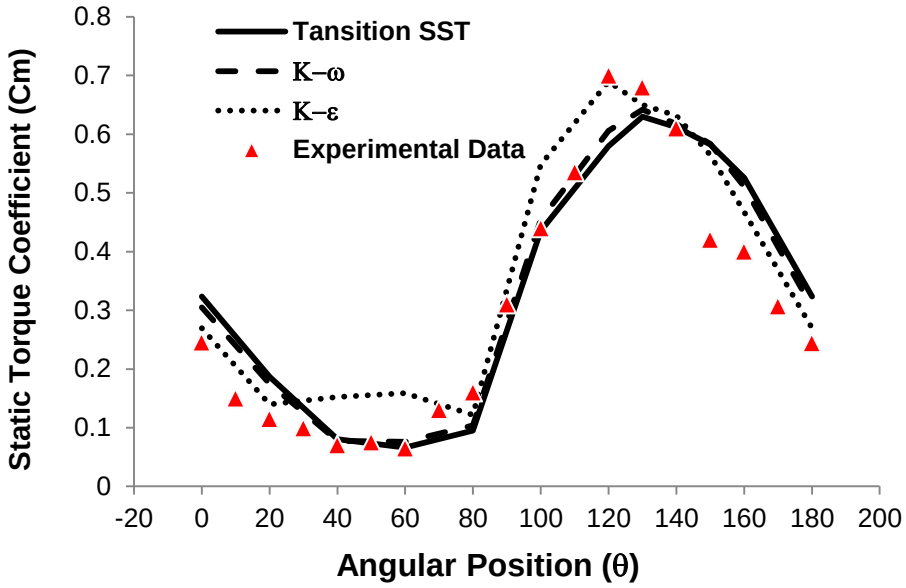
- K-ε model
- K-ω SST model
- Transition SST model

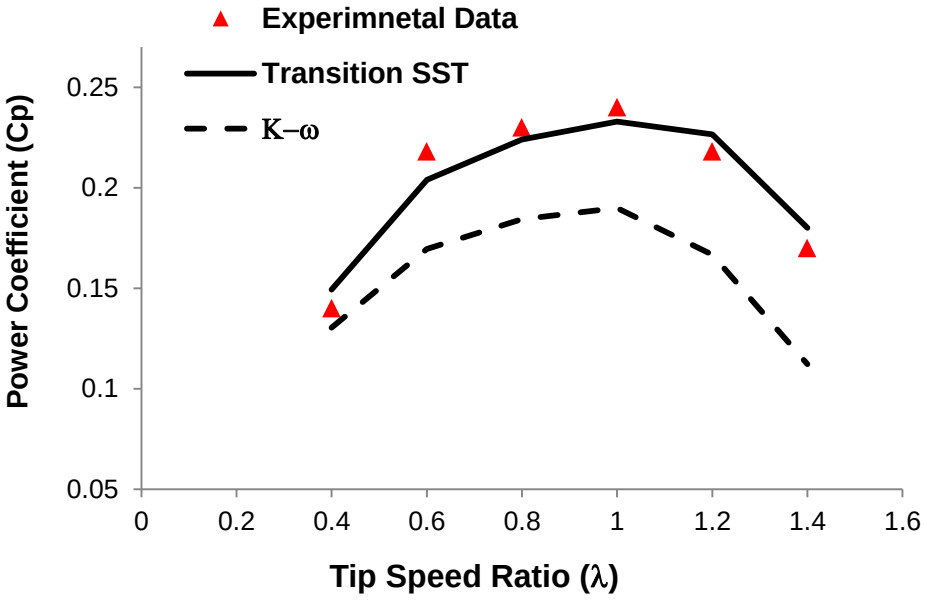
The **transition SST turbulence** model shows closer agreement to the **experiments data** in the numerical results for:

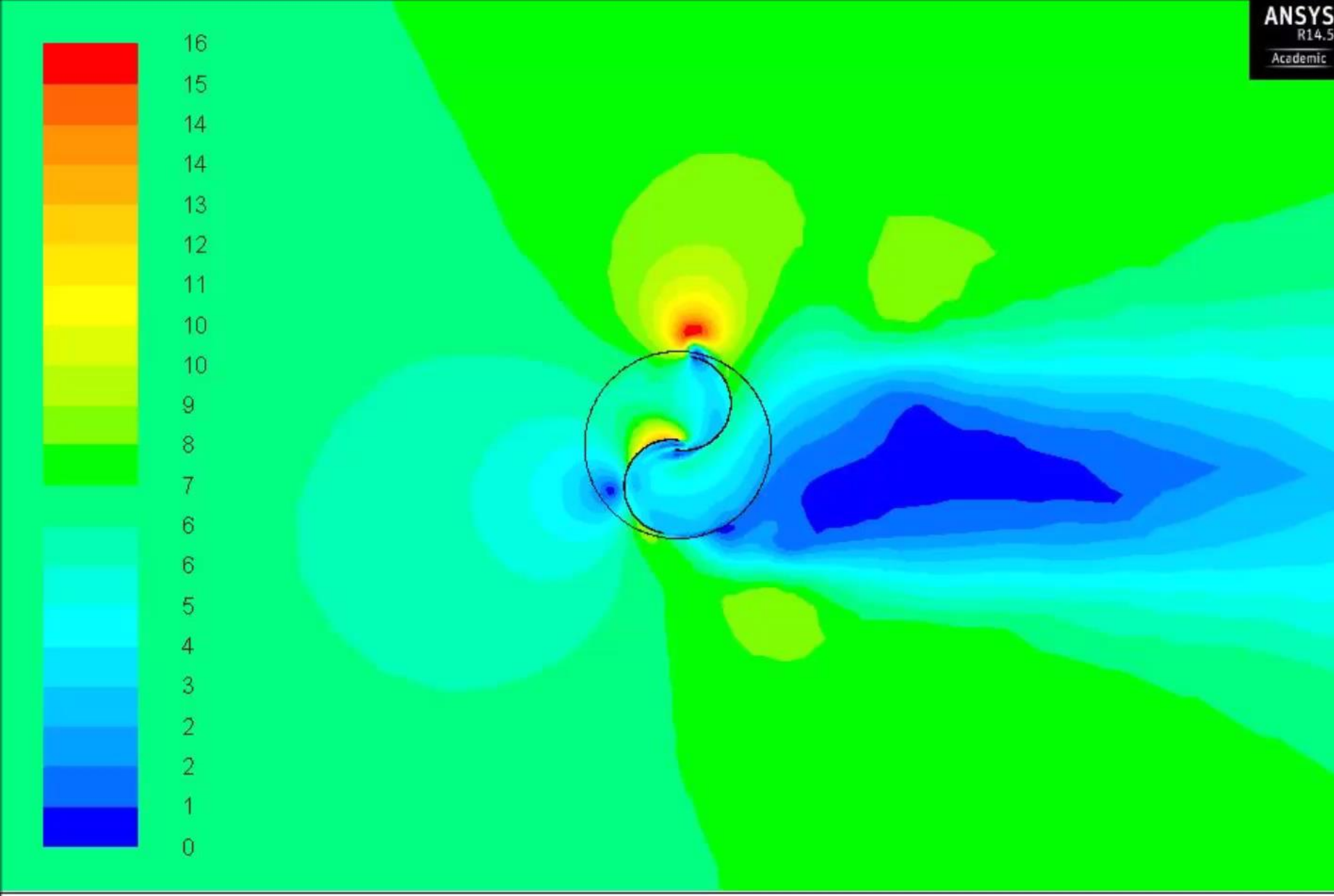
- Static torque coefficient at different azimuth angles (θ)
- Power coefficient at different tip speed ratios (λ)

The maximum power coefficient:

$Cp_{max} = 0.23$ at $\lambda = 1$



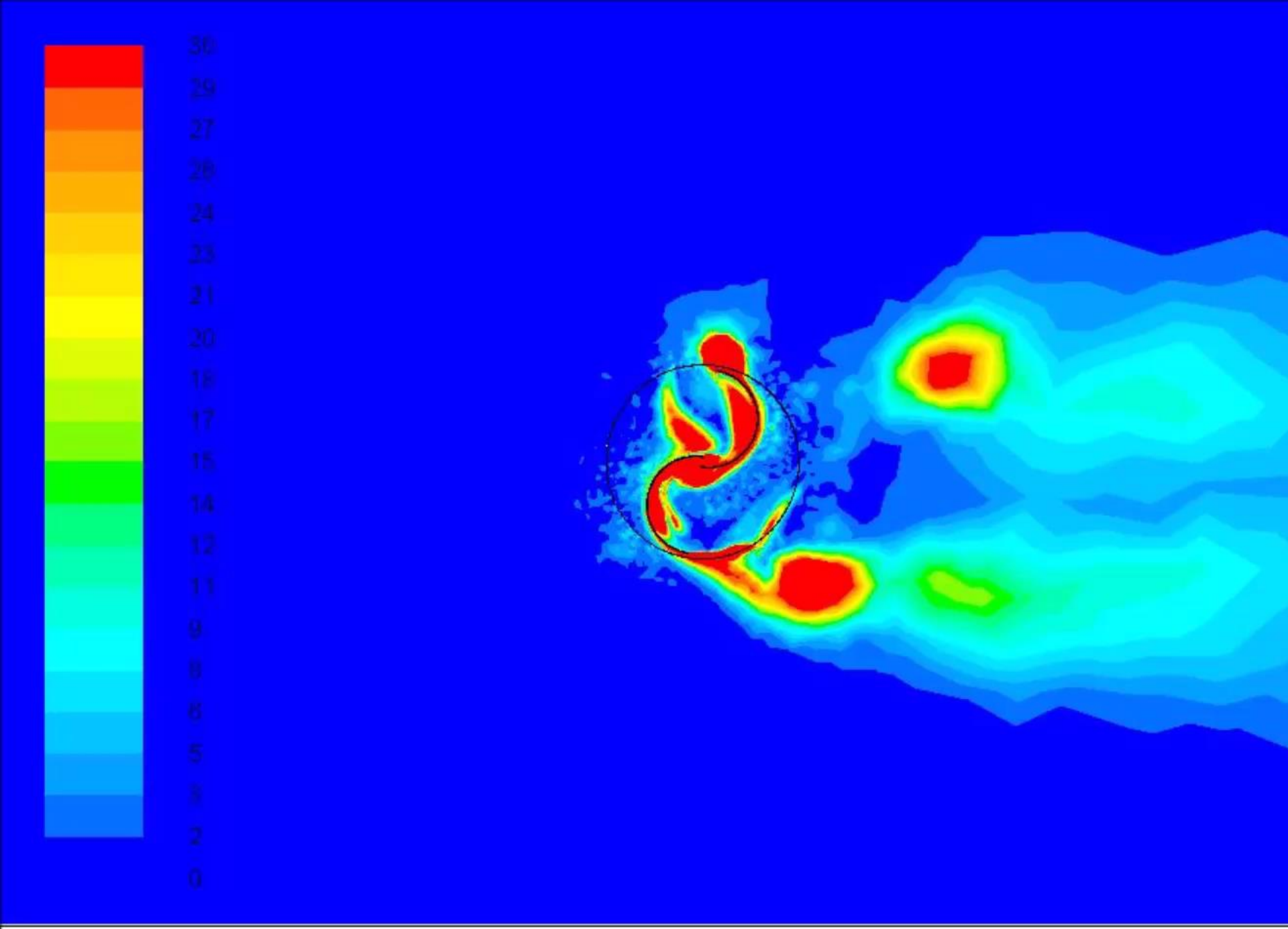




Contours of Velocity Magnitude (m/s) (Time=3.8263e+00)

May 13, 2015

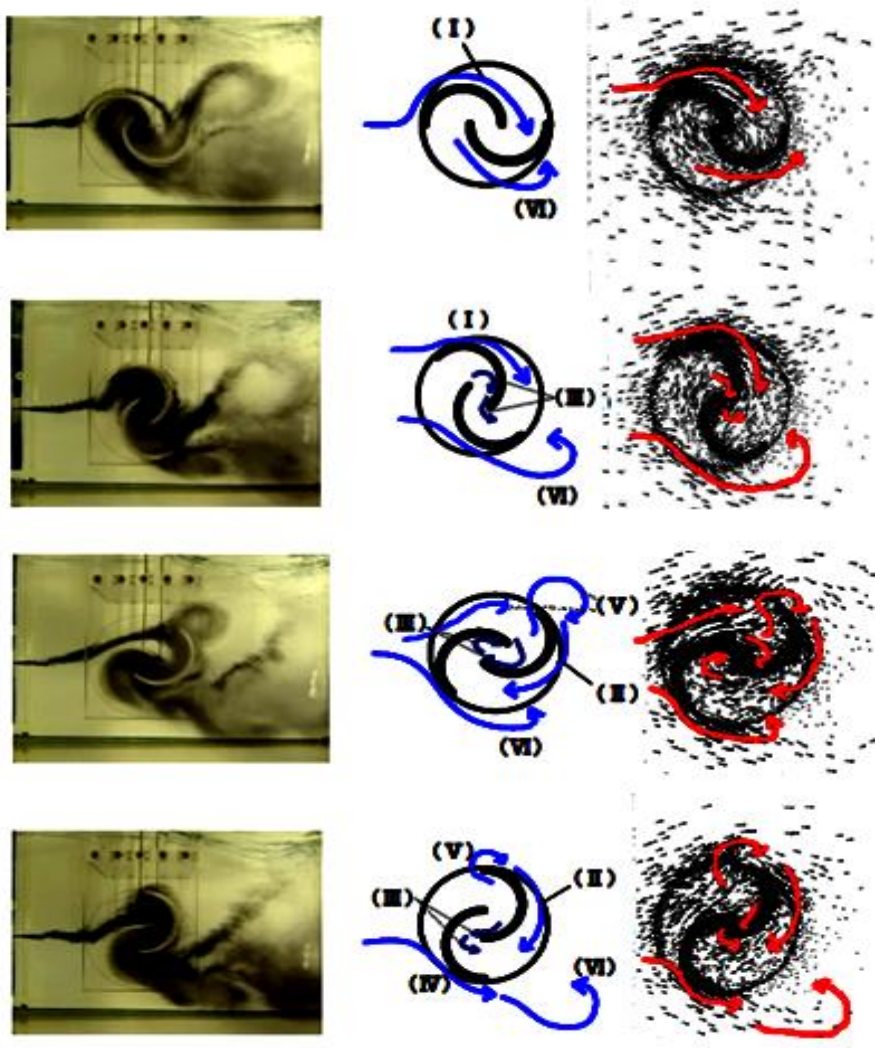
ANSYS Fluent 14.5 (2d, pbns, trans-sst, transient)


30
29
27
26
24
23
21
20
18
17
15
14
12
11
9
8
6
5
3
2
0

Flow Pattern around a Single Savonius Rotor

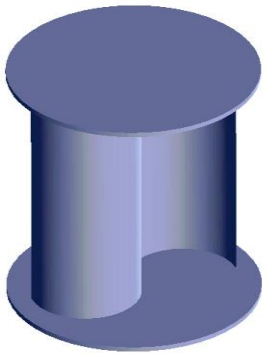
The flow patterns around the rotor are identified and found comparable to the experimental data:

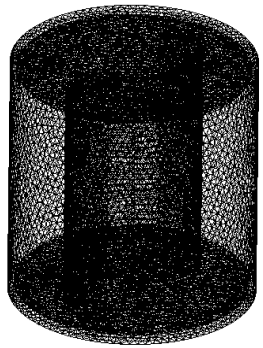
- **Flow (I):** Coanda flow (Attached to the advancing blade convex side).
- **Flow (II):** Dragging flow (from the advancing blade convex side to the returning blade concave side).
- **Flow (III):** Overlap flow though the overlapping area.
- **Flow (IV):** Stagnation flow from upstream to the returning blade convex side.
- **Flow (V):** Shedding vortex at the advancing blade tip.
- **Flow (VI):** Shedding vortex from the returning blade tip.

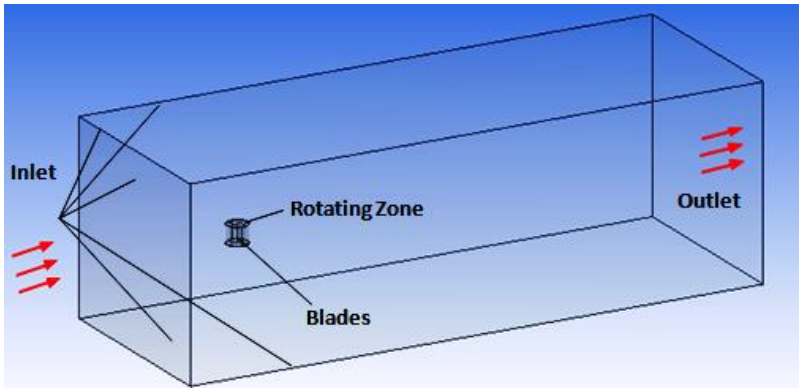


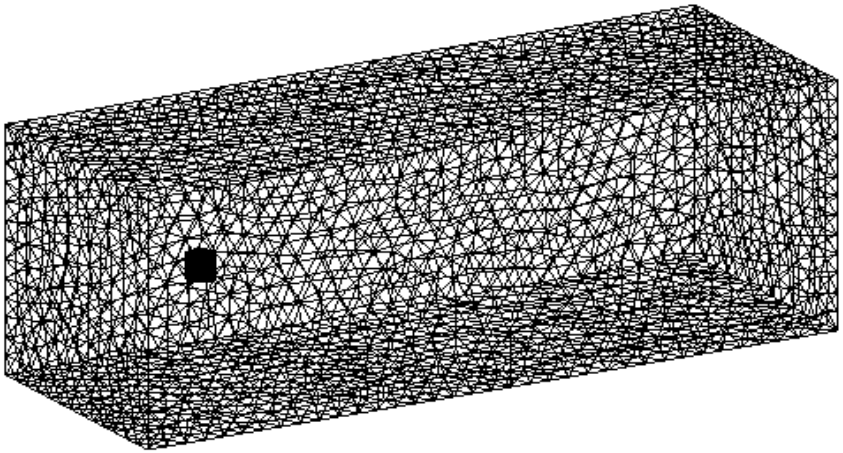
Nakajima, M., IIO, S., Ikeda, T., Performance of double-step Savonius rotor for environmentally friendly hydraulic turbine. Journal of Fluid Science and Technology 3, (2008)

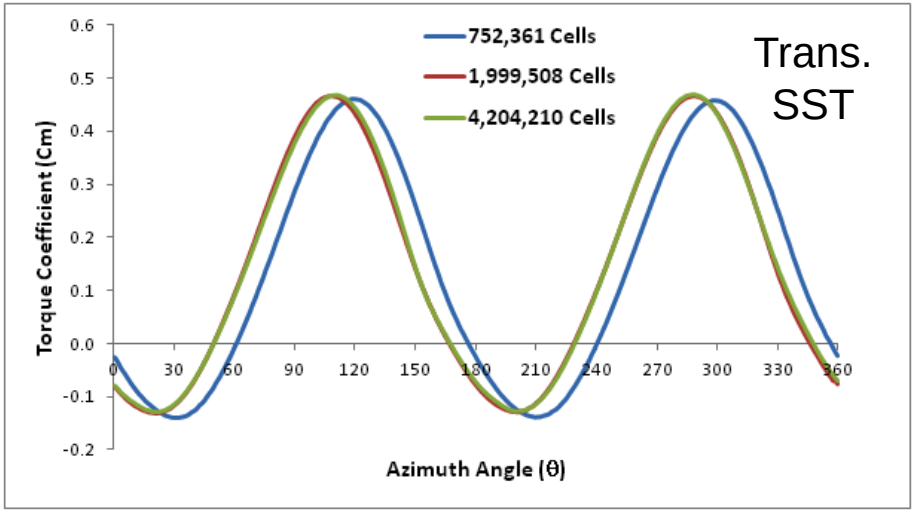
3D Validation for a Single Savonius Turbine

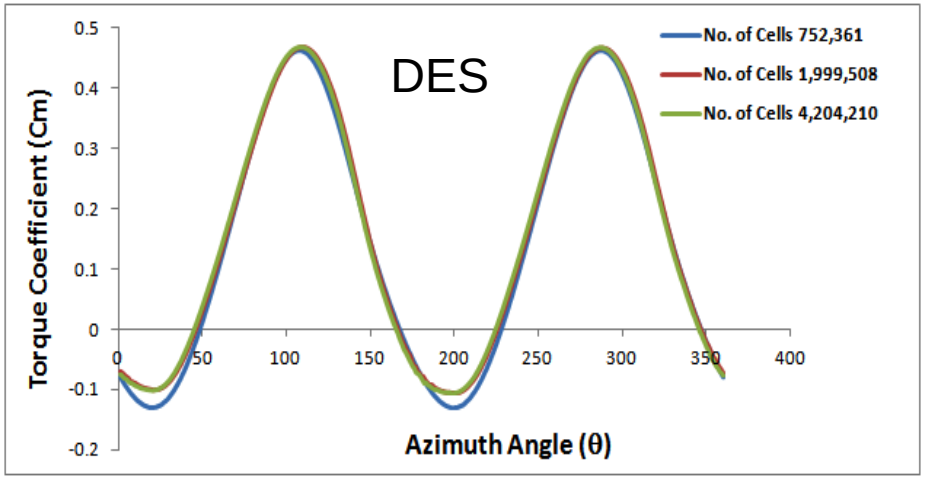




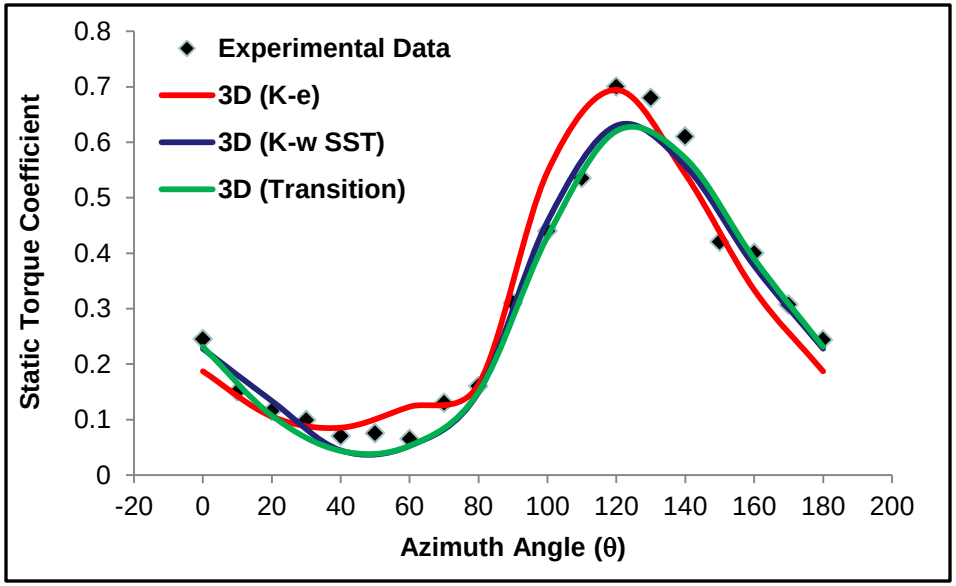


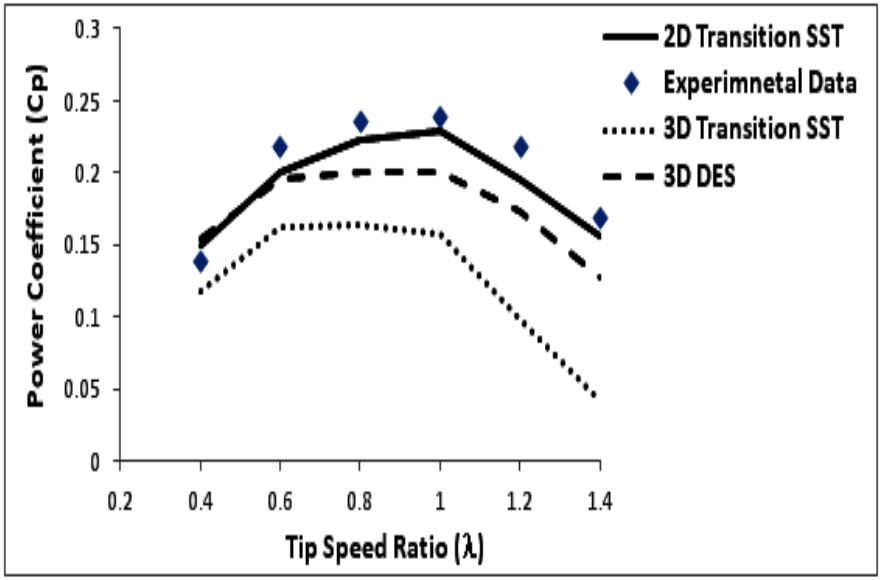






Grid Level	No. of Cells	Cm Transition SST	Cm DES
1	752,361	0.1461	0.1806
2	1,999,508	0.1561	0.1909
3	4,204,210	0.1557	0.1901

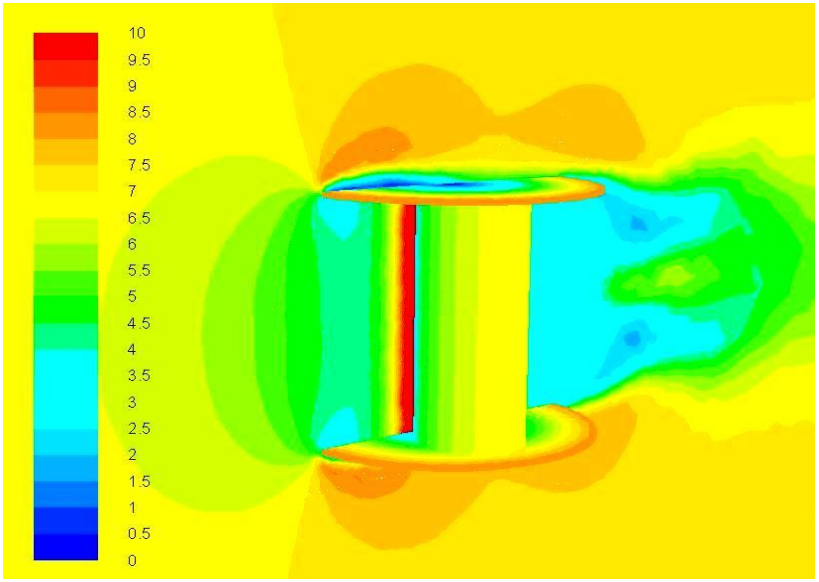




Transition SST model in the 3D Solution under predicted the single turbine performance compared to experimental data, this results are in consistence with the literature review on 3D solutions

To obtain better rsults, **detached eddy simulation (DES)** model is used for the flow simulation, the obtained results are **closer to the experimental data** for different TSR

The max. difference between DES and experimental data is about 15%

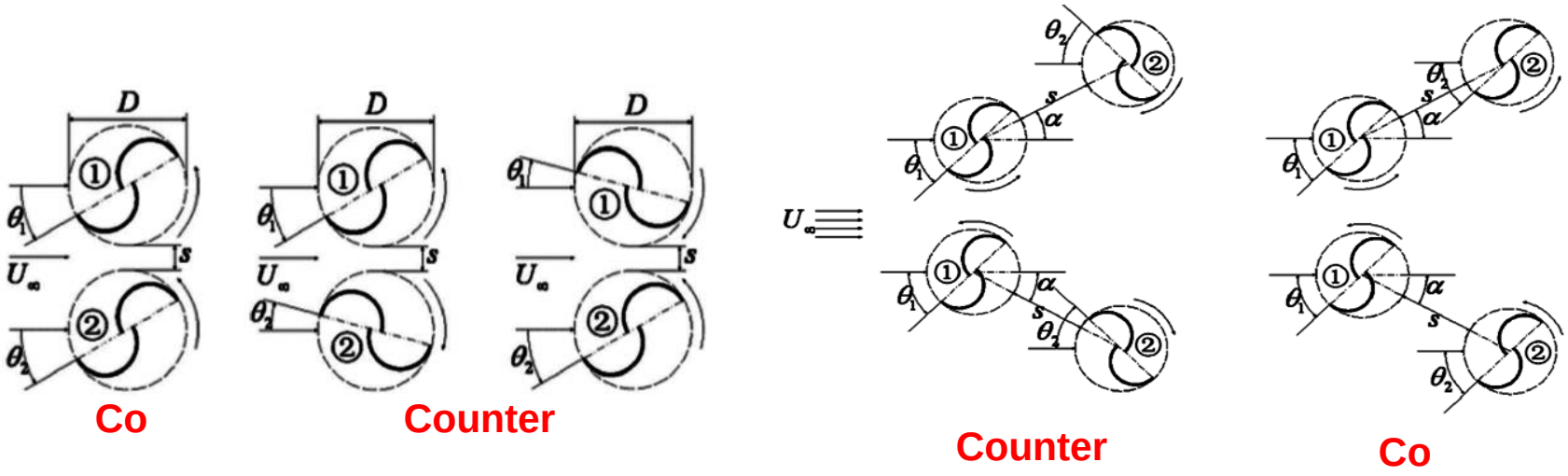


Velocity Contours

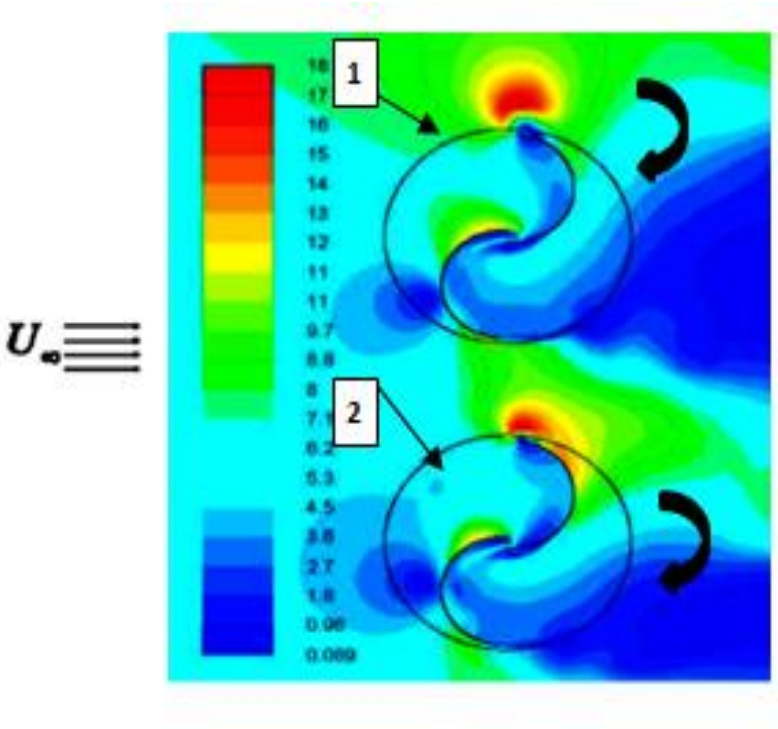
Numerical Solution of Two Savonius Wind Turbine Clusters

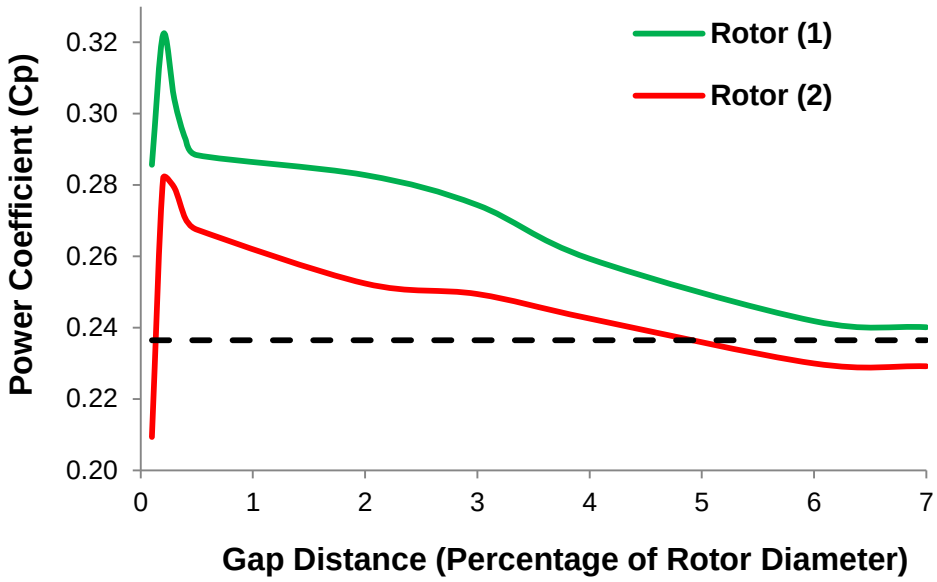
The development of an efficient cluster requires the study of different possibilities of multiple turbine cluster

Two **Co-rotating** and **Counter-rotating** turbine clusters in parallel and oblique configurations are numerically simulated



1- Two Parallel Co-Rotating Savonius Turbines:



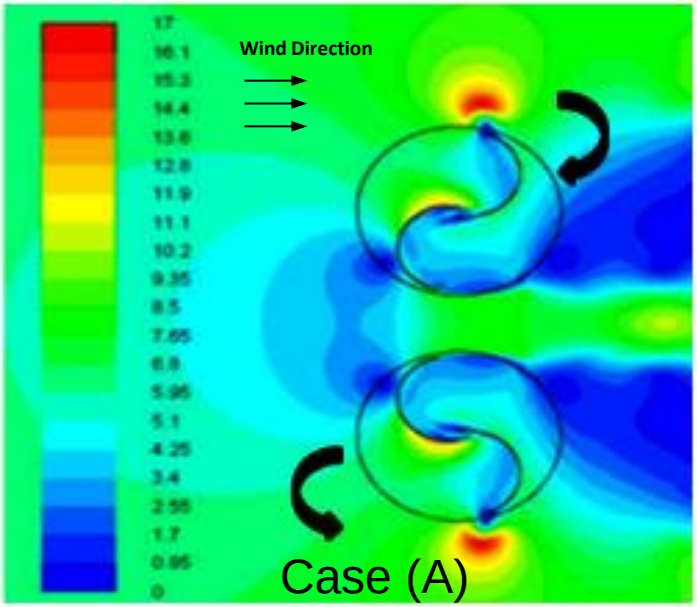


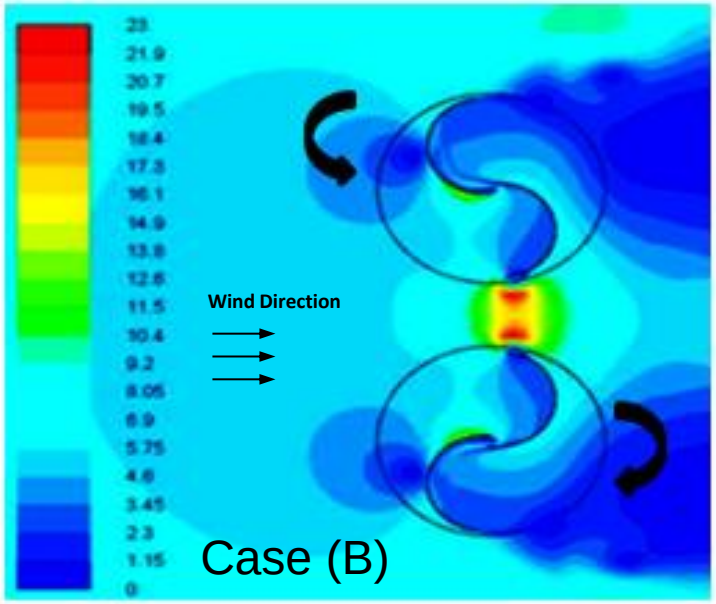
Rotor (1) has higher efficiency enhancement than Rotor (2) due to the direction of rotation

Cp_{avg} max is 0.3 at **0.2D** gap distance enhancement of **30%** higher than isolated turbines

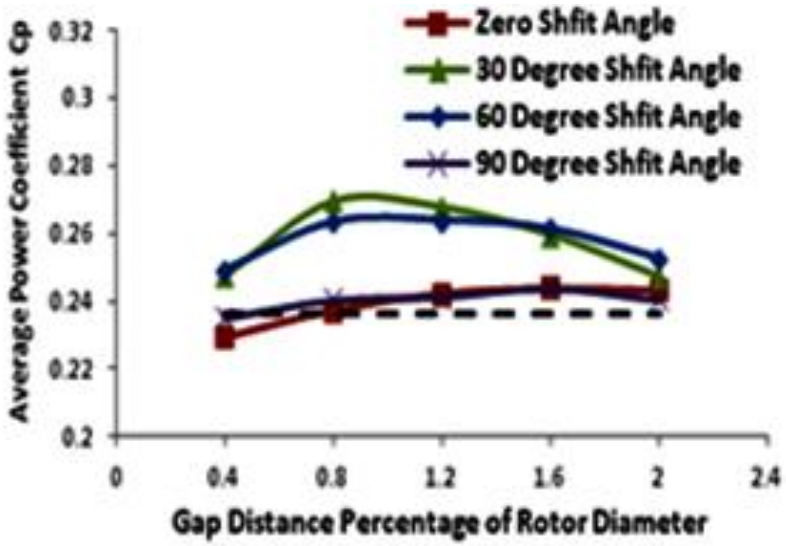
Reaches isolated turbine performance placed at approximately 5-6 D

2- Two Parallel Counter-Rotating Savonius Turbines

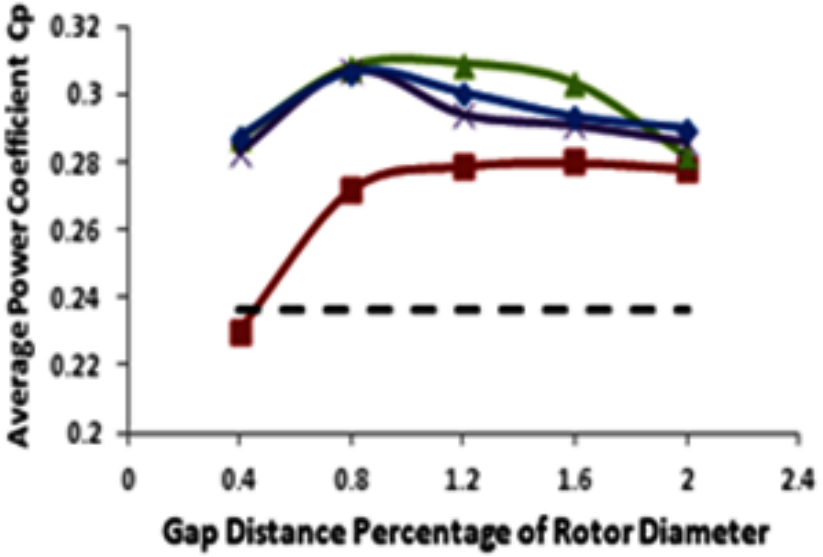




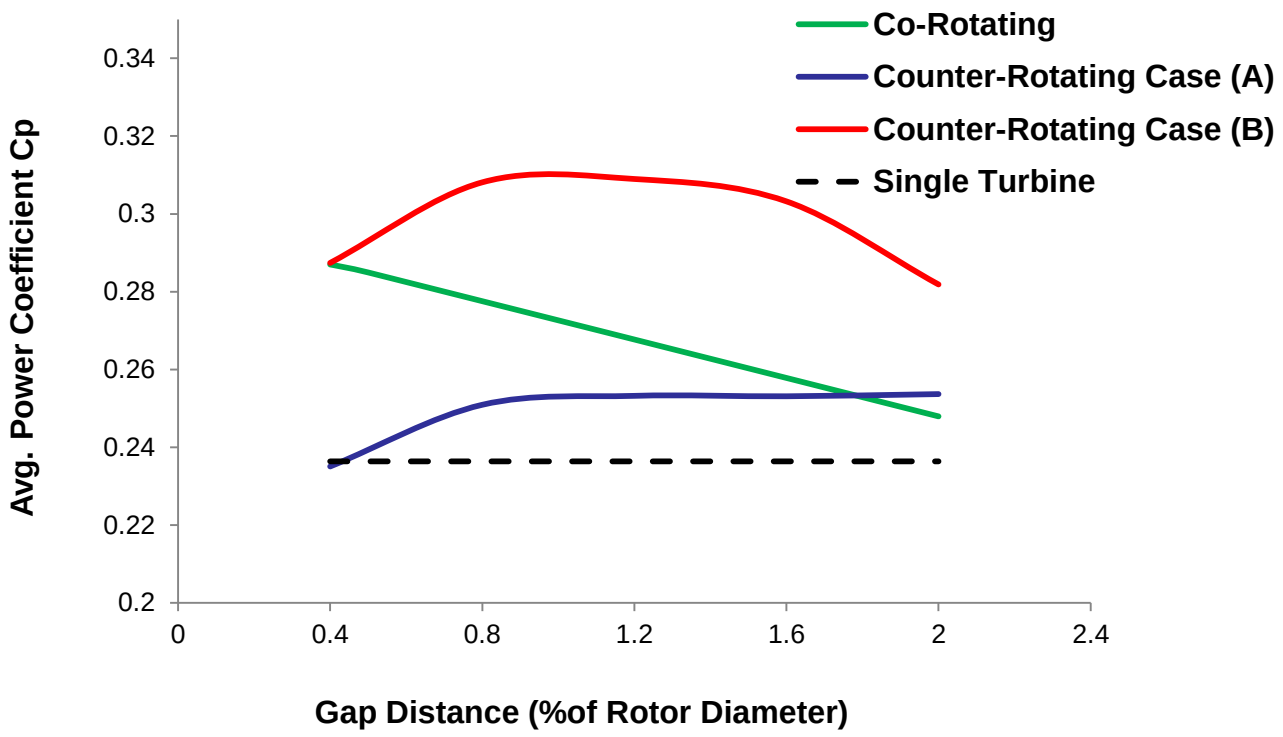
Cp_{avg} max is 0.26 at 0.8D gap distance



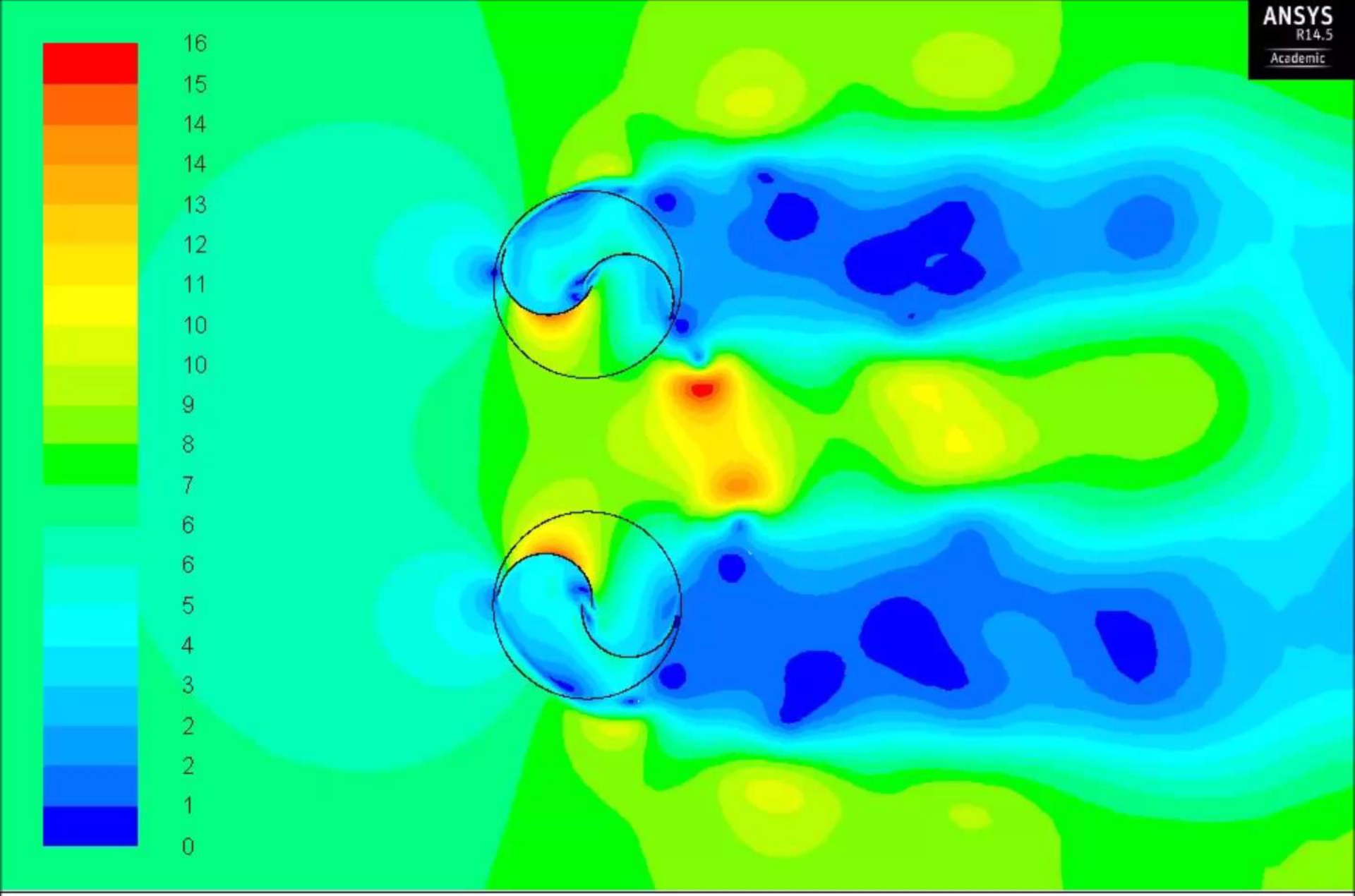
Cp_{avg} max is 0.3 at 0.8D gap distance



Comparison Between Co- and Counter-Rotating Two Parallel Turbines

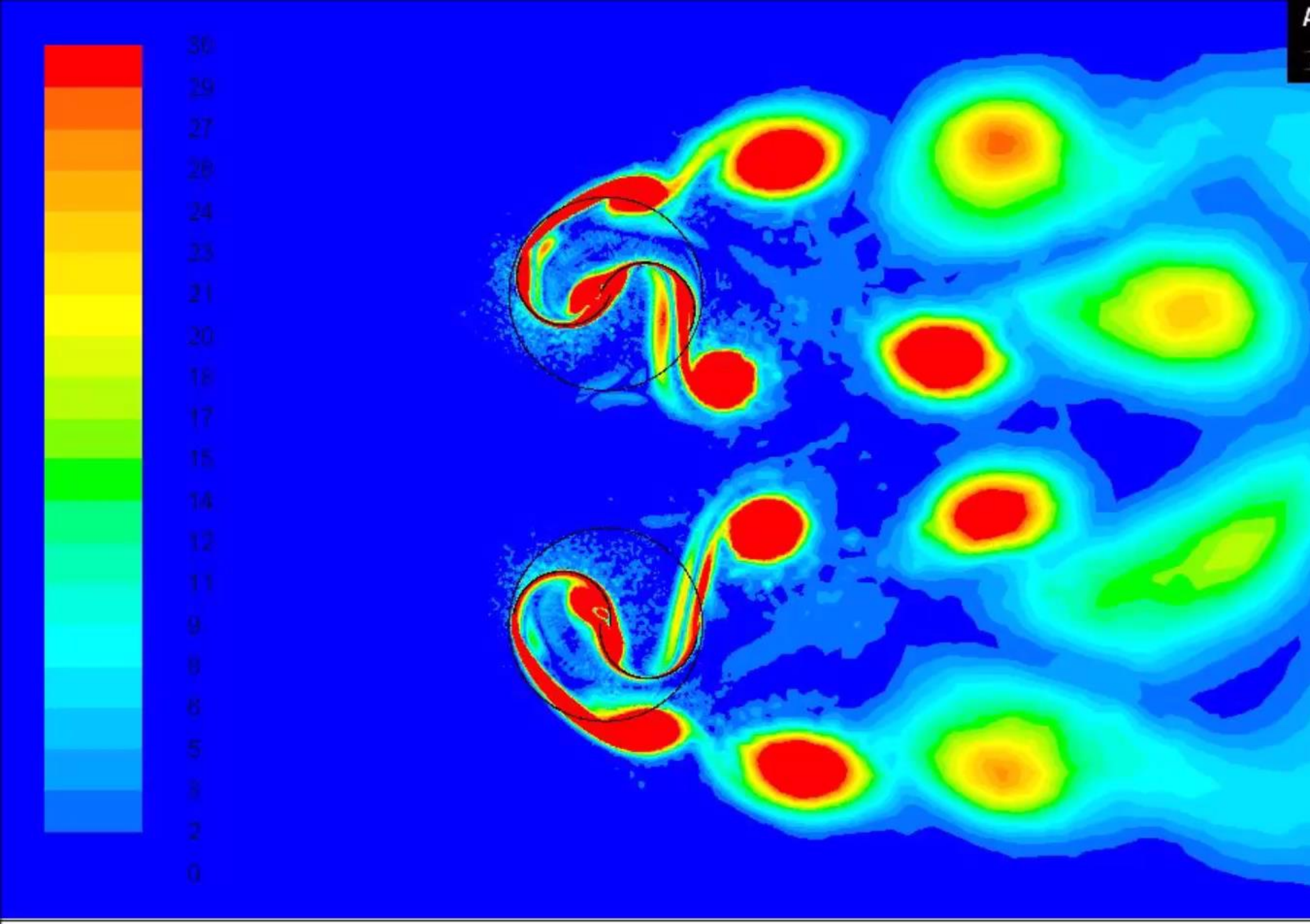


case (B) for counter-rotating rotors at a relative phase angle 30^{o} is the most efficient for two parallel counter-rotating Savonius rotors, where the inward buckets are advancing buckets



Contours of Velocity Magnitude (m/s) (Time=2.2525e+00)

May 13, 2015
ANSYS Fluent 14.5 (2d, pbns, trans-sst, transient)

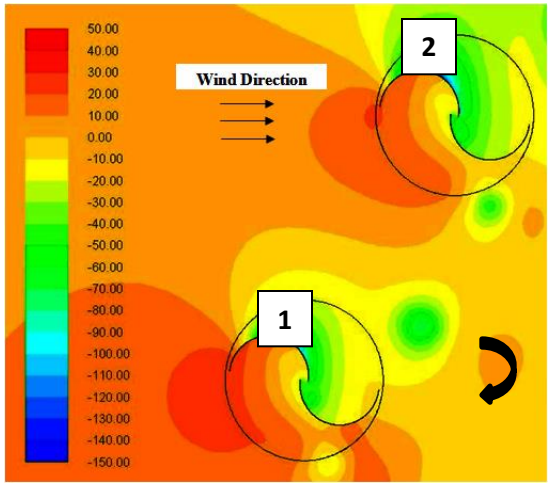


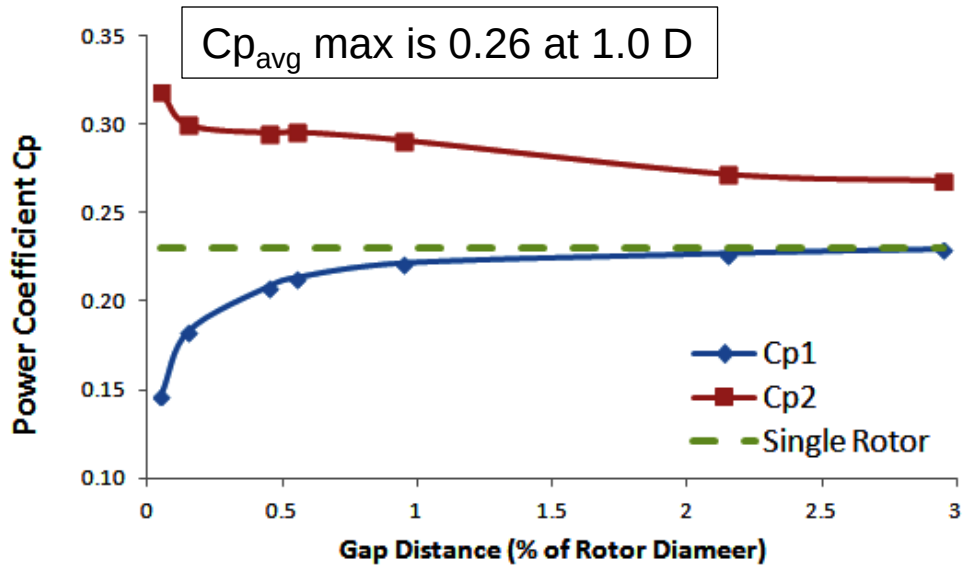
Contours of Vorticity Magnitude (1/s) (Time=2.2525e+00)

May 13

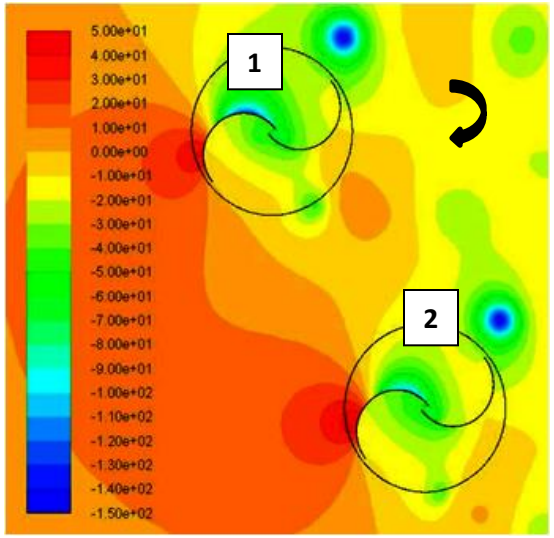
3- Two Oblique Co-Rotating Savonius Turbine Clusters

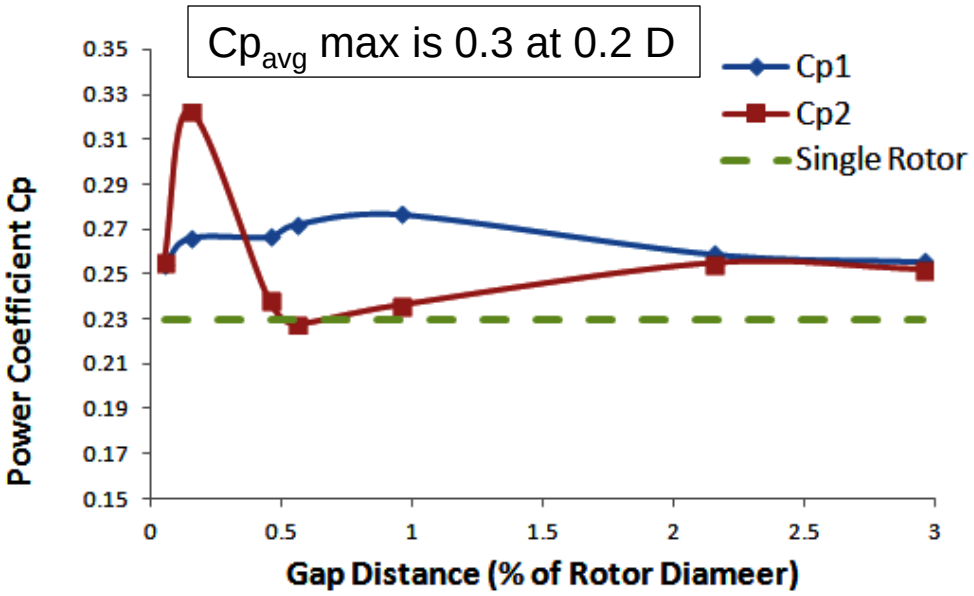
Case (A)



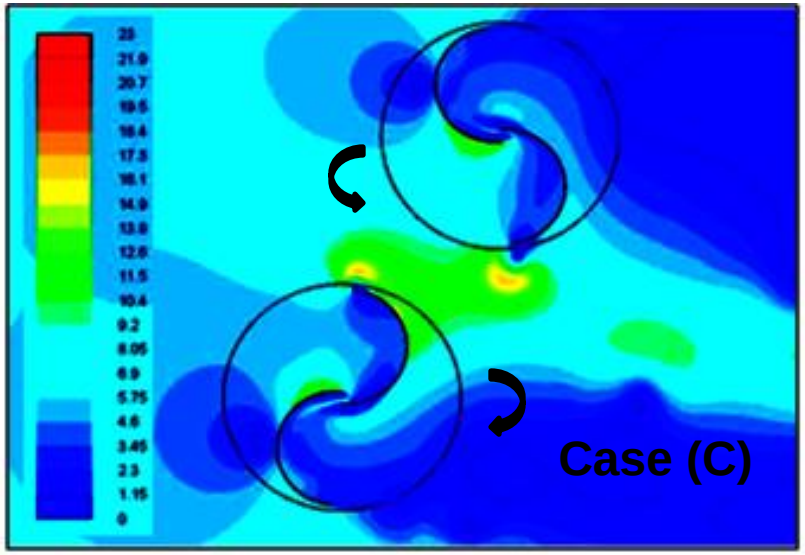


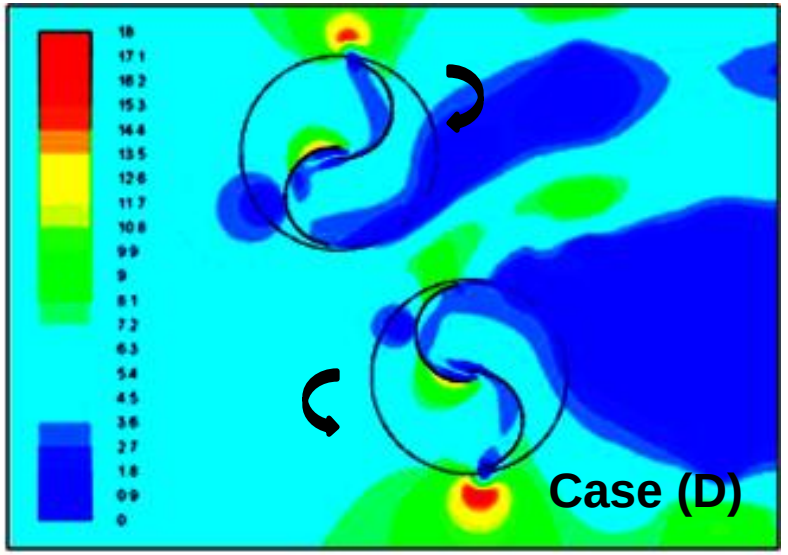
Case (B)



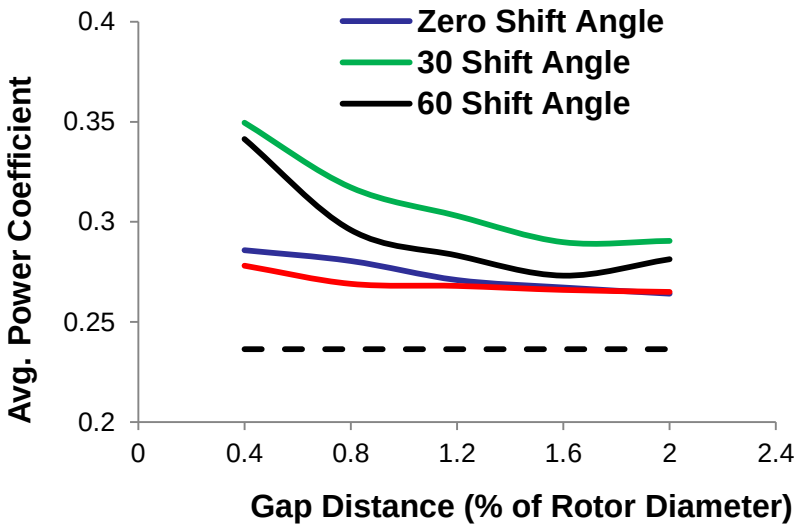


4- Two Oblique Counter-Rotating Savonius Turbine Clusters

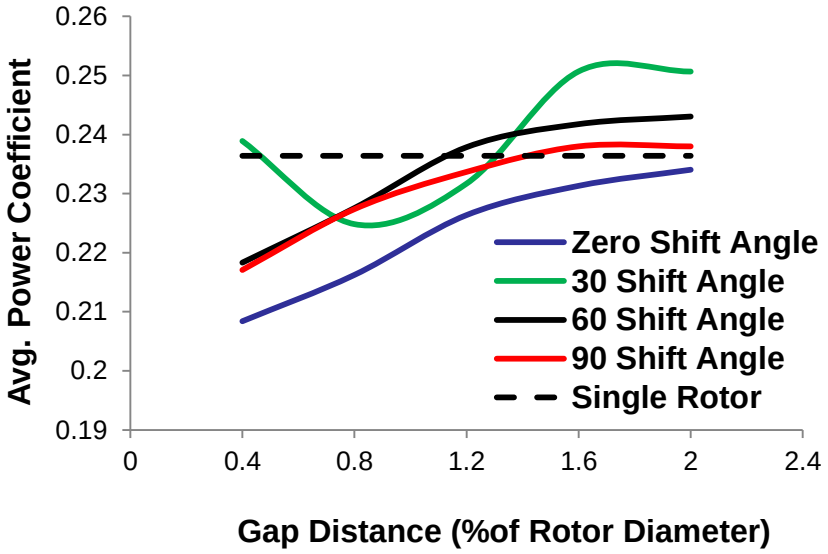




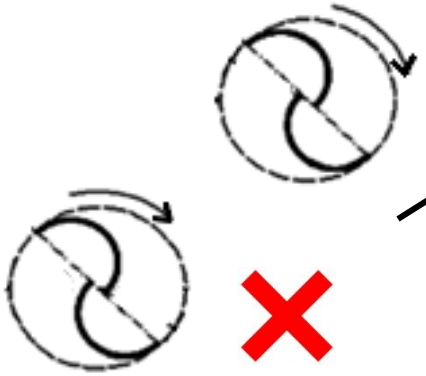
Cp_{avg} max is 0.35 at 0.4D

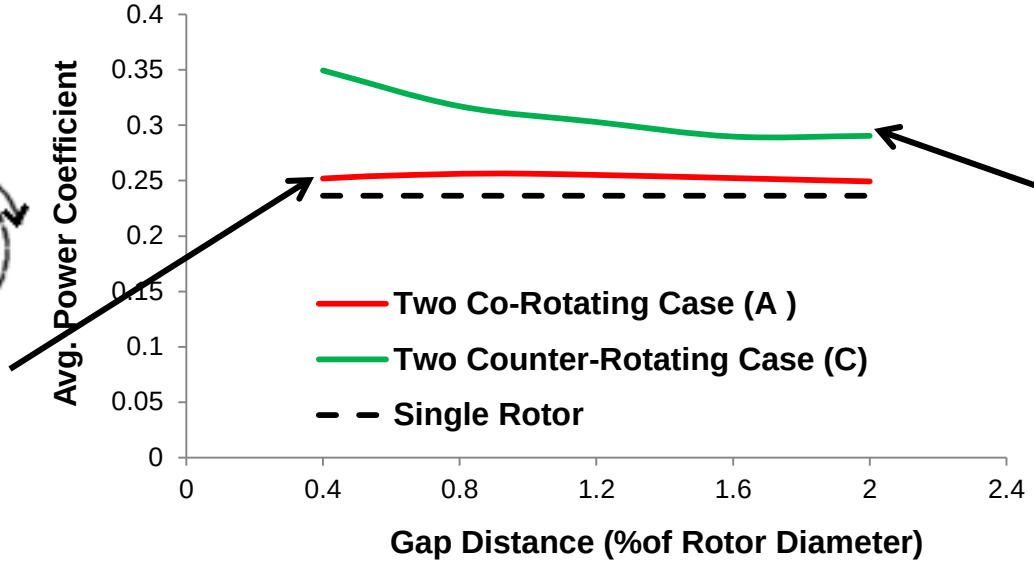


Cp_{avg} max is 0.25 at 1.6D

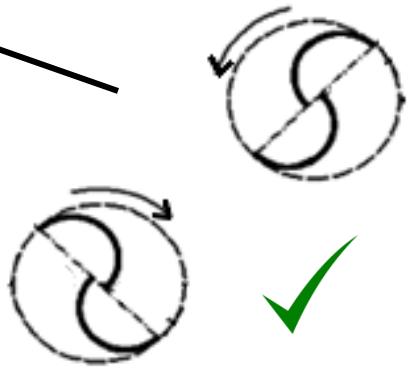


Co-rotating Case (A)

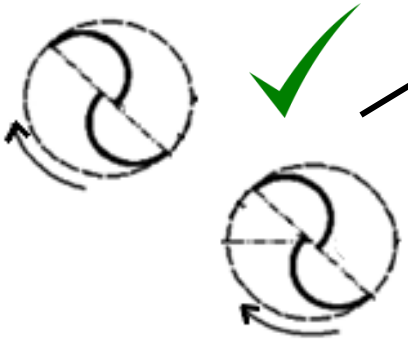


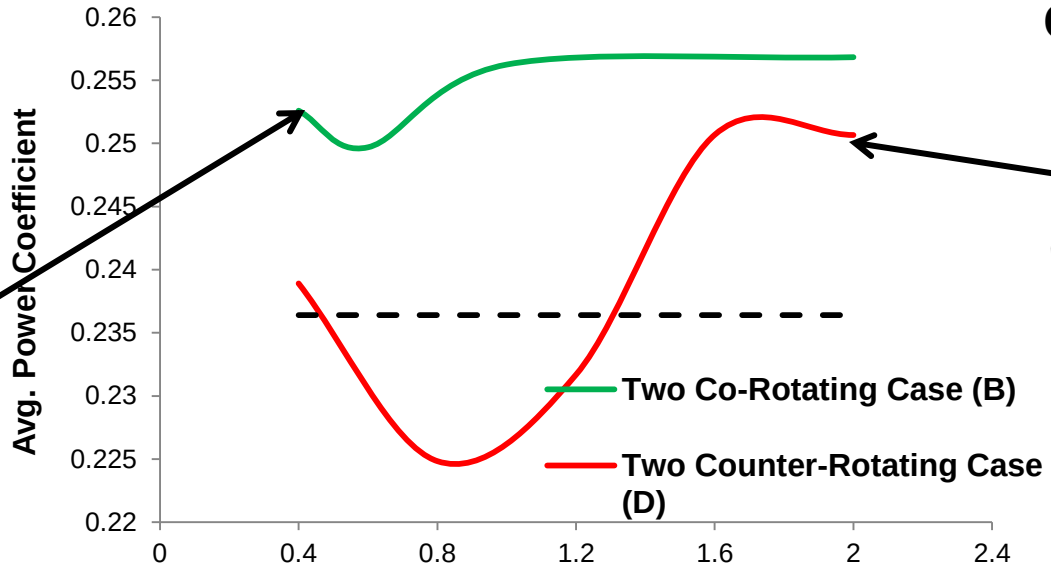


Counter-rotating Case (C)

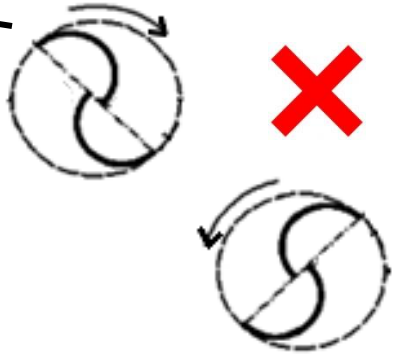


Co-rotating Case (B)





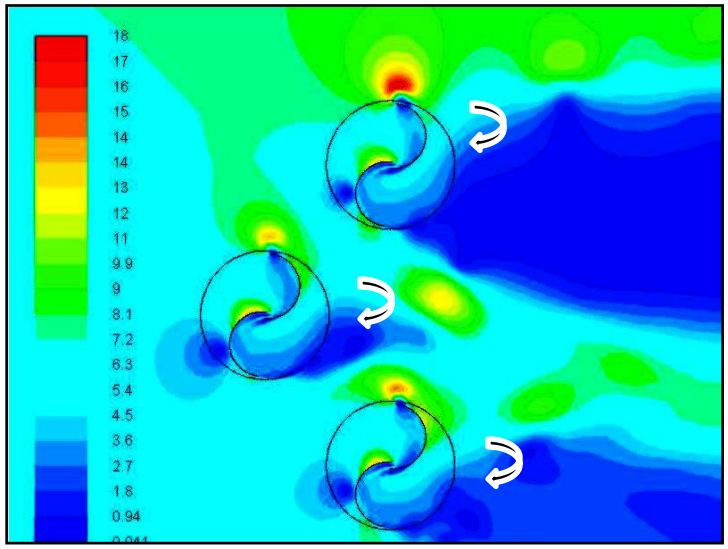
Counter-rotating Case (D)



Numerical Simulation of Three Turbine Savonius Clusters

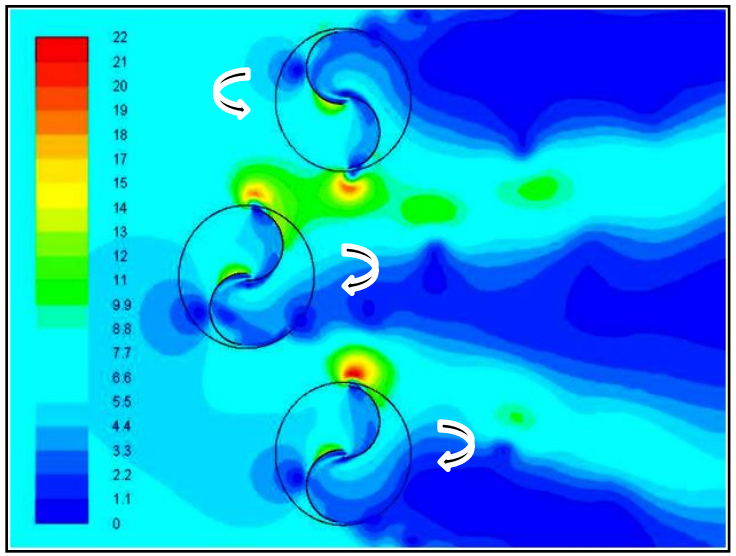
Co-Rotating Cluster

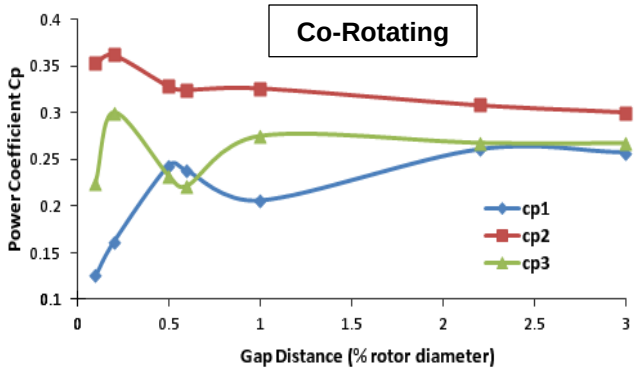
Cp = 0.29

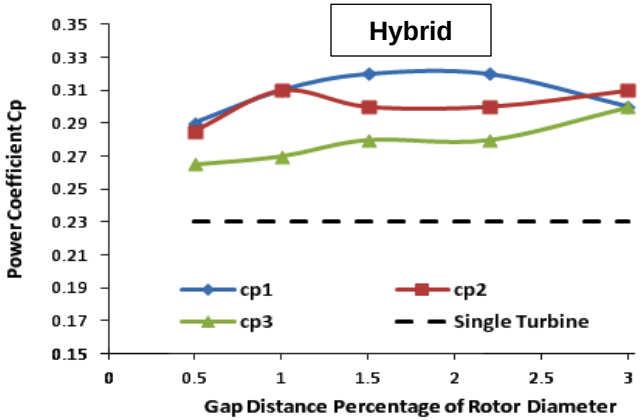


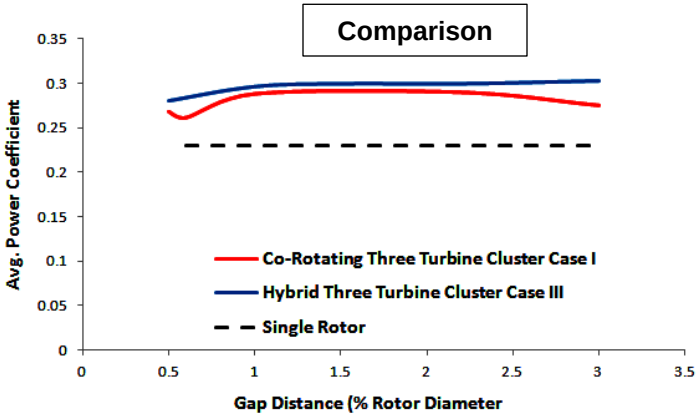
Hybrid Cluster

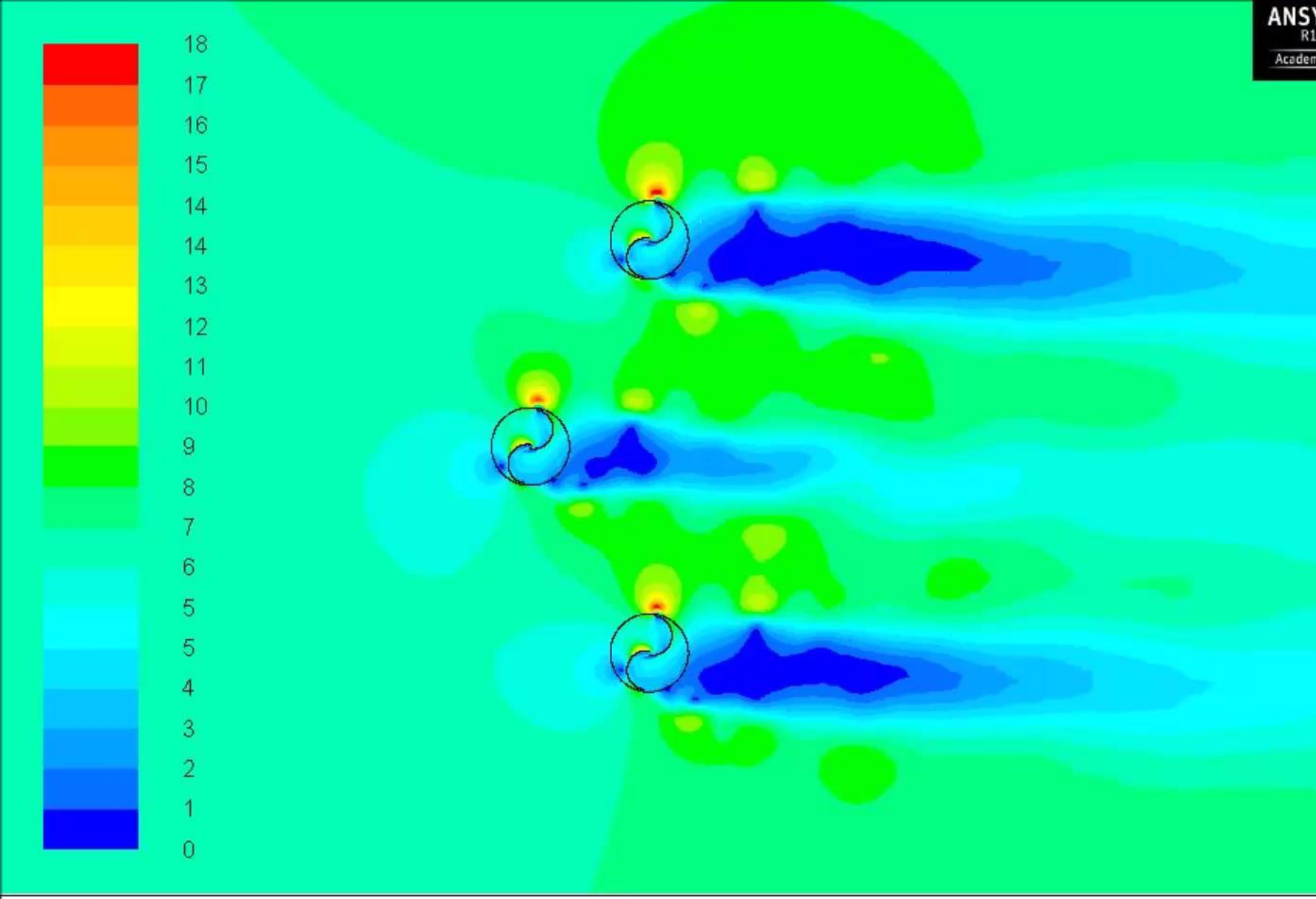
Cp=0.3







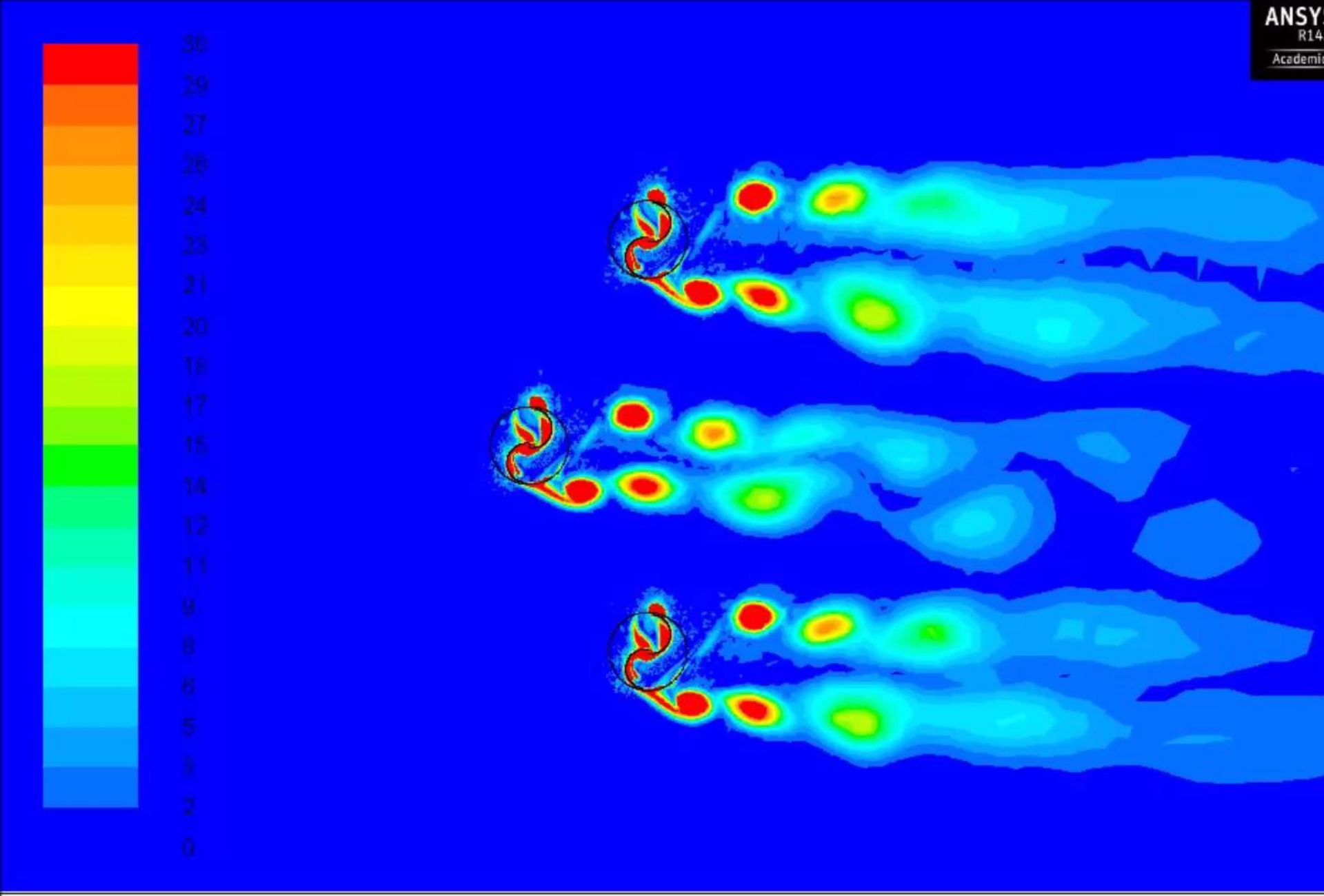




Contours of Velocity Magnitude (m/s) (Time=4.0512e+00)

May 13, 20

ANSYS Fluent 14.5 (2d, pbns, trans-sst, transie



Contours of Vorticity Magnitude (1/s) (Time=4.0512e+00)

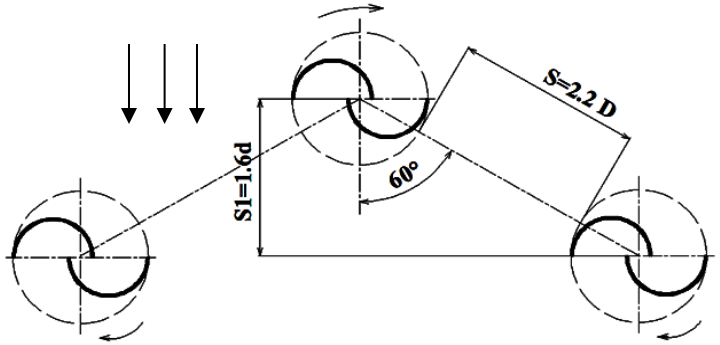
May 13, 201

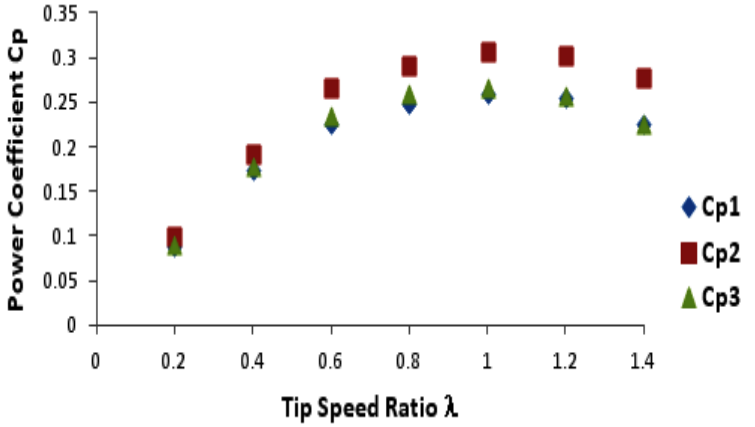
ANSYS Fluent 14.5 (2d, pbns, trans-sst, transien

Three Turbine Cluster Performance Confirmation

Co-Rotating Three turbine Cluster has an enhancement in average power coefficient of 26 % compared to isolated turbines

	Isolated Rotor	Rotor (1)	Rotor (2)	Rotor (3)
Power Coefficient (Cp)	0.23	0.26	0.327	0.289
Enhancement % Compared to Isolated Rotor		13%	42%	25%
Ratio Compared to Rotor (1)		1	1.23	1.07

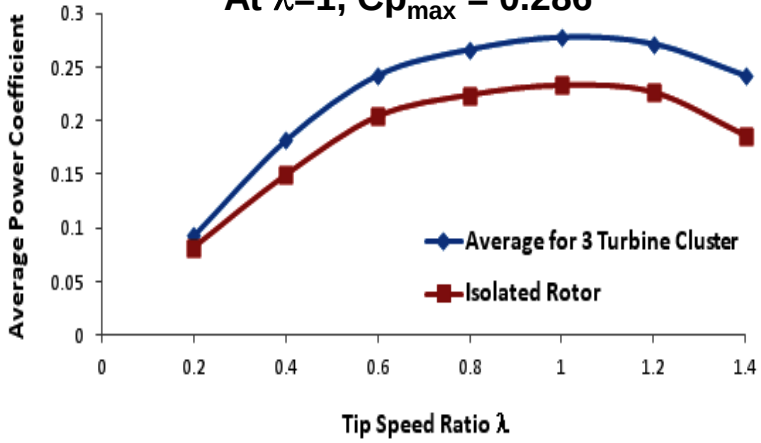




The results show that the ratio 1:1.2:1 between the power coefficients of the three rotors is consistent for λ>0.6

We focus here on the flow field at λ>0.6 in order to observe the flow-inducing action of the turbine revolutions rather than the flow-stagnating action at lower tip-speed ratios

At λ=1, Cp_{max} = 0.286





Development of Patterned Vertical Axis Wind Turbine Farm

Nine Savonius Wind Turbine Farm

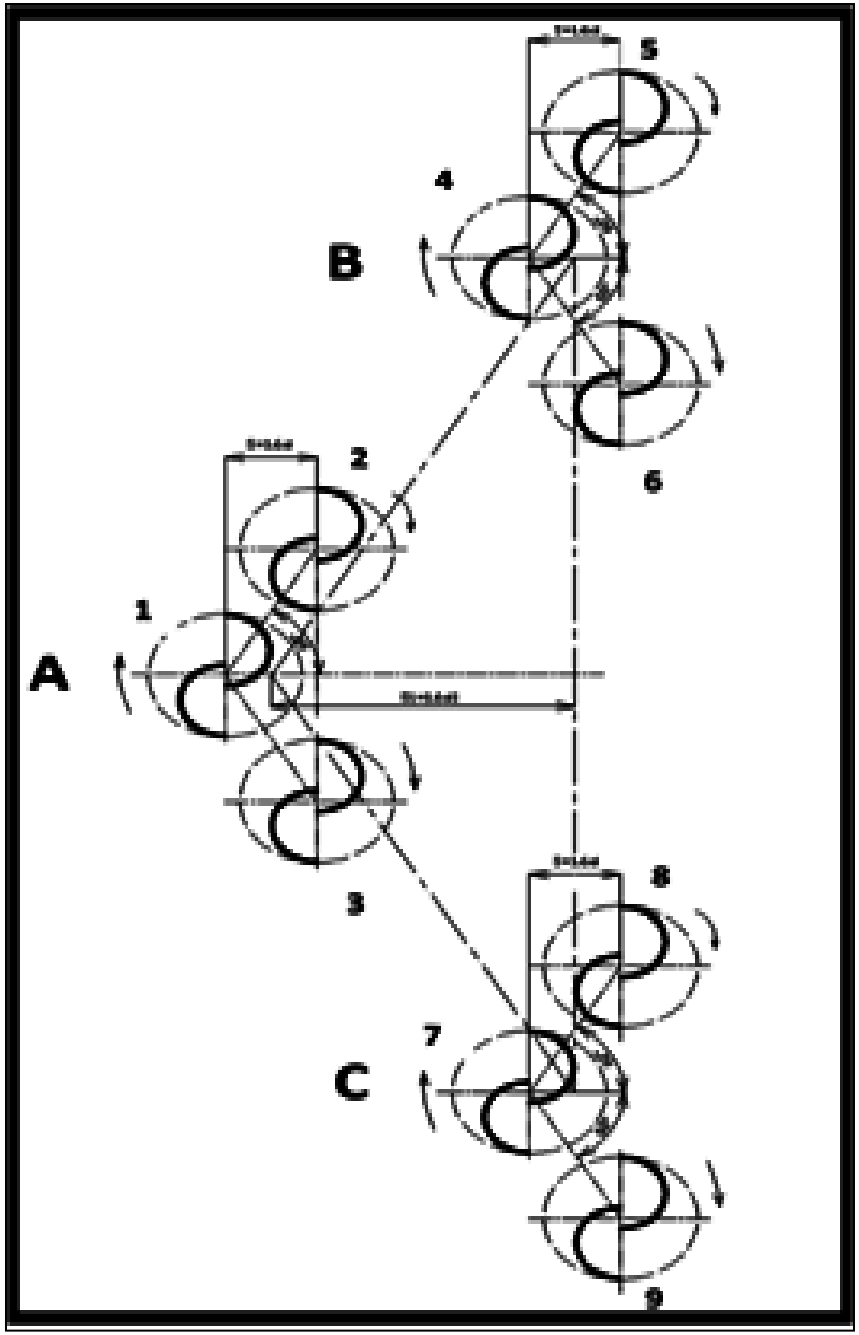
The **nine turbine farm** is **triangular** and has the **same topology** of the three turbine **cluster**

Each vertex of the triangle has a **three turbine cluster**

The domain, solver setting and turbulence model are similar to that of the three turbine cluster simulation

The same grid topology is used, this results in a grid having a number of cells equal to 817,253 cells for the nine turbine farm simulation

The simulation time is about 32 hours



Numerical Results for the Nine Savonius Wind Turbine Farm

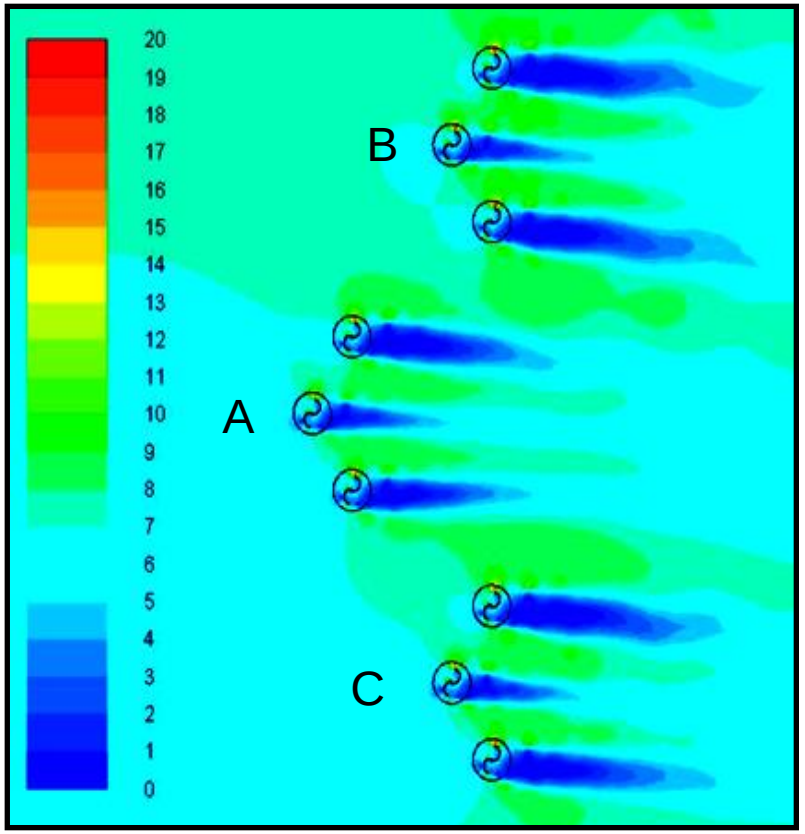
The ratio between Cp of the clusters (A:B:C) is 1:1.2:1

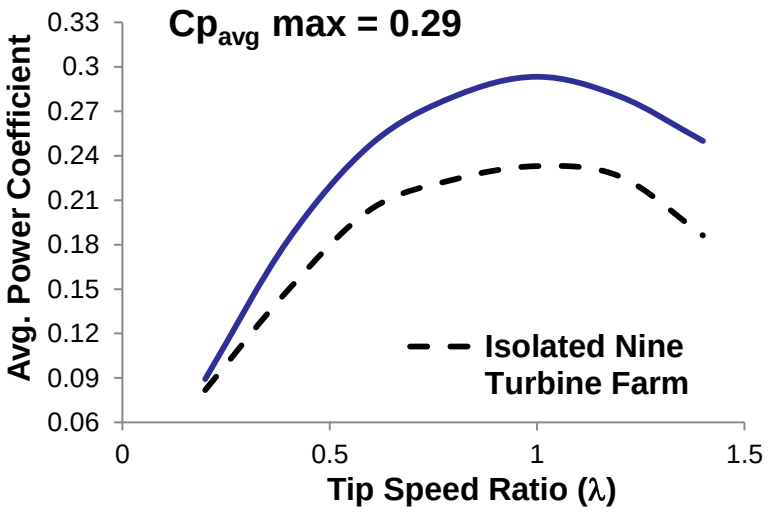
The ratio between Cp of individual turbines is (1:1.2:1)

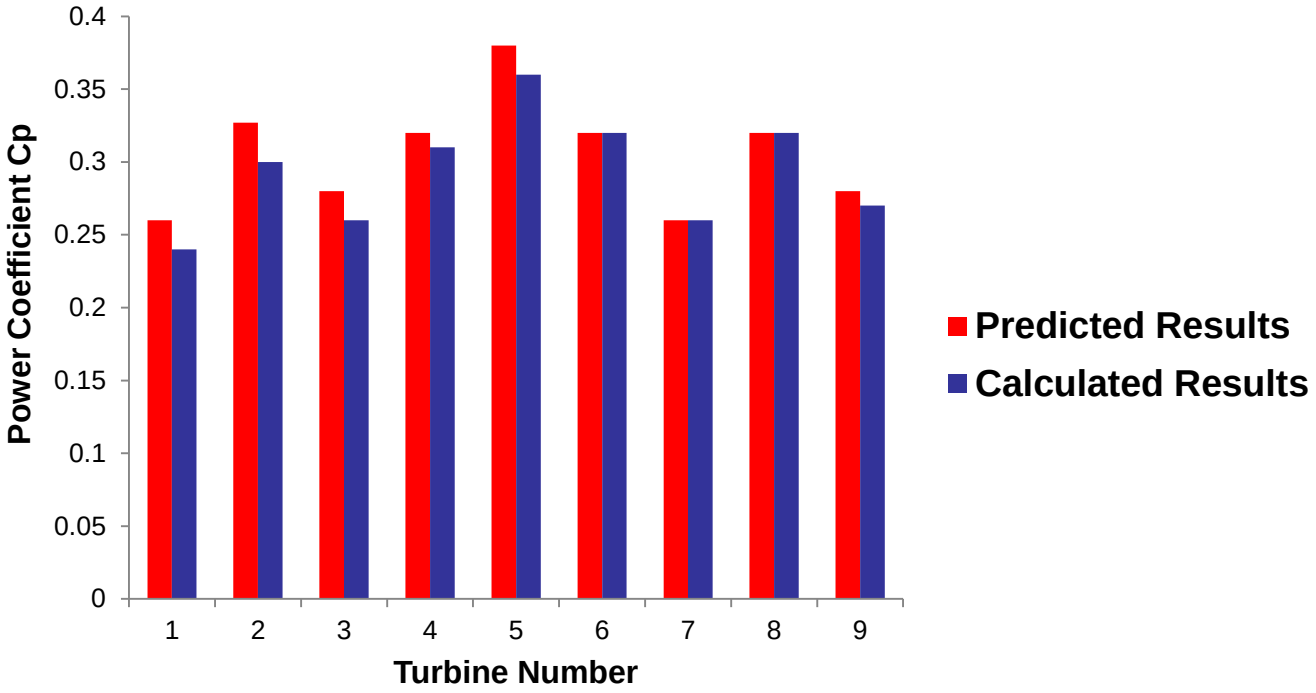
The average power coefficient achieved by the developed nine turbine farm at λ=1 is 26% higher than that of isolated nine turbine farm

Cluster A	Isolated Rotor	Rotor (1)	Rotor (2)	Rotor (3)
Power Coefficient (Cp)	0.23	0.24	0.3	0.26
Enhancement % Compared to Isolated Rotor		4%	30%	13%
Ratio Compared to Rotor (1)		1	1.25	1.08
Cluster B	Isolated Rotor	Rotor (4)	Rotor (5)	Rotor (6)
Power Coefficient (Cp)	0.23	0.31	0.36	0.32
Enhancement % Compared to Isolated Rotor		34%	56%	39%
Ratio Compared to Rotor (4)		1	1.16	1.03
Cluster C	Isolated Rotor	Rotor (7)	Rotor (8)	Rotor (9)
Power Coefficient (Cp)	0.23	0.26	0.32	0.27
Enhancement % Compared to Isolated Rotor		13%	39%	17%
Ratio Compared to Rotor (7)		1	1.23	1.03

	Cluster (A)	Cluster (B)	Cluster (C)
Power Coefficient (Cp)	0.26	0.33	0.28
Ratio Compared to Cluster (A)	1	1.23	1.04



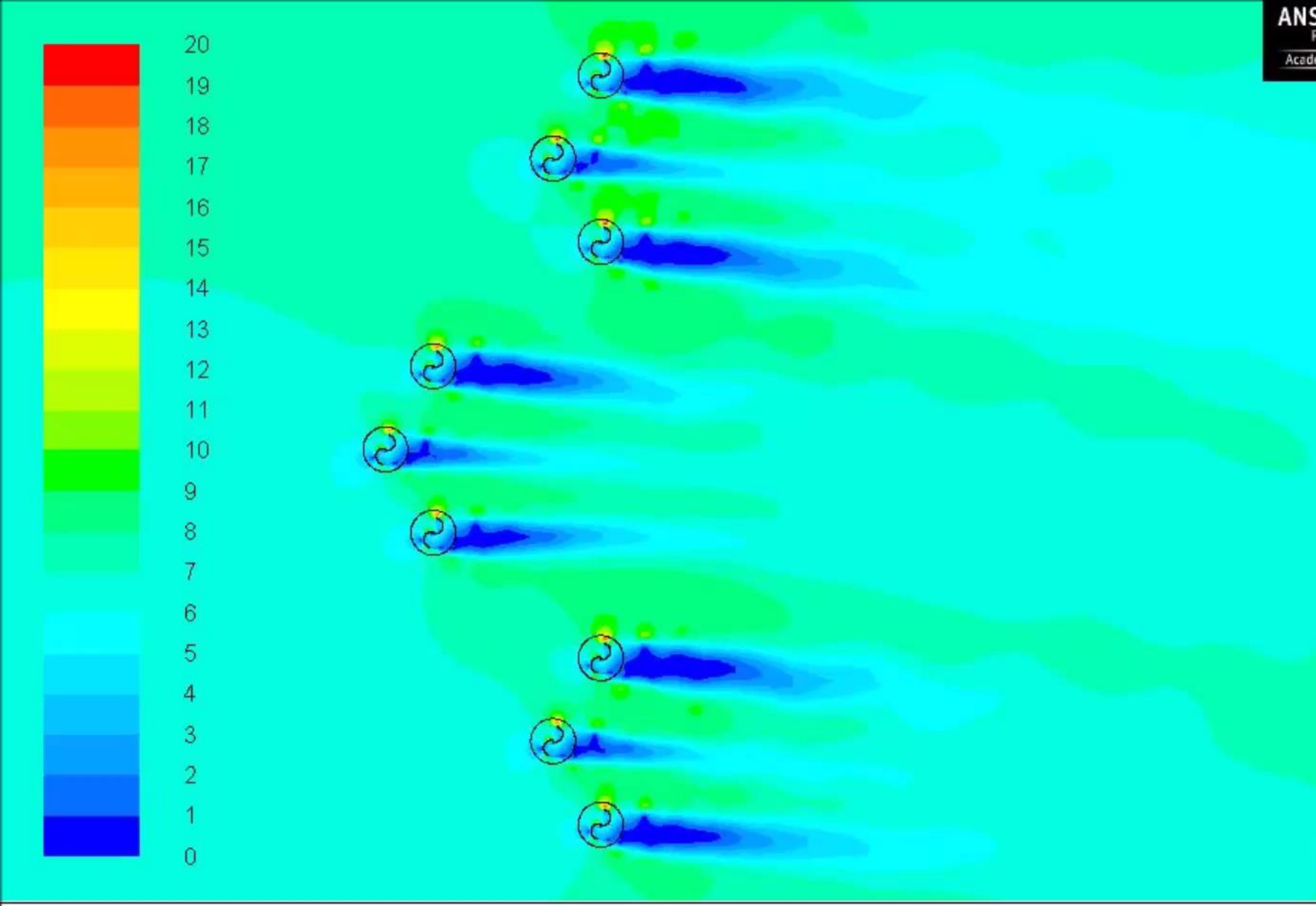




The nine turbine farm is patterned, the performance of the farm can be predicted by simulation of a three turbine cluster

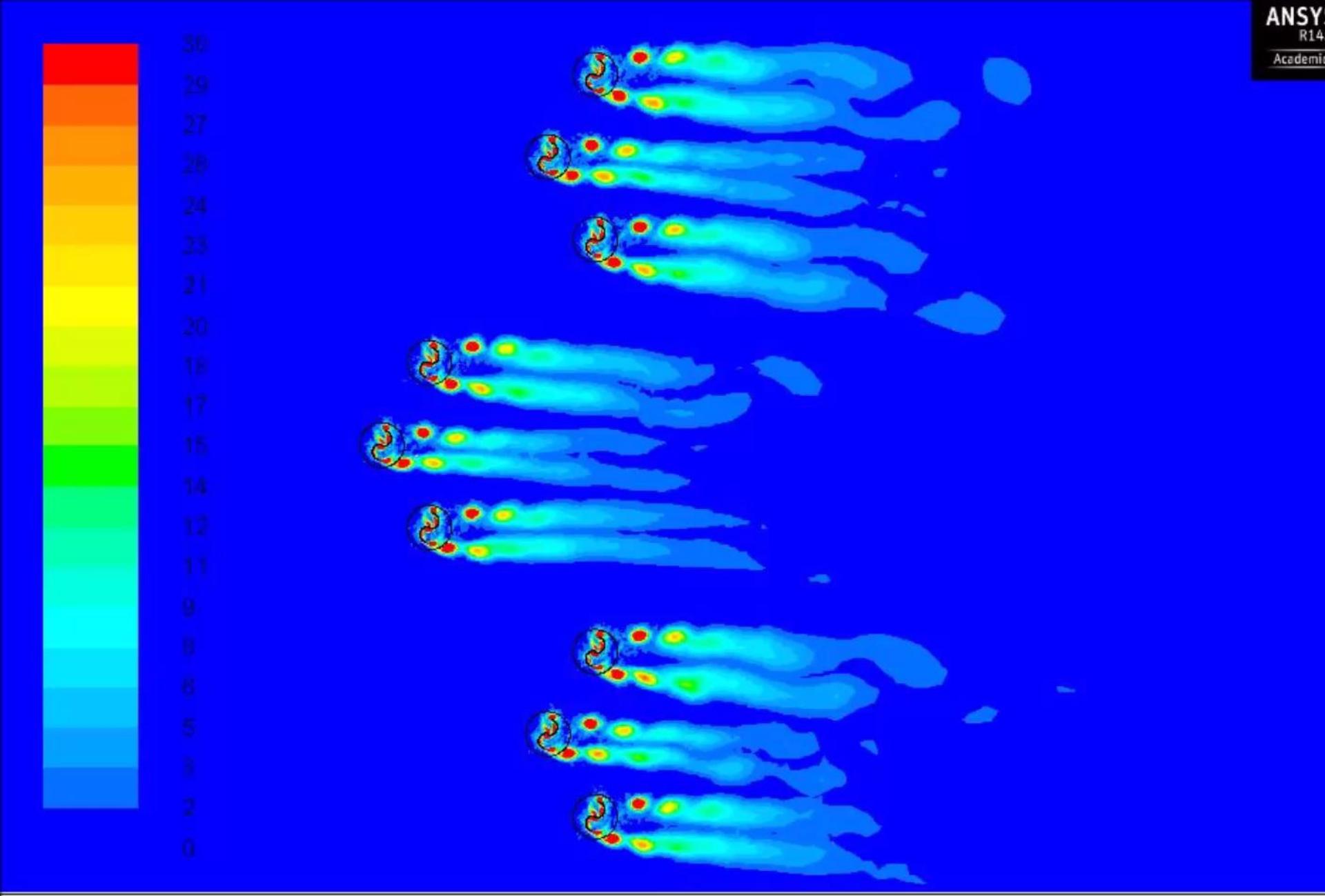
Using the ratio 1:1.2:1 and the results of the three turbine cluster, the nine turbine farm efficiency is predicted and compared to the calculated results

The error in the predicted average power coefficient (Cp=0.3) of the farm compared to the calculated value (Cp=0.292) is less than 2%



Contours of Velocity Magnitude (m/s) (Time=5.4050e+00)

May 13, 20



Contours of Vorticity Magnitude (1/s) (Time=5.4050e+00)

May 13, 201

ANSYS Fluent 14.5 (2d, pbns, trans-sst, transien

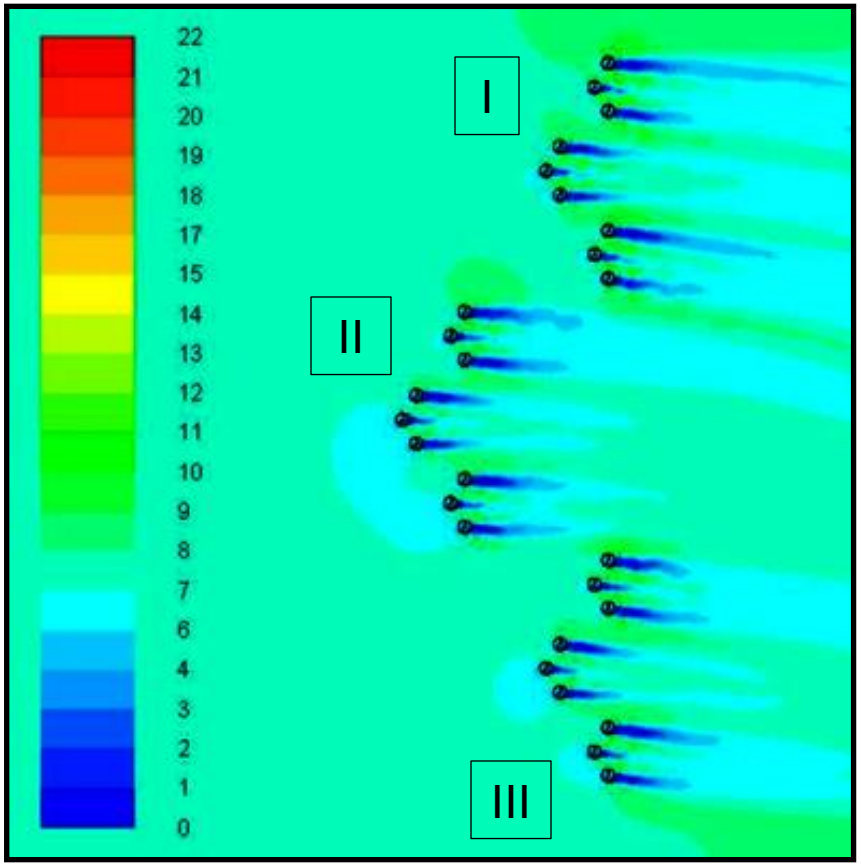
Numerical Results for the Twenty-Seven Savonius Wind Turbine Farm

The ratio between Cp of individual turbines is (1:1.2:1)

The ratio between average Cp of the clusters is 1:1.2:1

The ratio between average Cp of the nine turbine farms I, II and III is 1:1.2:1

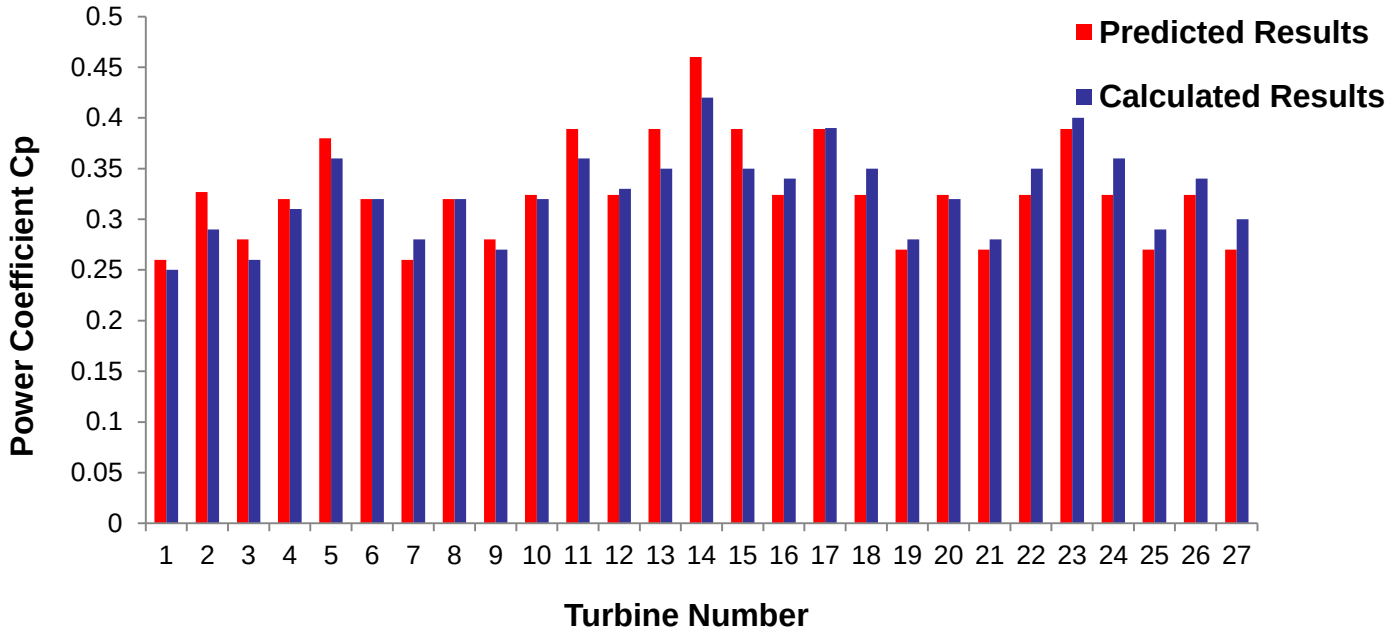
The average power coefficient achieved by the developed nine turbine farms at λ=1 is 39% higher than that of isolated nine turbine farm



	Total Power (watt)	Ratio Compared to Cluster (A)
Cluster (A)	170	1
Cluster (B)	208	1.22
Cluster (C)	182	1.07
	Total Power (watt)	**Ratio Compared to Cluster (D)**
Cluster (D)	214	1
Cluster (E)	233	1.09
Cluster (F)	226	1.05
	Total Power (watt)	**Ratio Compared to Cluster (A)**
Cluster (G)	181	1
Cluster (H)	233	1.27
Cluster (I)	195	1.06

	Cluster (I)	Cluster (II)	Cluster (II)
Total Power (watt)	567	680	604
Ratio Compared to Cluster (I)	1	1.2	1.06

The average power achieved by the developed twenty-seven turbine farm is 0.32 at λ =1

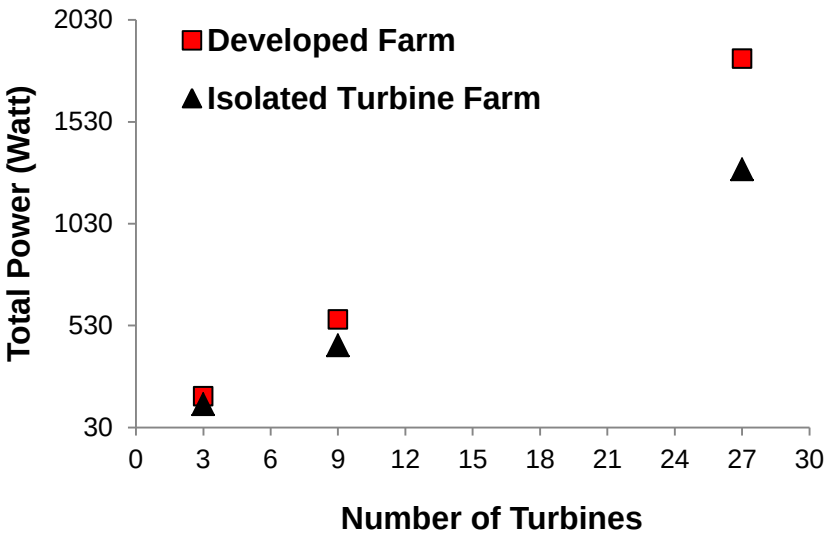


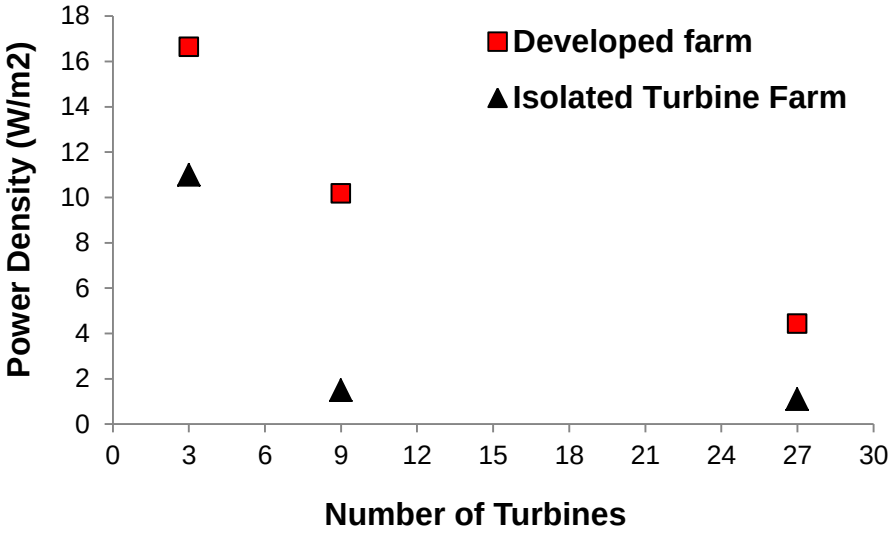
The 27 turbine farm is patterned, this means that the performance of the farm can be predicted by simulation of only three turbines.

Using the ratio 1:1.2:1 and the results of the simulation of the three turbine cluster, the 27 turbine farm efficiency is predicted and compared to the calculated results.

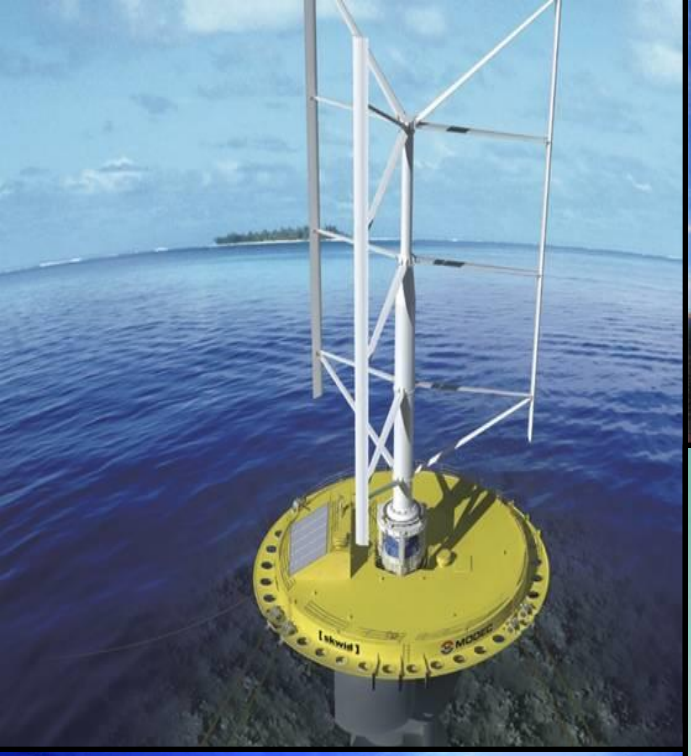
The error in the predicted average power coefficient (Cp=0.326) of the farm compared to the calculated value (Cp=0.325) is less than 0.4%

Power and Power Density of the Developed VS Isolated Farms (One meter Diameter and One meter Height Turbines)

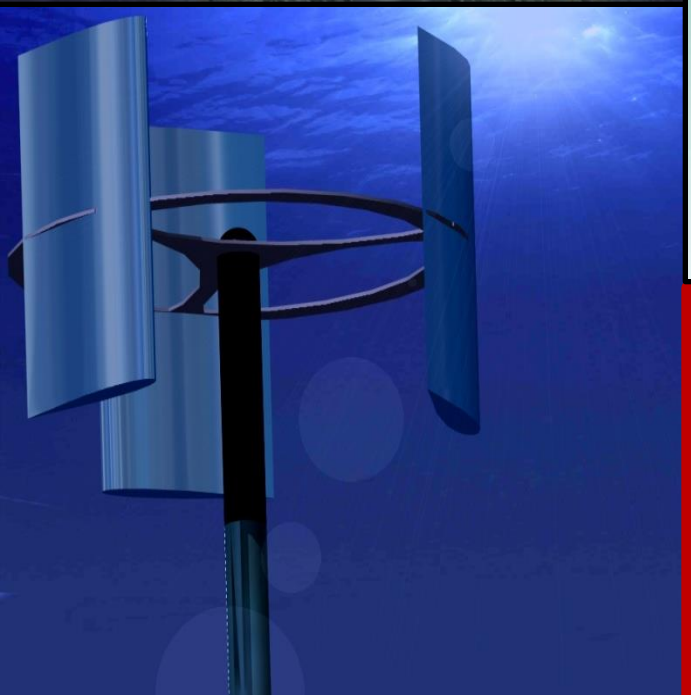


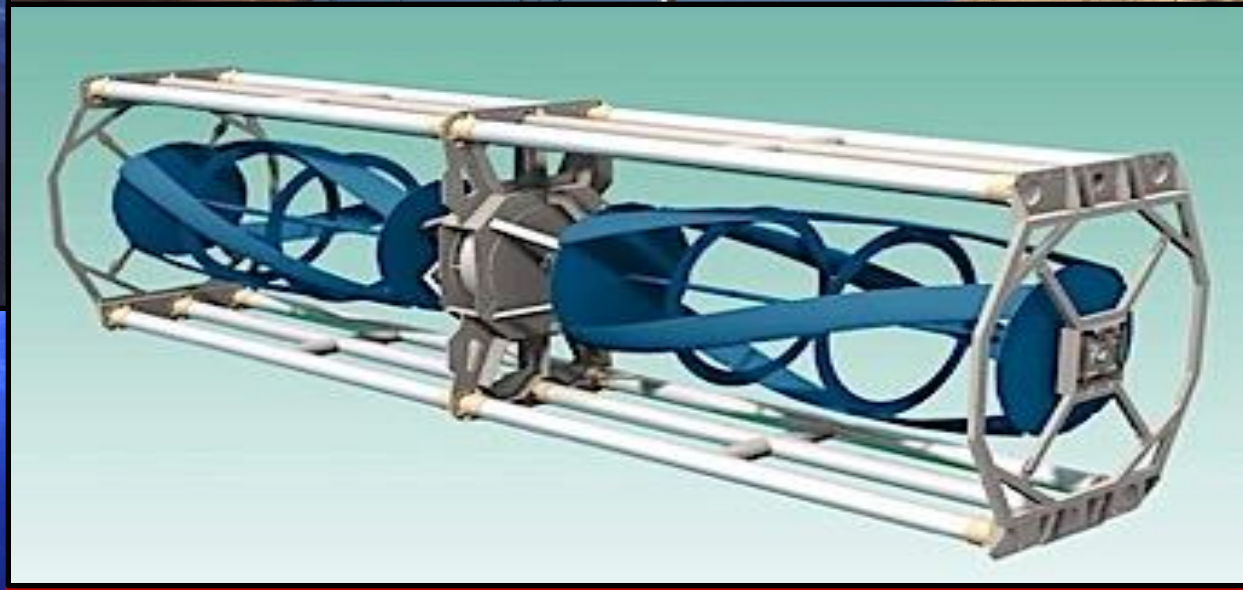


	Power (W/m)		Enhancement In Power	Power Density (W/m^2)		Enhancement In Power Density
	Developed	Isolated		Developed	Isolated	
3 Turbines	182	145	26%	17	13	1.3 times
9 Turbines	554	435	26%	10	1.3	7 times
27 Turbines	1841	1304	39%	4.5	1.1	4 times







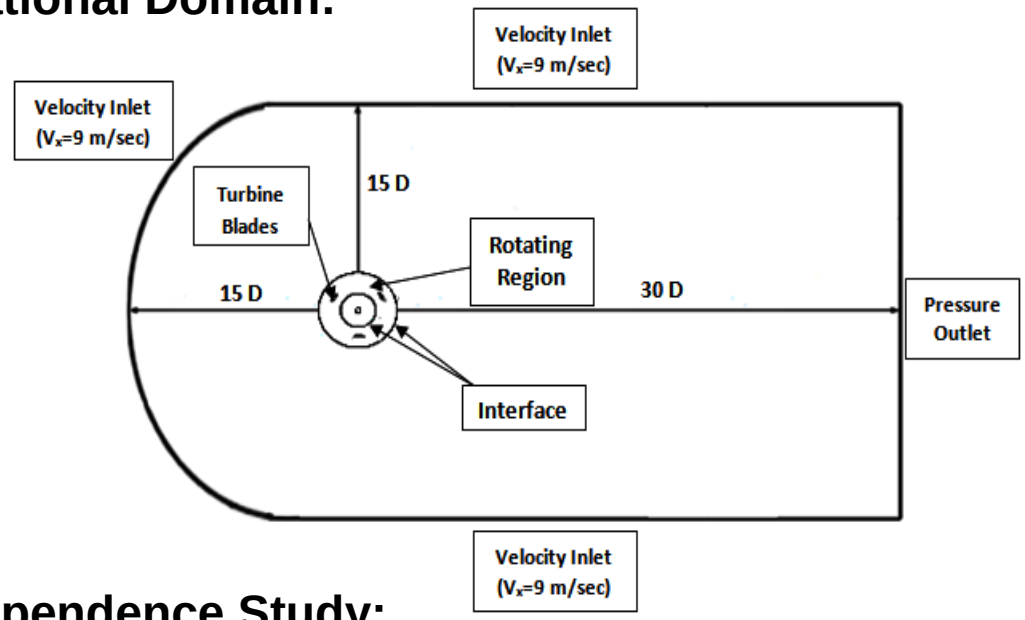


Case Study (II)

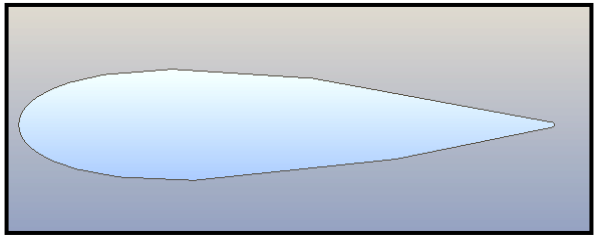
Darrieus Wind Turbine

Numerical Unsteady Simulation
Solution of a Single Darrieus Wind Turbine

Computational Domain:



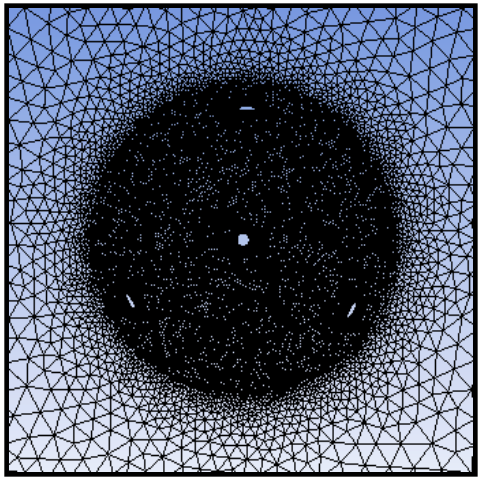
Aerfoil: NACA 0021

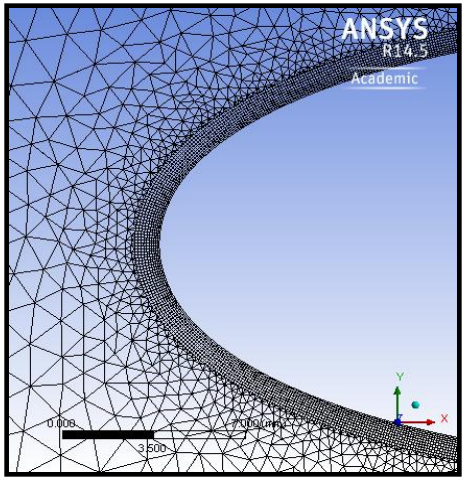


Grid independence Study:

Grid level	Number of cells	Cm	Cp
1	47,591	0.059	0.166
2	81,034	0.093	0.259
3	173,768	0.129	0.362
4	235,451	0.131	0.367
5	492,605	0.129	0.361

y+ < 1 as required by the transition SST turbulence model

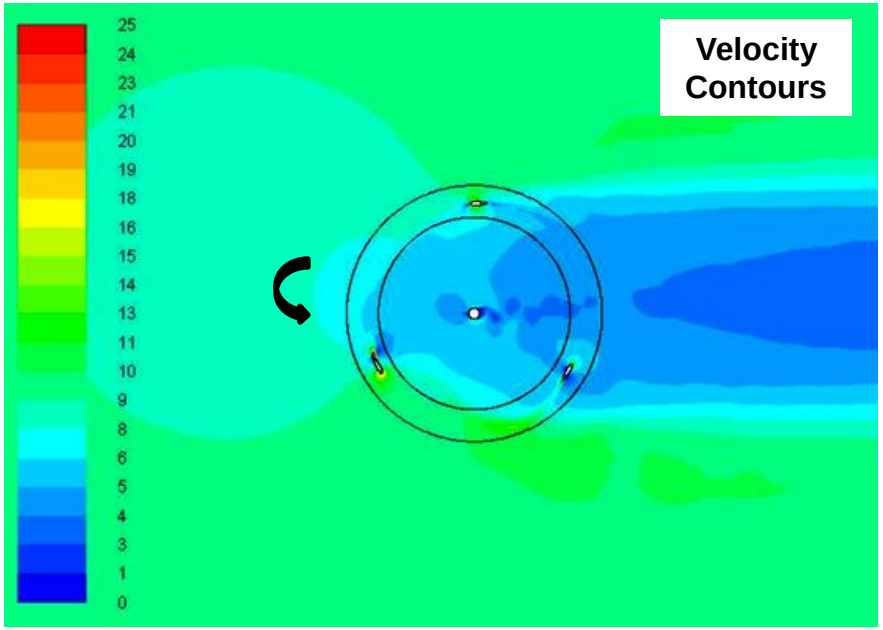


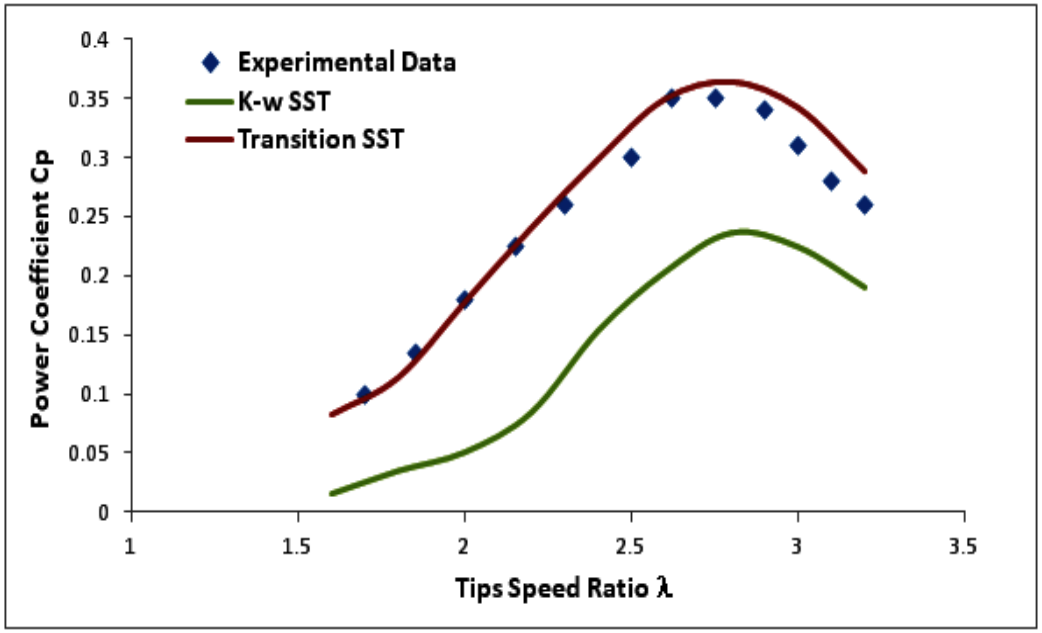


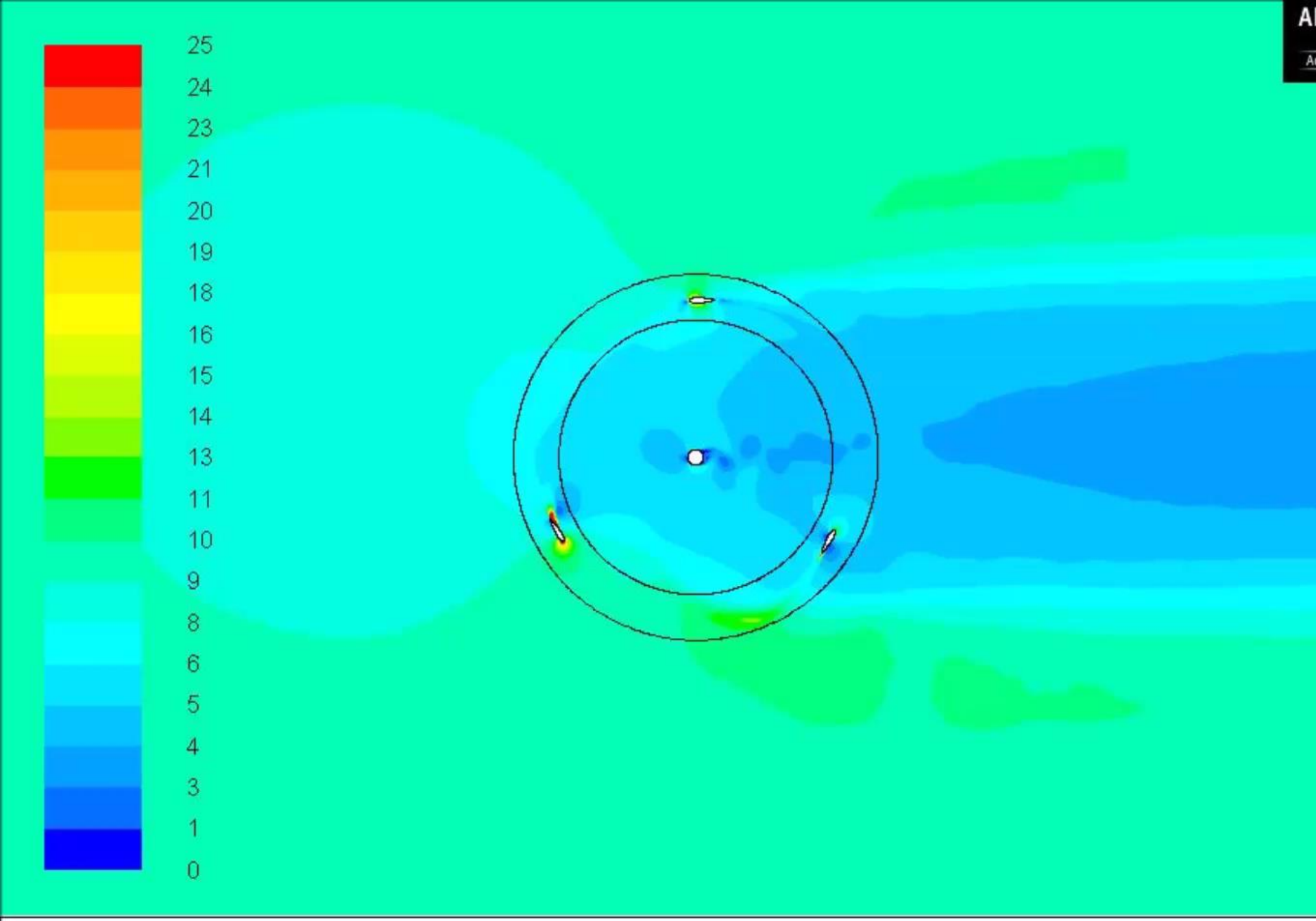
2D Numerical Model Validation:

The transition SST turbulence shows closer agreement to the experiments data in the numerical results for Power coefficient at different tip speed ratios (λ)

Peak Cp=0.36 at λ=2.8

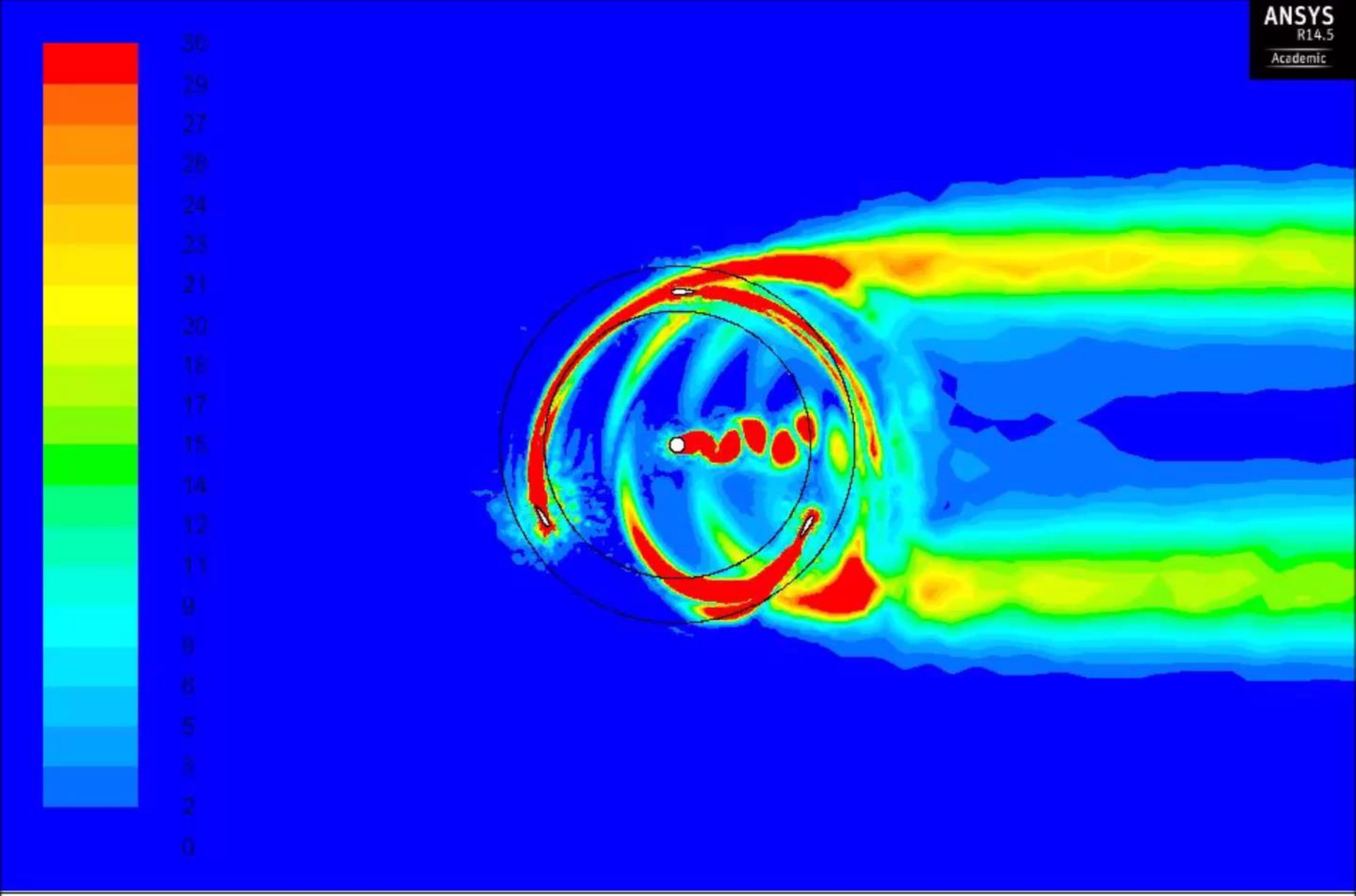






Contours of Velocity Magnitude (m/s) (Time=1.3832e+00)

May 11,



Contours of Vorticity Magnitude (1/s) (Time=1.3832e+00)

May 11, 2015
ANSYS Fluent 14.5 (2d, pbns, trans-sst, transient)

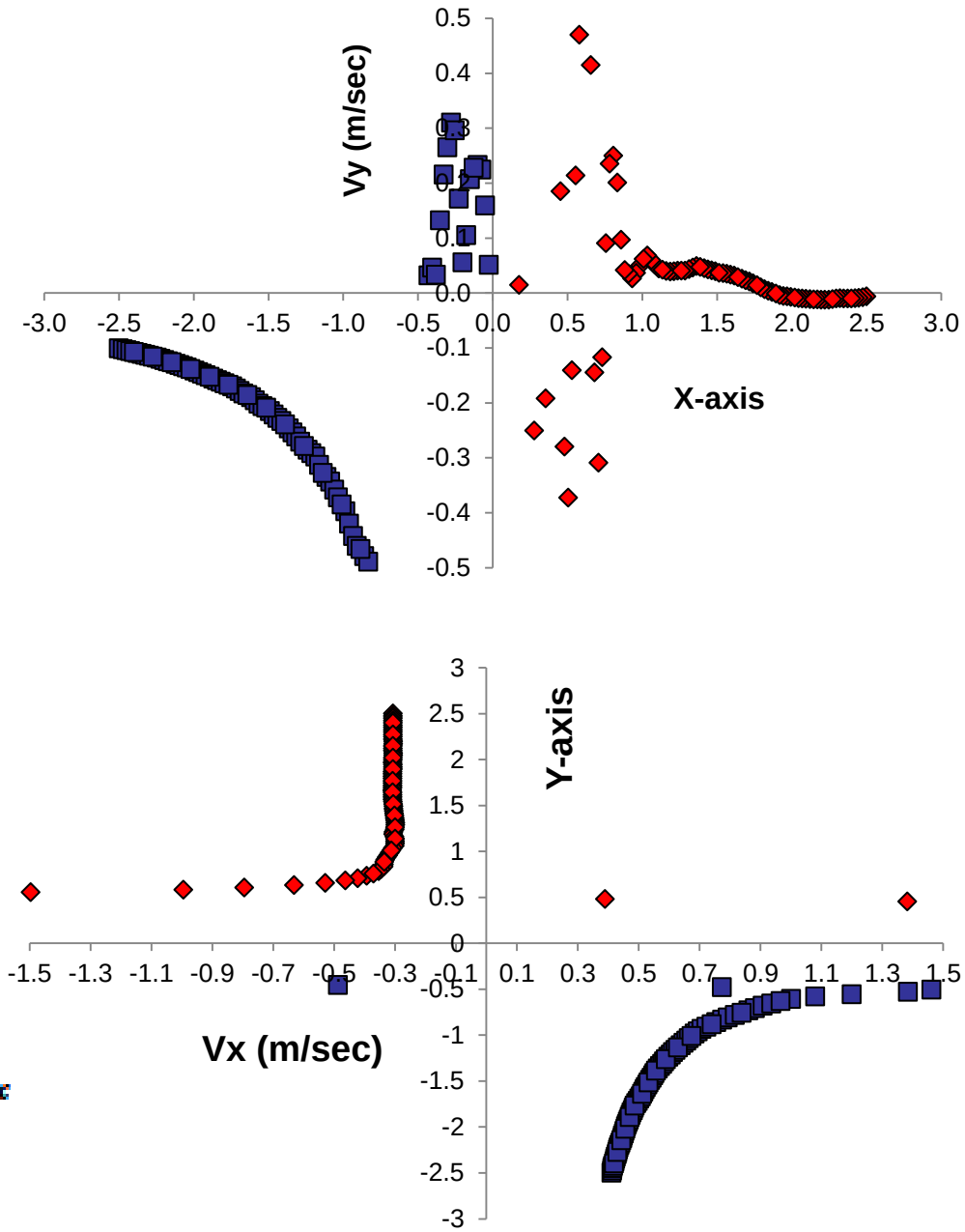
A preliminary analysis of the mean velocity field around the turbine blades at tip speed ratios is obtained

The mean tangential velocity distribution is studied by plotting the mean x-velocity component on the Y-axis and the mean y-velocity component on the X-axis

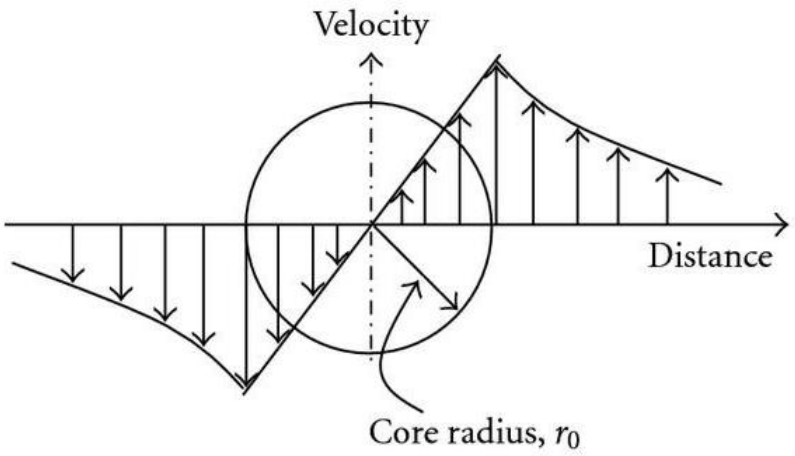
The mean x-velocity is a combination of the undisturbed free stream velocity, the velocity induced due to the expansion of the streamlines and an additional component due to the rotational flow which is generated due to a vortex similar to a non-perfect Rankine vortex

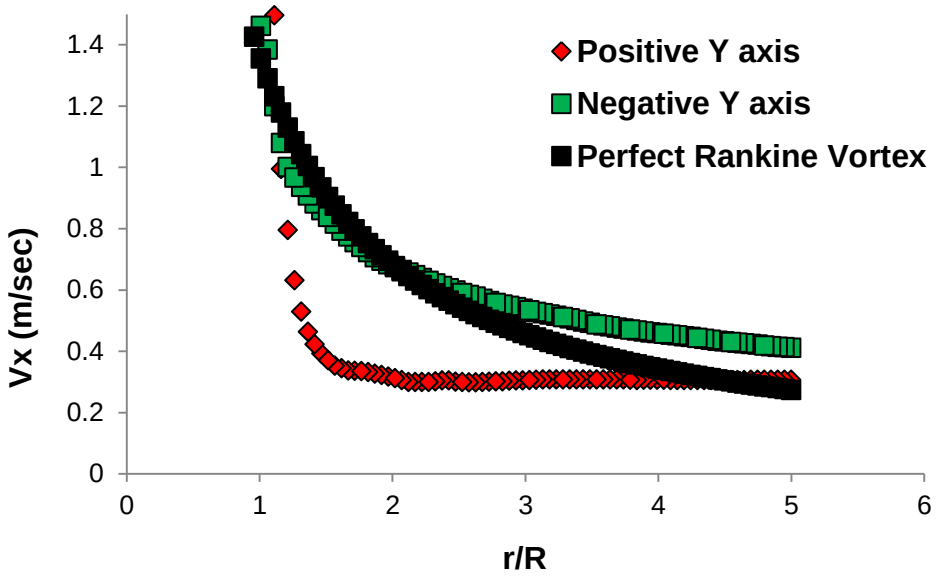
$$Vx = V_{x-undisturbed} + V_{x-induced} + V_{x-vortex}$$

The undisturbed flow component is taken out of the x-velocity plot



Combining the mean x-velocity on both the positive and negative Y-axes on one plot, they are found to approximately fit a perfect Rankine vortex having a circulation (Γ) 4.3

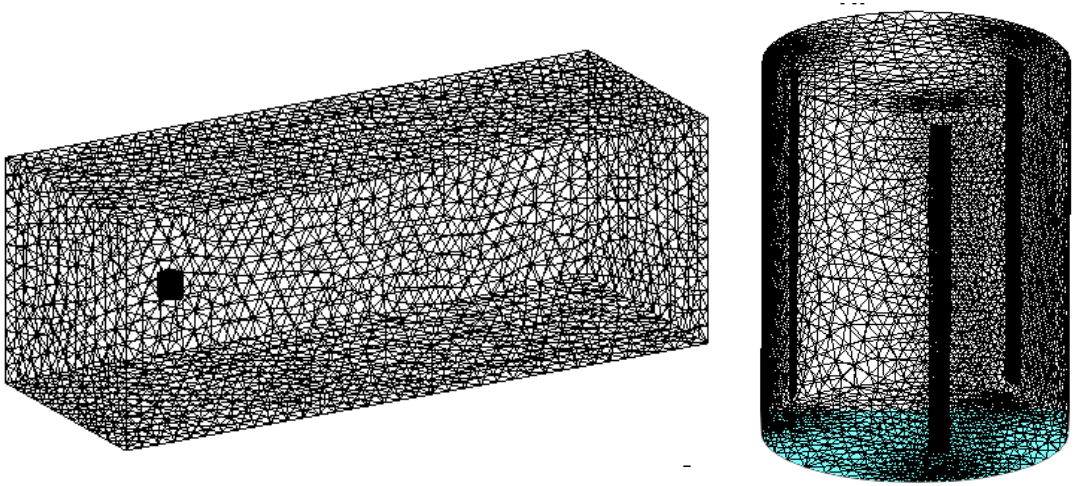




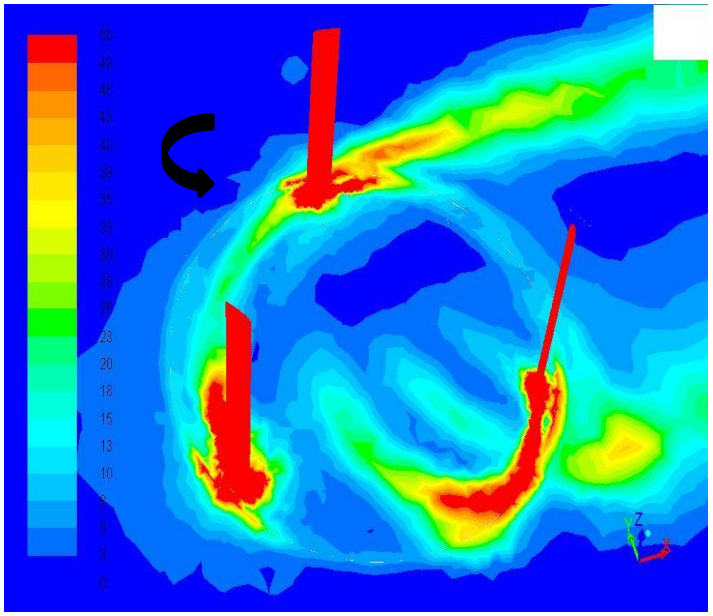
$$u_\theta(r) = \begin{cases} \Gamma r/(2\pi R^2) & r \le R, \\ \Gamma/(2\pi r) & r > R. \end{cases}$$

This provides a preliminary description of the Darrieus turbine as a Rankine vortex combined with the free stream. A further analysis will be done in a future work in order to give a detailed and more accurate vortex modeling for the Darrieus turbine.

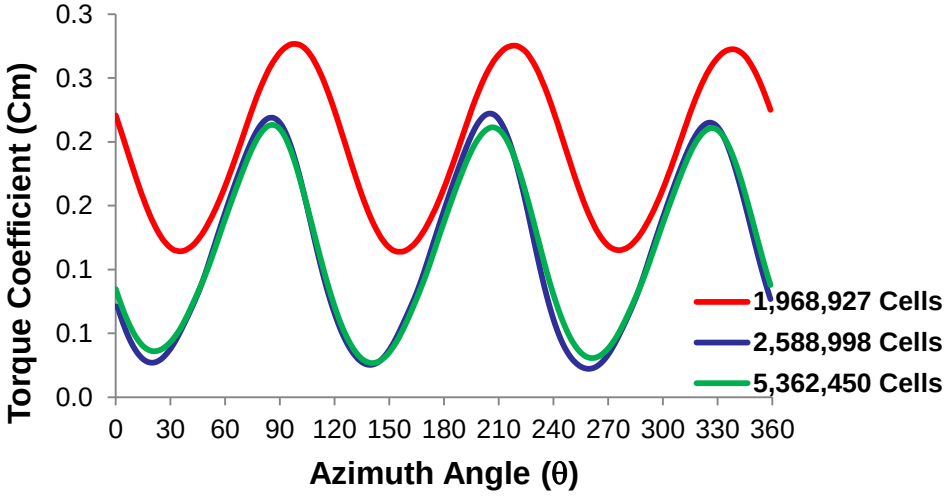
3D Validation for a Single DarrieusTurbine

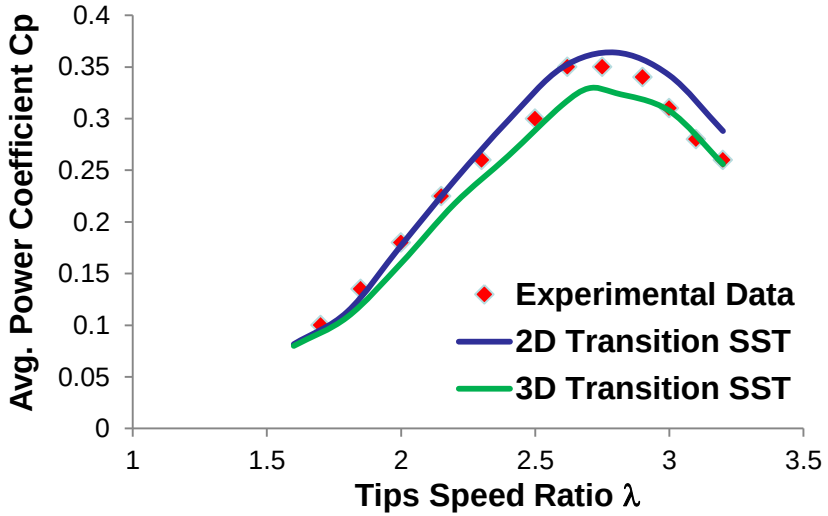


Vorticity Contours



Grid Level	No. of Cells	Cm	Cp
1	1,968,927	0.1807	0.506
2	2,588,998	0.1125	0.315
3	5,362,450	0.1121	0.314

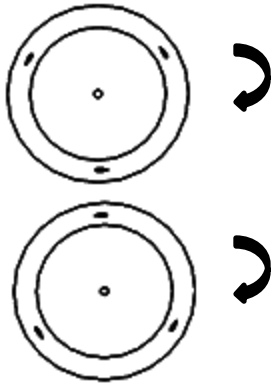




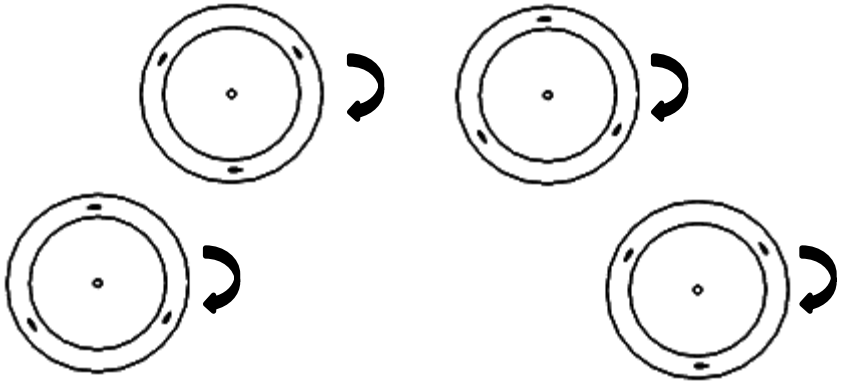
Numerical Solution of Two Darrieus Wind Turbine Clusters

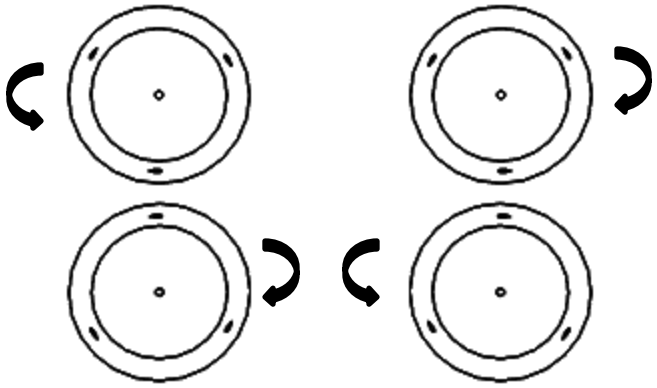
The development of an efficient cluster requires the study of different possibilities of multiple turbine cluster

Two Co-rotating and Counter-rotating turbine clusters in parallel and oblique configurations are numerically simulated

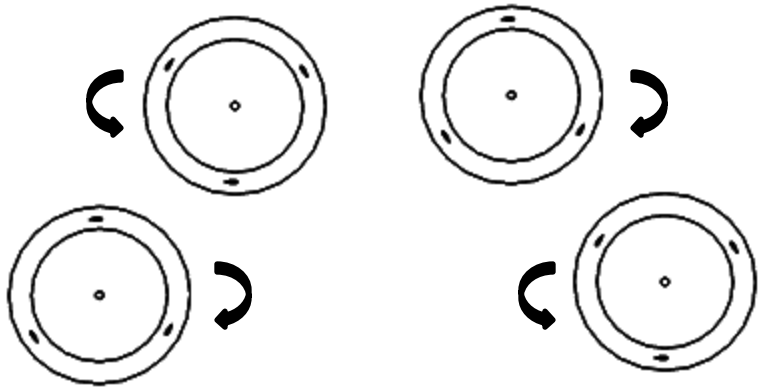


Co-Rotating





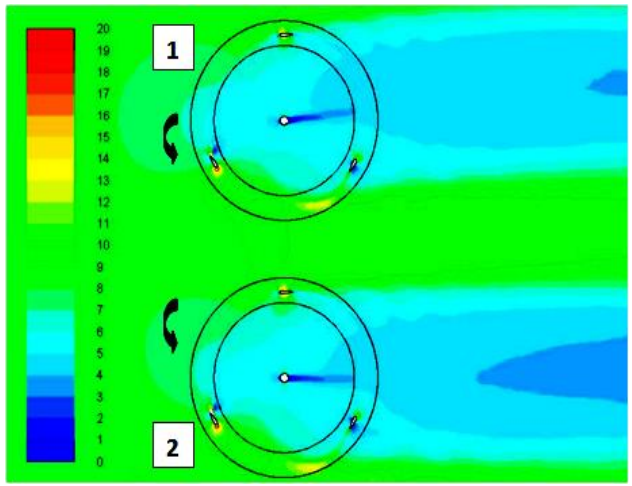
Counter-Rotating



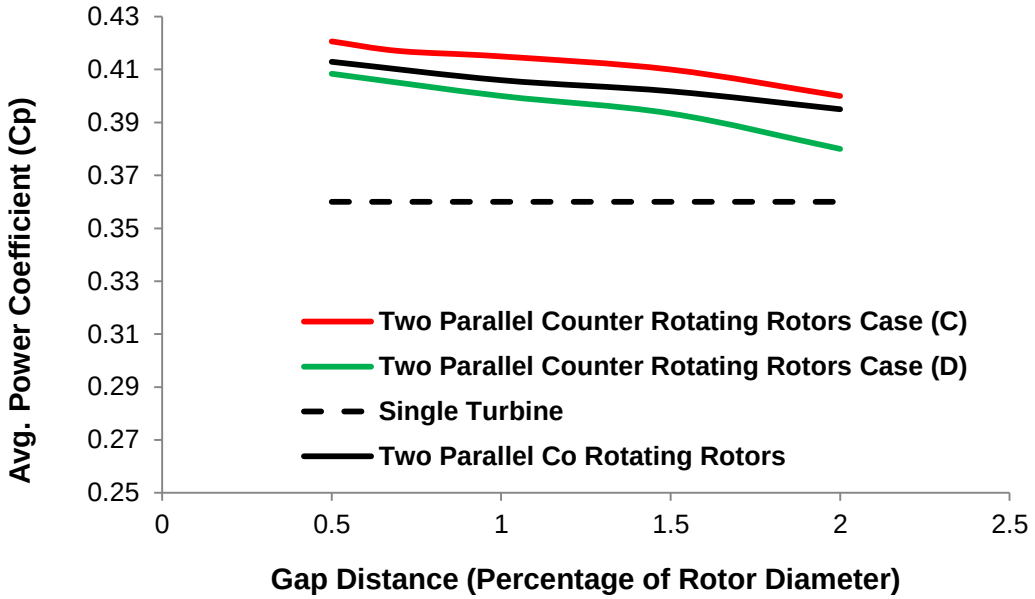
Parallel Configurations

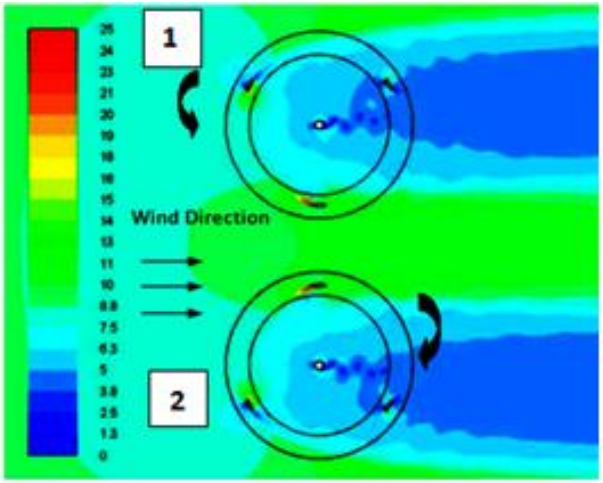
Oblique Configurations

Two Parallel Turbines

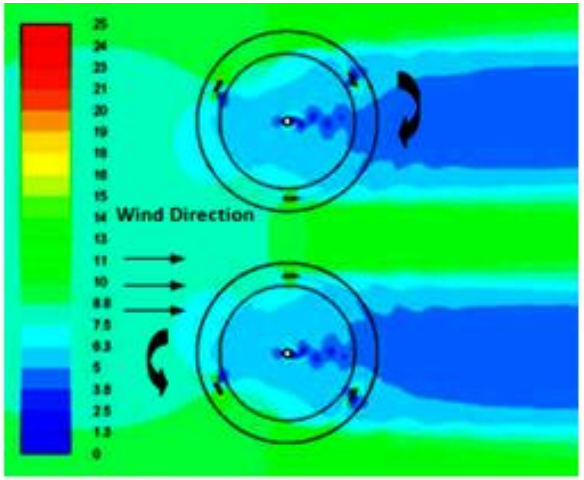


Co-Rotating





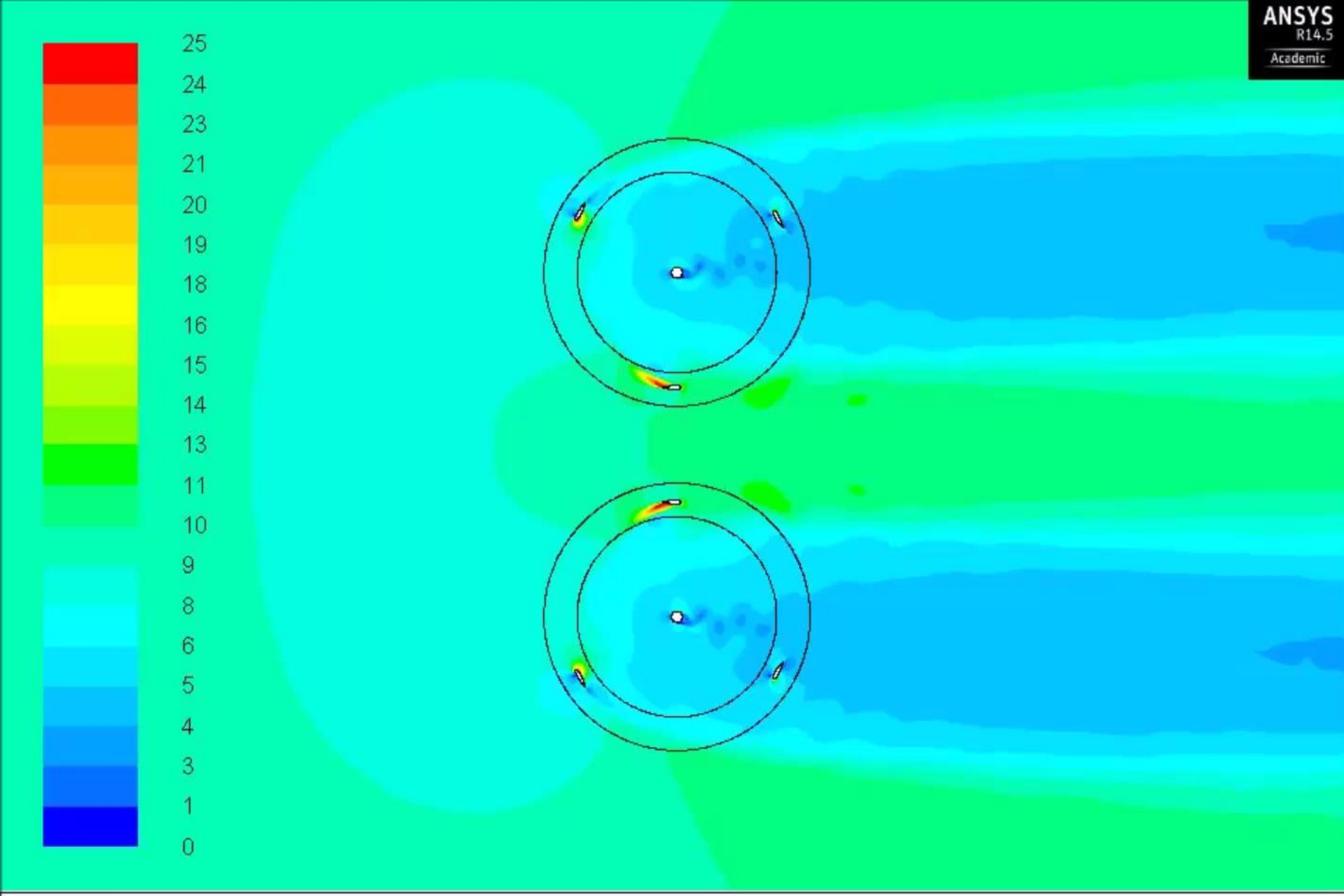
Counter-Rotating (Case C)



Counter-Rotating (Case D)

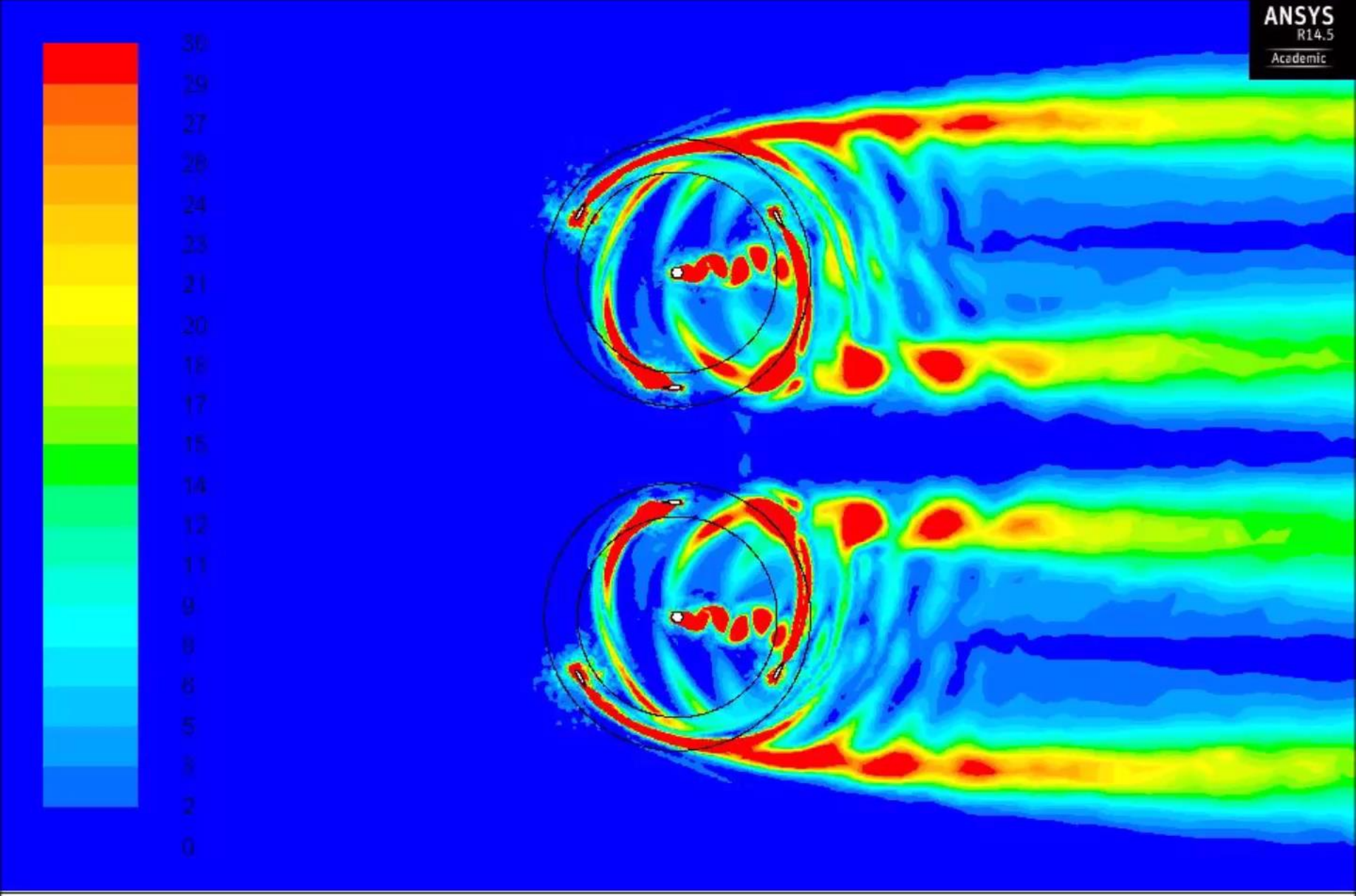
Cpmax = 0.42 for Case (C)

Velocity Contours



Contours of Velocity Magnitude (m/s) (Time=1.7843e+00)

May 14, 2015
ANSYS Fluent 14.5 (2d, pbns, trans-sst, transient)

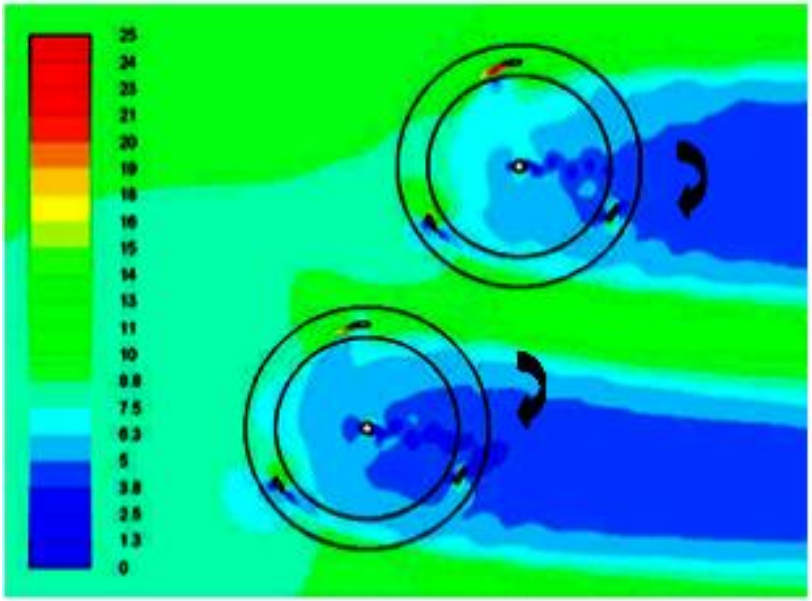


Contours of Vorticity Magnitude (1/s) (Time=1.7843e+00)

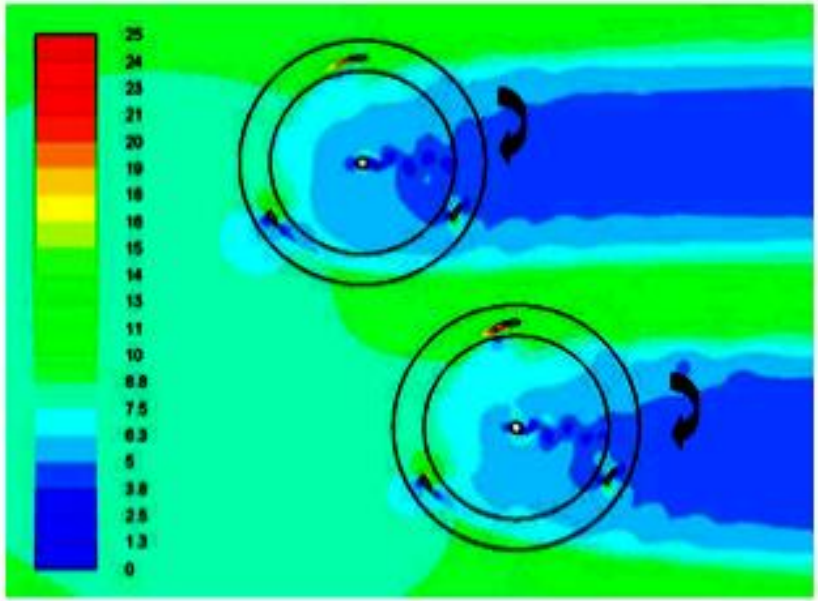
May 14, 2015
ANSYS Fluent 14.5 (2d, pbns, trans-sst, transient)

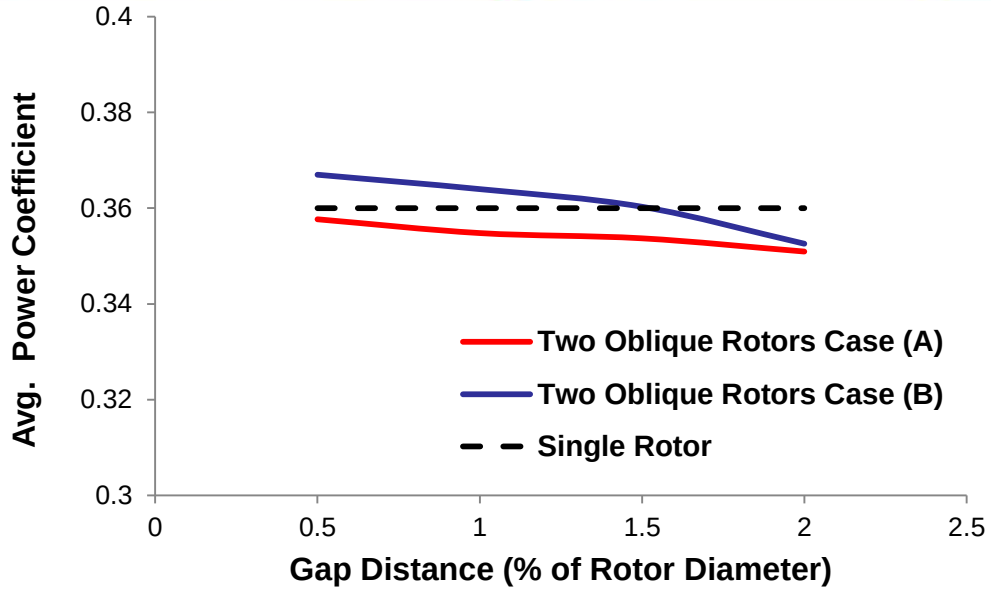
Two Oblique Co-Rotating Turbines:

Co-Rotating (Case A)



Counter-Rotating (Case B)

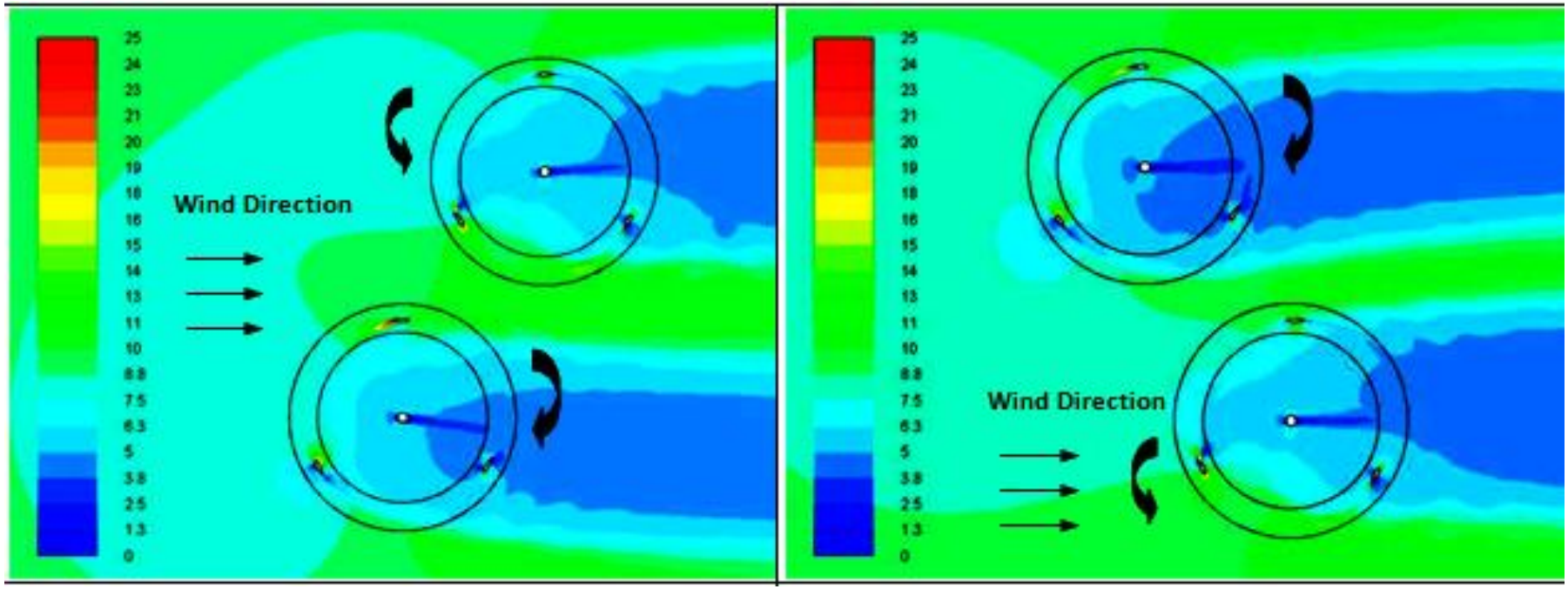


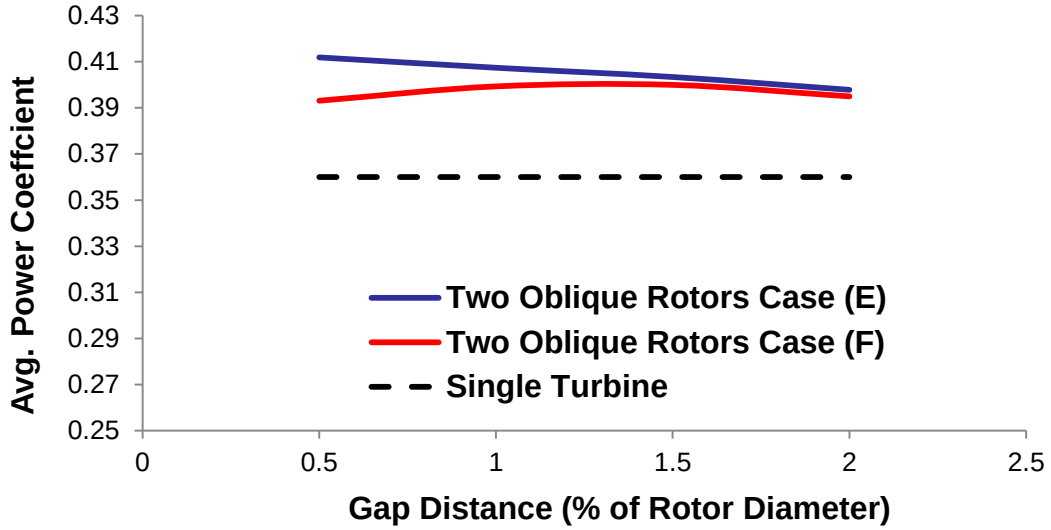


Two Oblique Counter-Rotating Turbines:

Counter-Rotating (Case E)

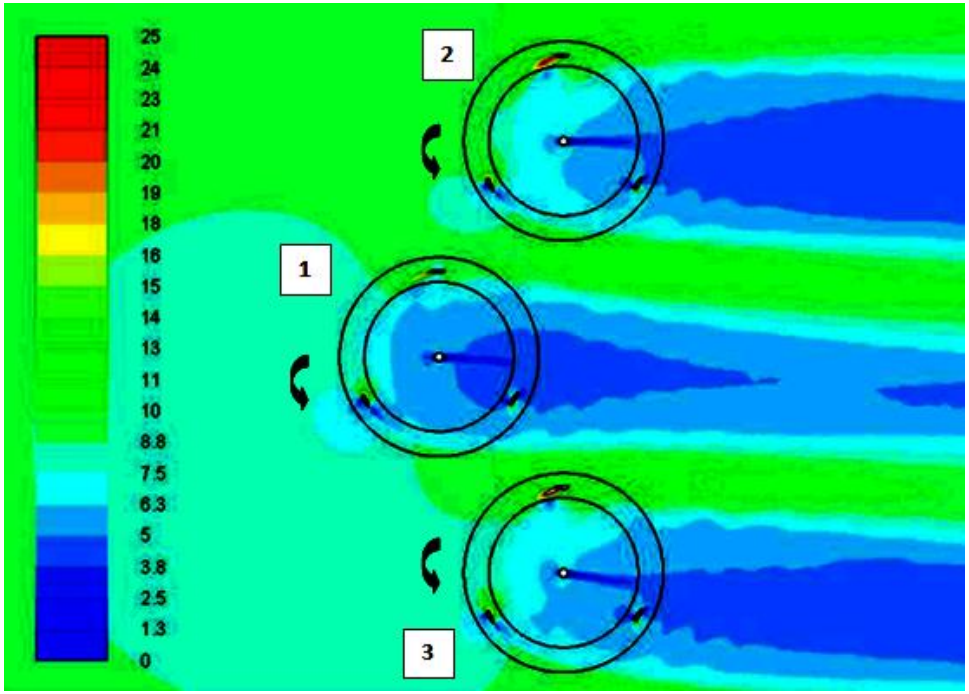
Counter-Rotating (Case F)

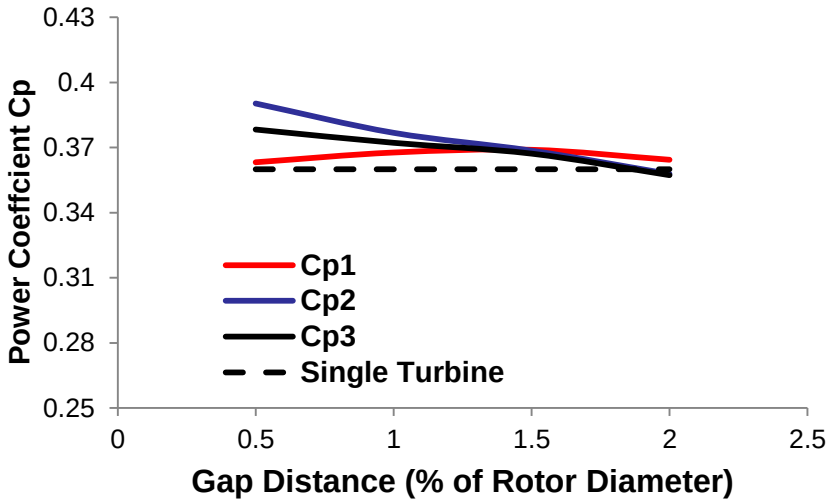


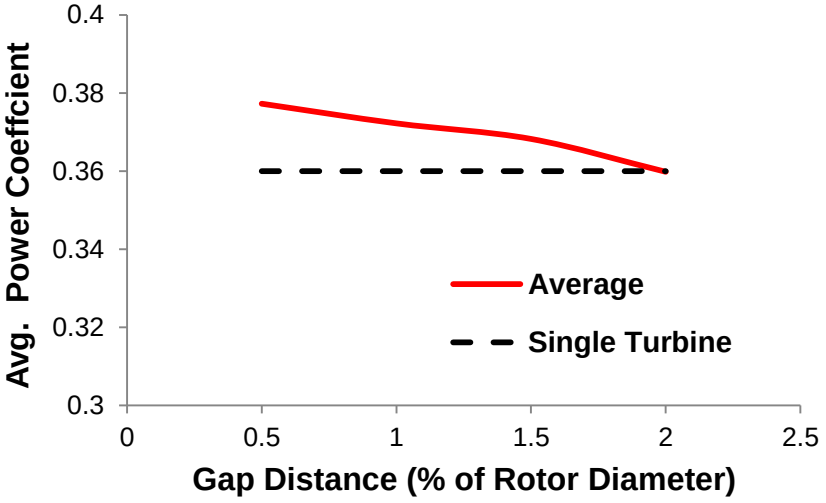


Numerical Simulation of Three Turbine Clusters

Three Co-Rotating Turbine Cluster (I):



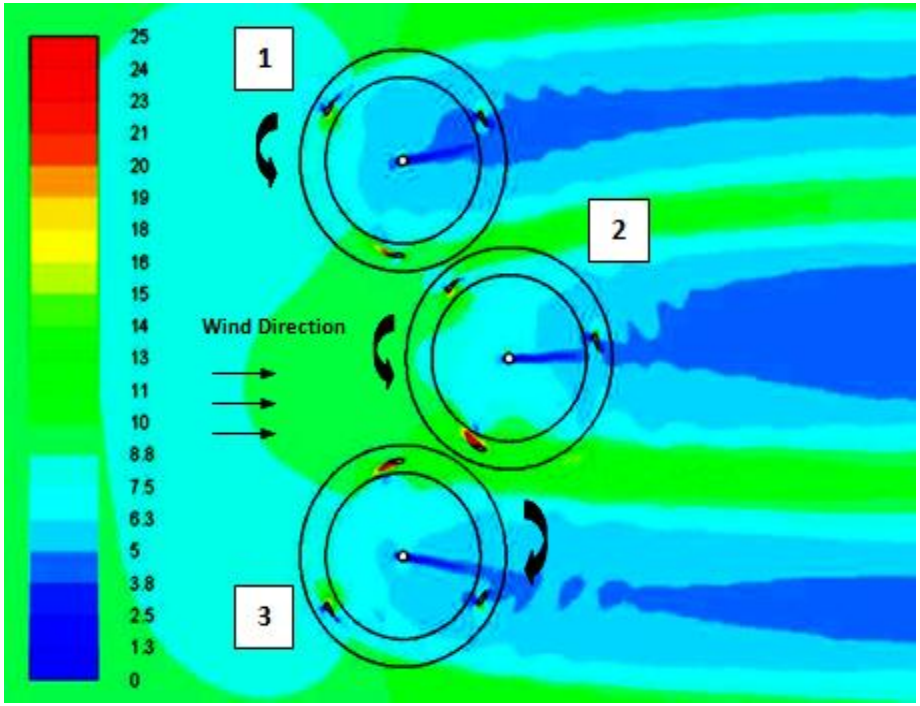




Cp_{max} = 0.377 at 0.5D gap distance

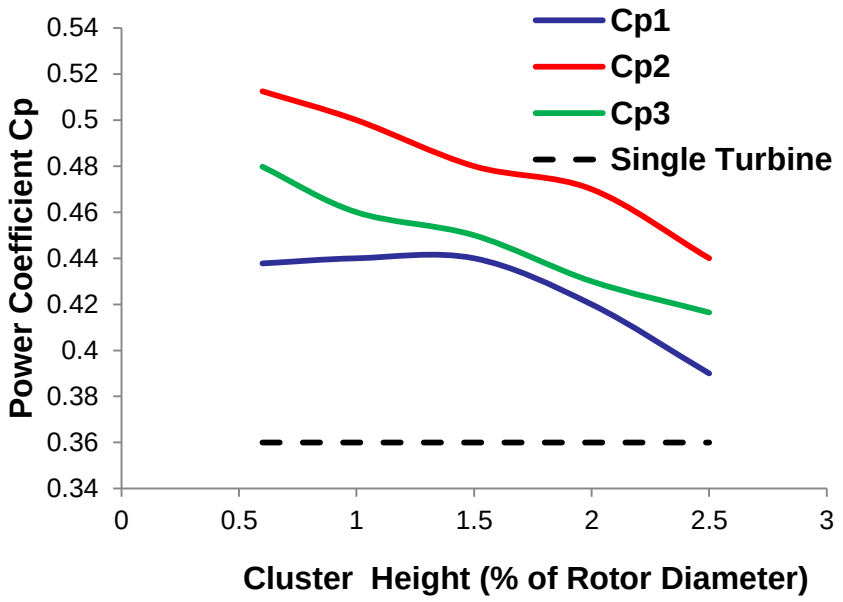
5% higher than isolated turbines

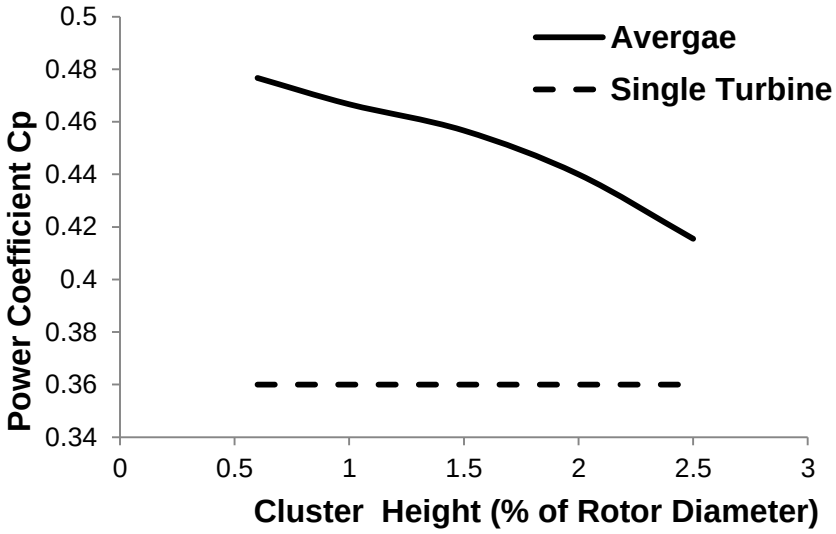
Three Turbine Hybrid Clusters (II):



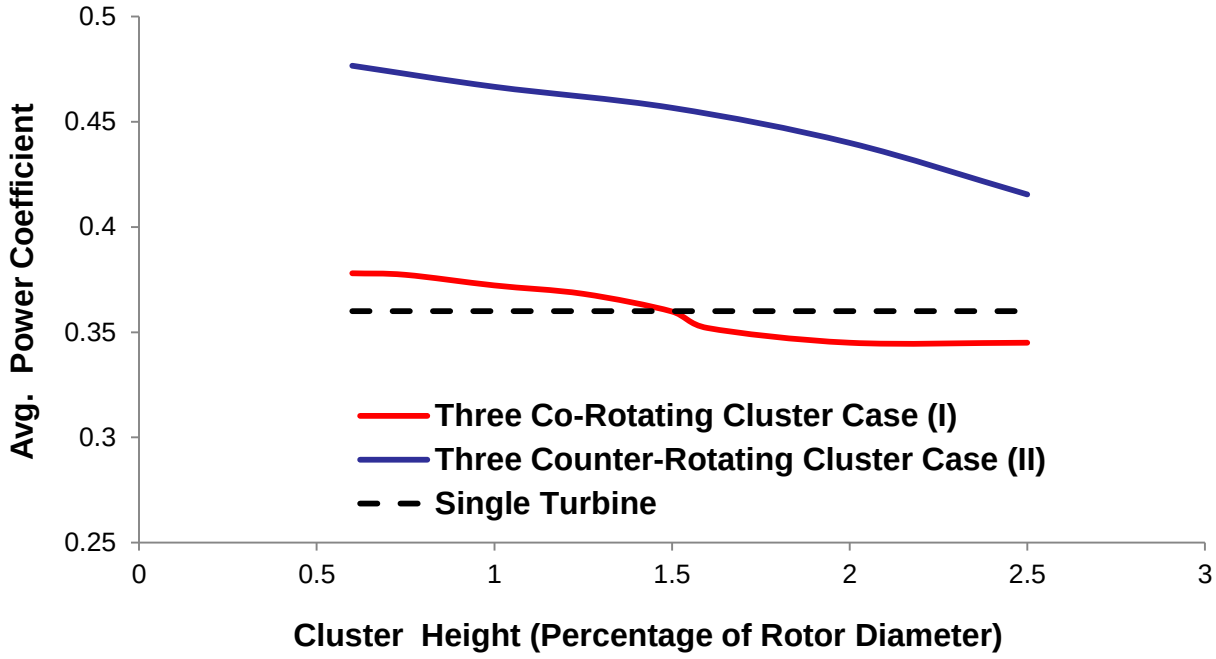
Cp_{max} = 0.47 at 0.6D

30% higher than isolated turbines





Comparison between Counter-Rotating (Hybrid) and Co-Rotating Triangular Darrieus Three Turbine Clusters

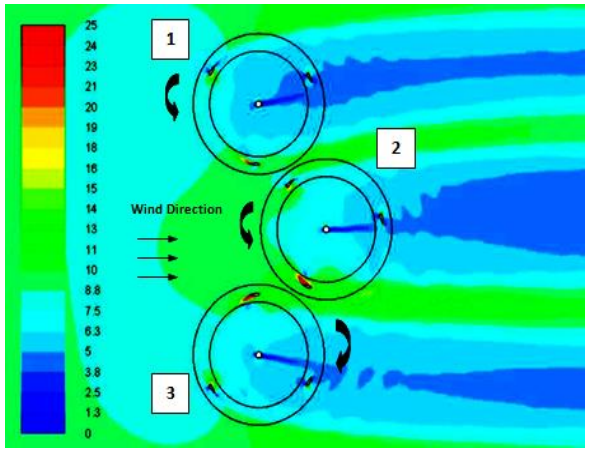


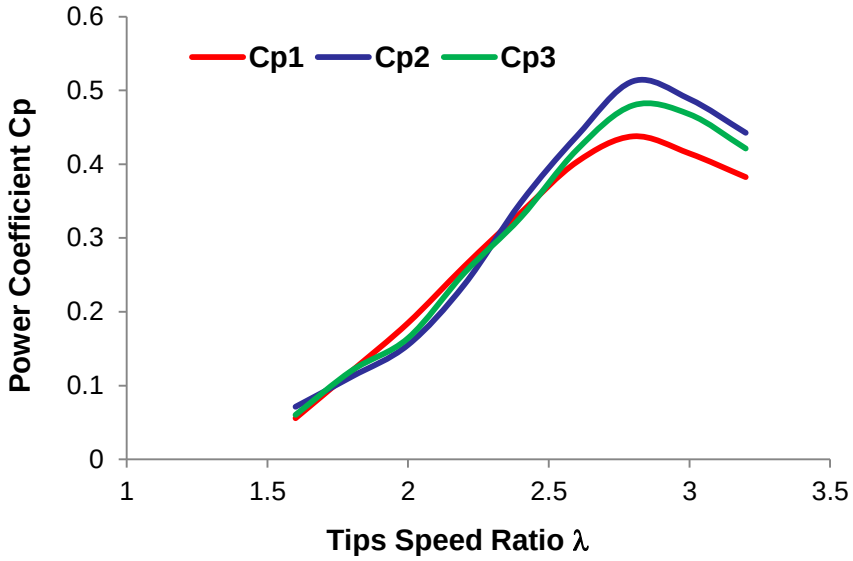
The counter rotating cluster (II) is the most efficient triangular cluster to be used as a building unit for an efficient triangular Darrieus wind turbine farm

The efficient cluster (II) height is 0.6D and base 2D with an average power coefficient of 0.47, this represents an enhancement of 30% compared to a isolated turbines.

The ratio between the power coefficients of the three turbines (1), (2) and (3) is 1 : 1.1 : 1

Hybrid Three Turbine Cluster (II) Performance Confirmation





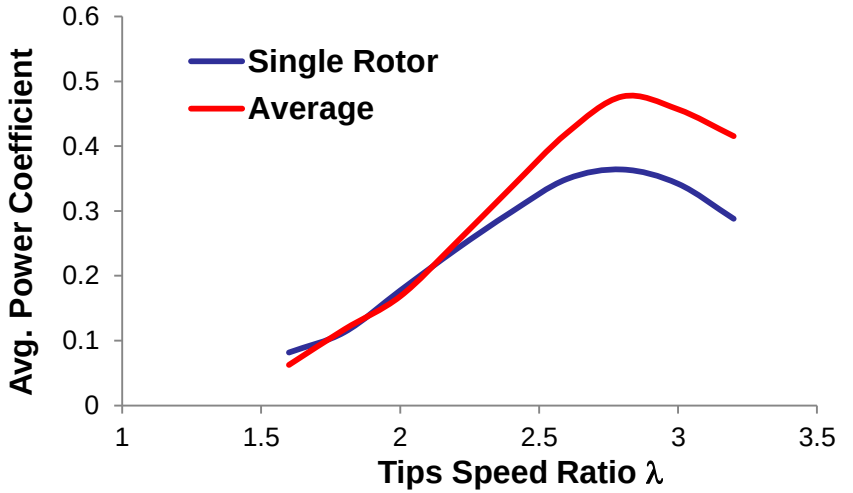
To **confirm** the enhancement, the cluster is simulated at **different tip speed ratios**

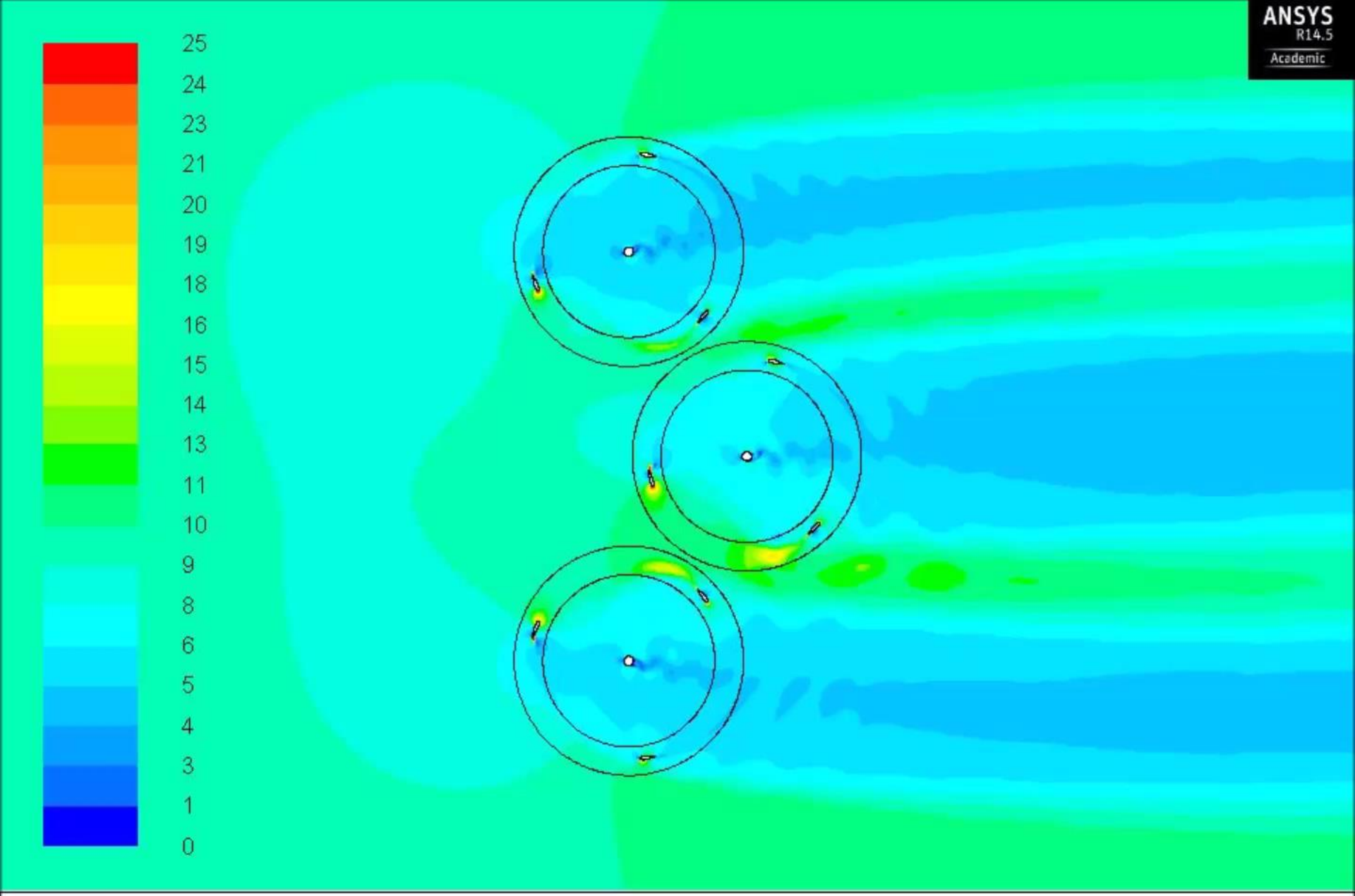
The **ratio** between the **power coefficients** of its three rotors (1),(2) and (3) is approximately **1:1.1:1** respectively

The results show that the **ratio 1:1.1:1** between the power coefficients of the three rotors is consistent for **λ>2.4**

The **developed** three turbine cluster is **30% higher** than three **isolated** turbines, and has **4 times** their **power density**

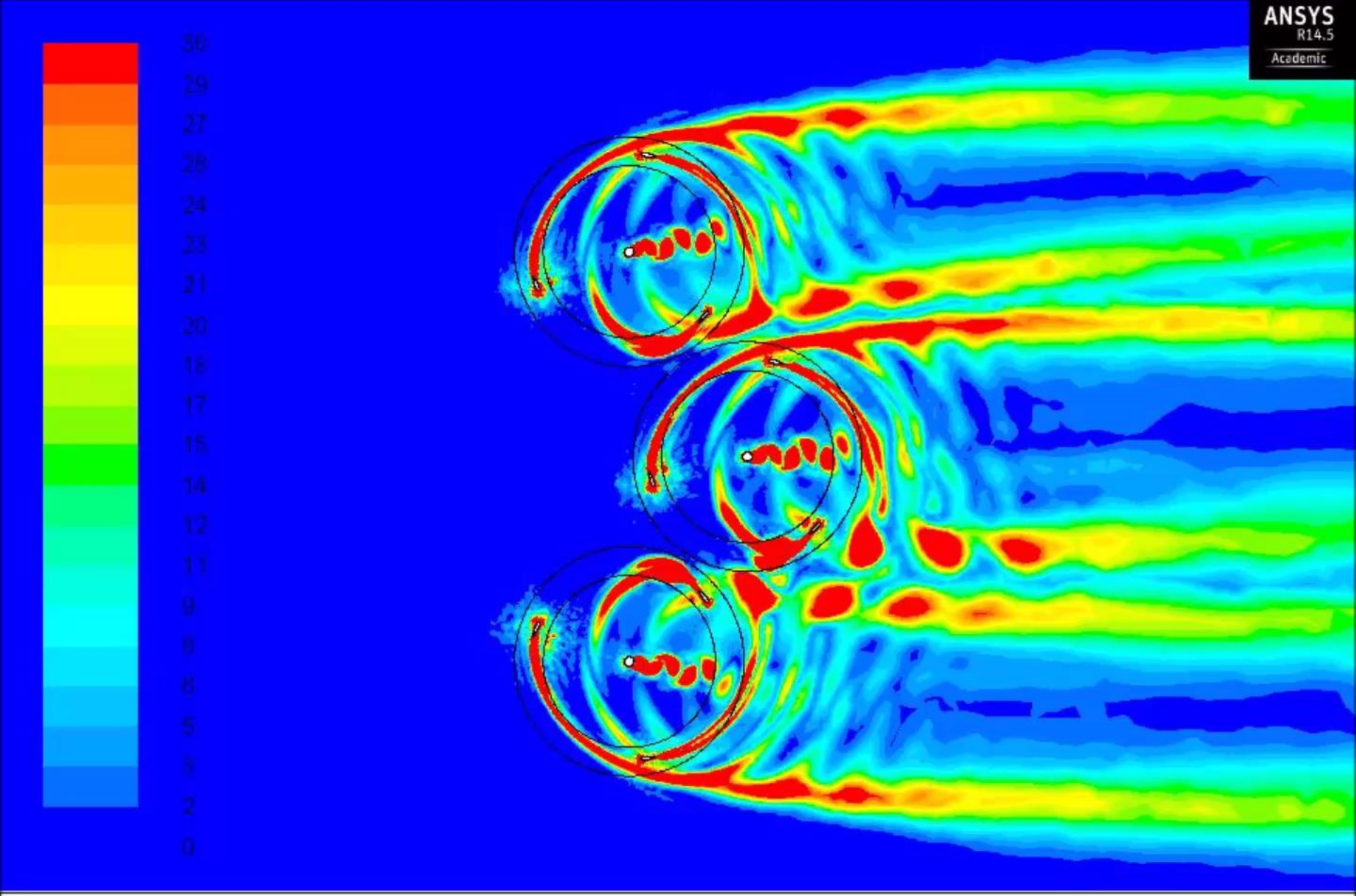
At λ=2.8, Cp_{avg} =0.47





Contours of Velocity Magnitude (m/s) (Time=1.0982e+00)

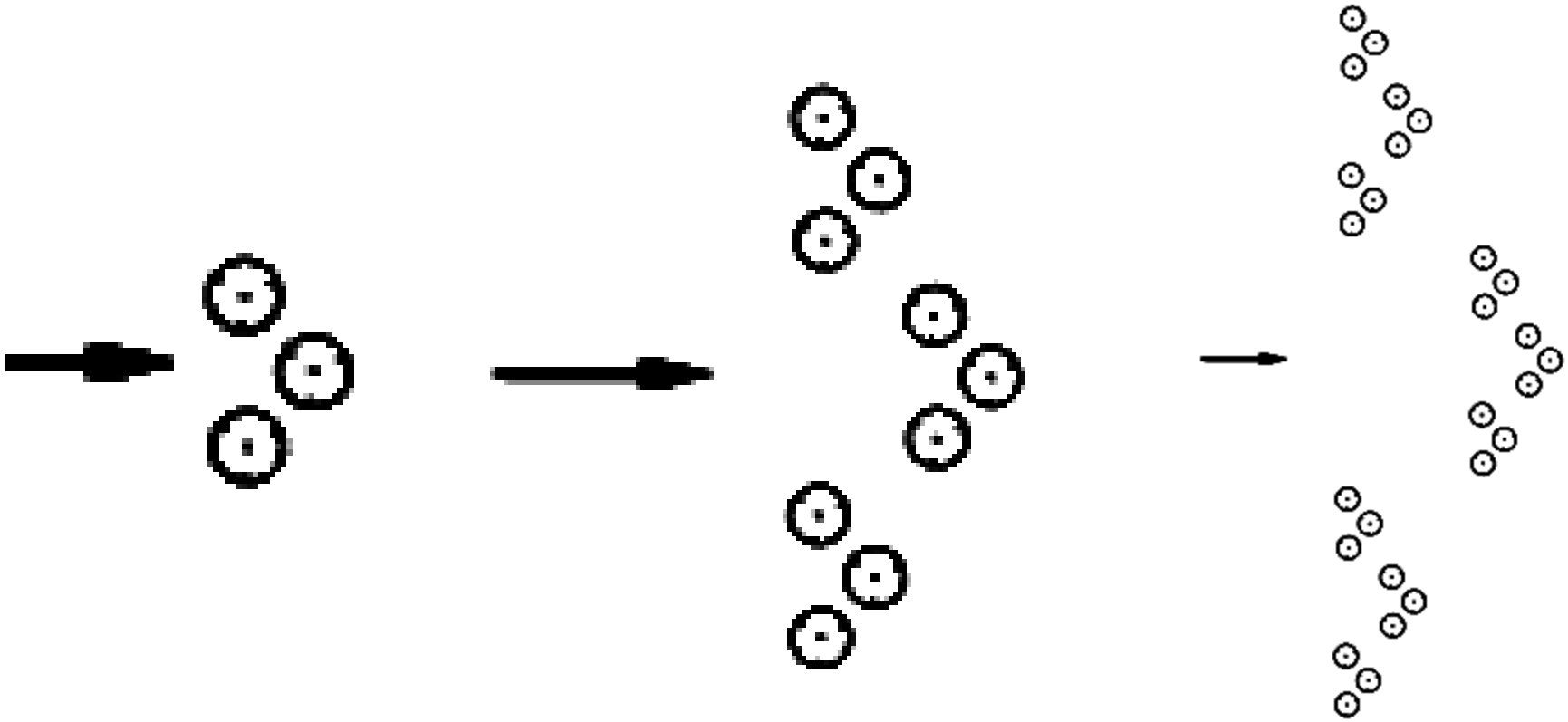
May 13, 2015
ANSYS Fluent 14.5 (2d, pbns, trans-sst, transient)



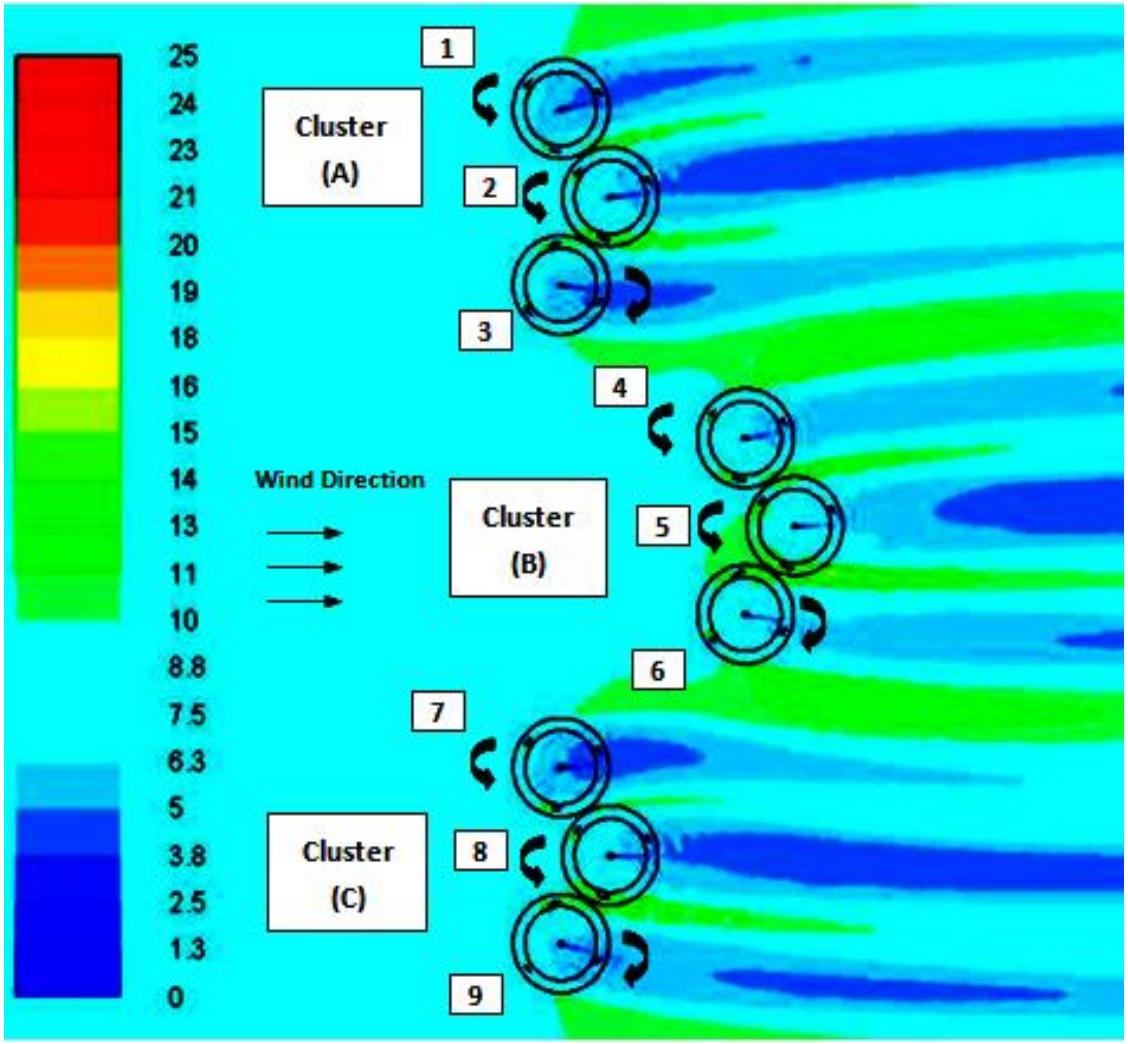
Contours of Vorticity Magnitude (1/s) (Time=1.0982e+00)

May 13, 2015
ANSYS Fluent 14.5 (2d, pbns, trans-sst, transient)

Patterned Savonius Wind Turbine Farms



Nine Darrieus Vertical Axis Wind Turbine Farm

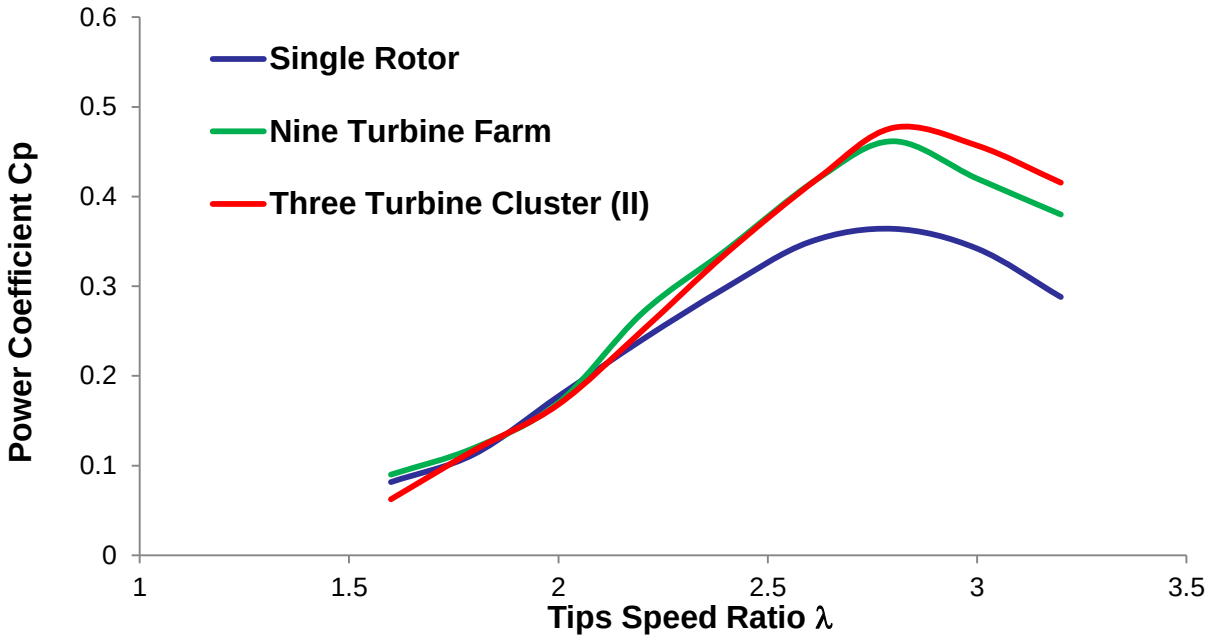


The three Darrieus turbine cluster (II) is used as a building unit for efficient Darrieus VAWT farms having the same topology of the cluster

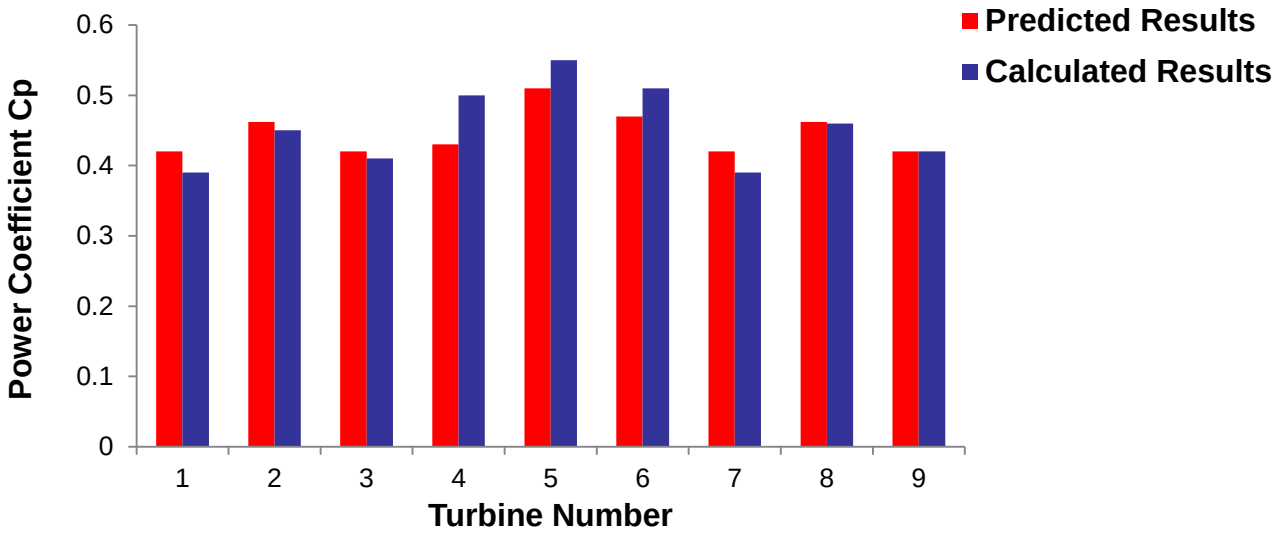
The same grid topology of the three turbine cluster is used, this results in 1,304,115 cells and computation time in 100 hrs for each tip speed ratio

The **ratio** between the **power coefficients** of the clusters (A),(B) and (C) is approximately **1:1.1:1** respectively

The **ratio** between the **power coefficients** of the three turbines in each cluster is approximately **1:1.1:1**



The maximum average power coefficient of the developed nine turbine farm is 0.46 which is 28% higher than that of isolated nine turbine farm



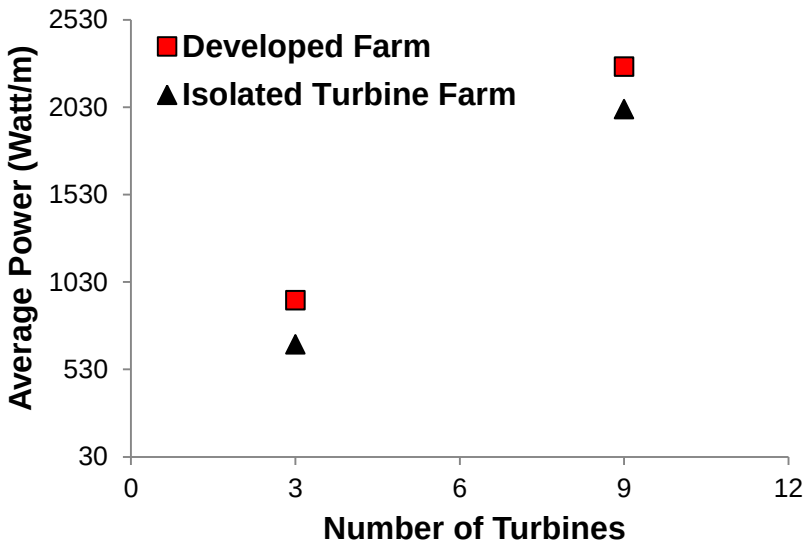
The nine turbine farm is patterned, this means that the performance of the farm can be predicted by simulation of only three turbines.

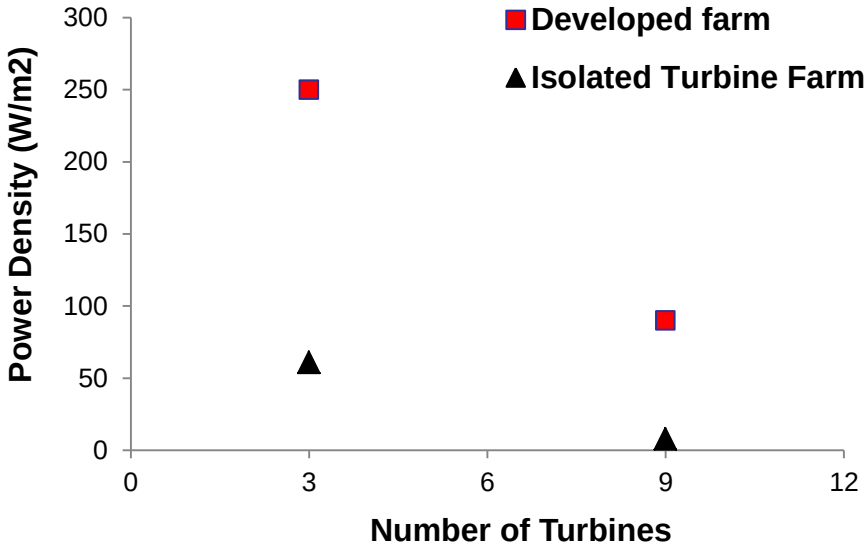
Using the ratio 1:1.1:1 and the results of the simulation of the three turbine cluster, the nine turbine farm efficiency is predicted and compared to the calculated results.

The error in the predicted average power coefficient (Cp=0.446) of the farm compared to the calculated value (Cp=0.453) is less than 2%

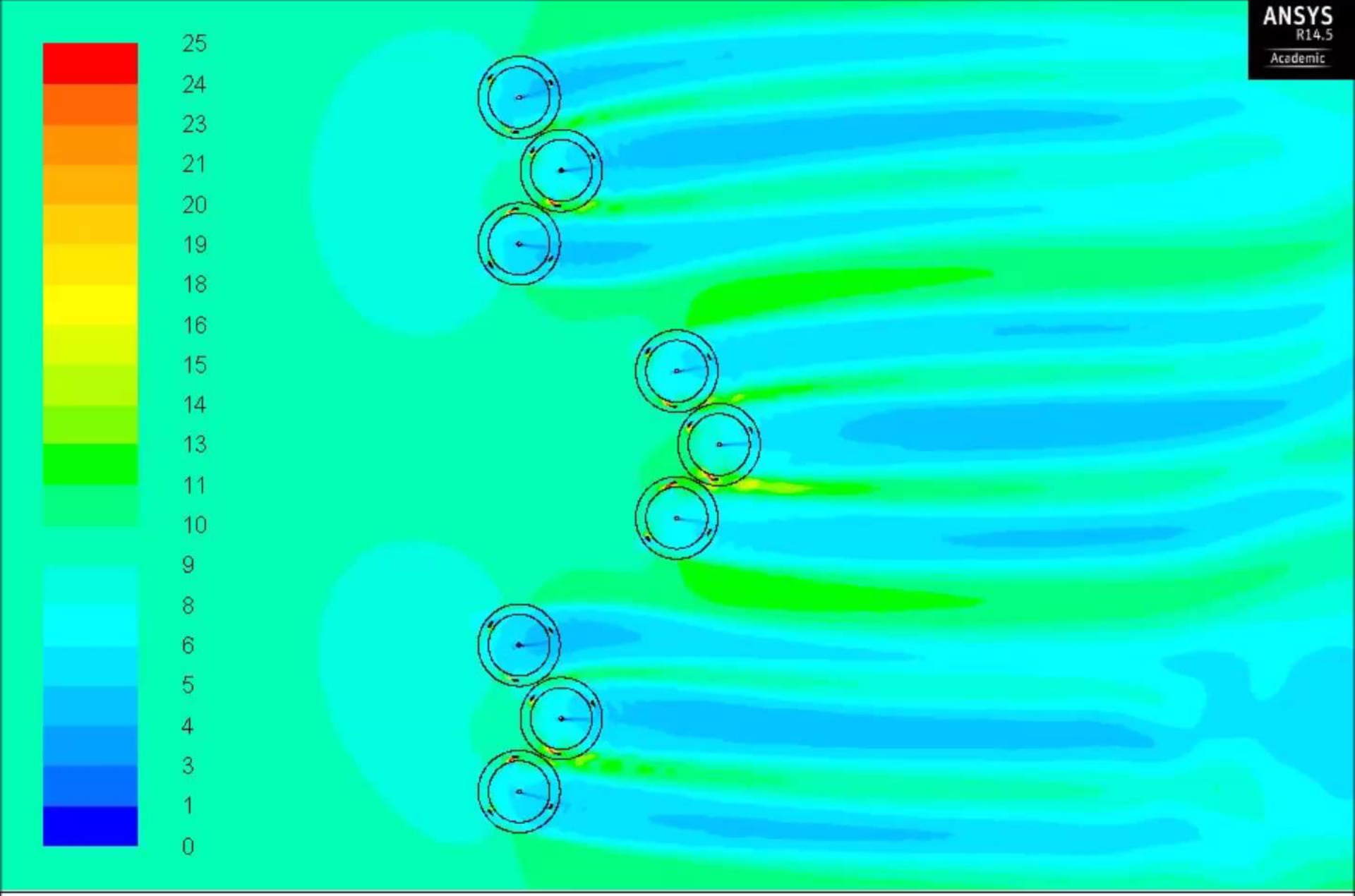
The power ratio is used to predict the performance of larger farms with the same topology to save processing time and man power

Power and Power Density of the Developed VS Isolated Farms



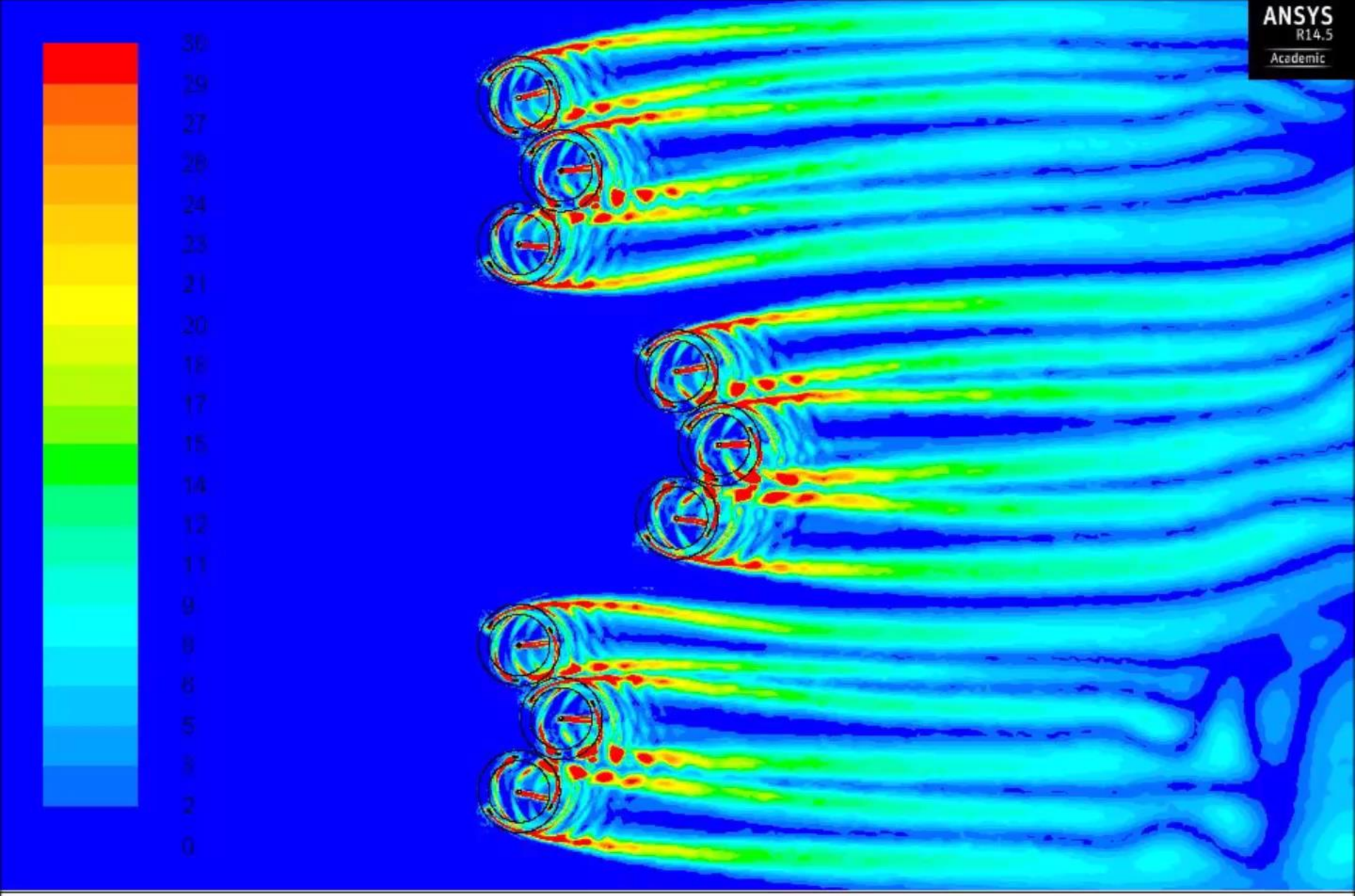


	Power (watt)		Enhancement In Efficiency	Power Density (watt/m^2)		Enhancement In Power Density
	Developed	Isolated		Developed	Isolated	
3 Turbines	926	702	30%	248	61	4 times
9 Turbines	2711	2017	28%	108	8	13 times



Contours of Velocity Magnitude (m/s) (Time=2.0577e+00)

May 13, 2015
ANSYS Fluent 14.5 (2d, pbns, trans-sst, transient)



Contours of Vorticity Magnitude (1/s) (Time=2.0577e+00)

May 13, 2015
ANSYS Fluent 14.5 (2d, pbns, trans-sst, transient)

Summary of Savonius Turbine Clusters
(Single Turbine Cp= 0.23 at λ=1)

	Co-Rotating				Counter-Rotating					Farms	
	Two Turbines			Three Turbines	Two Turbines				Three Turbines	Nine Turbines	27 Turbines
	Parallel	Oblique			Parallel		Oblique				
		Case A	Case B		Case A	Case B	Case C	Case D			
Cp	0.3	0.26	0.32	0.29	0.26	0.3	0.35	0.25	0.3	0.3	0.32
Gap Distance	0.2D	1.0D	0.2D	2.2D	0.8D	0.8D	0.4D	1.6D	2.2D		

Summary of Darrieus Turbine Clusters
(Single Turbine Cp= 0.36 at λ=2.8)

	Co-Rotating				Counter-Rotating					
	Two Turbines			Three Turbines	Two Turbines				Three Turbines	Nine Turbines
	Parallel	Oblique			Parallel		Oblique			
		Case A	Case B		Case C	Case D	Case E	Case F		
Cp	0.41	0.35	0.37	0.37	0.42	0.4	0.4	0.39	0.47	0.46
Gap Distance	0.5D	0.5D	0.5D	0.5D	0.5D	0.5D	0.5D	0.5D	0.5D	

Conclusion

- **Multiple Vertical axis wind Turbines arranged in closely configuration show enhancement in their performance compared to their isolated counter parts.**

- **The close arrangement enables to construct farms of higher power densities compared to conventional aligned isolated farms**

- **Two types of VAWTS are numerically studied:**
  Savonius and Darrieus turbines

- **The enhanced performance is numerically studied for two parallel and oblique co-rotating and counter rotating configurations**

- **The numerical results are used to develop an efficient triangular three turbine cluster**

- **The performance of the Savonius three Turbine cluster is higher than three isolated turbines by 26% , and its power density is 1.5 times the isolated turbines at λ=1**

- **The performance of the Darrieus three Turbine cluster is higher than three isolated turbines by 30% , and its power density is 4 times the isolated turbines at λ=2.8**

- **The clusters performance is confirmed at different tip speed ratios, and the power ratio between the turbines is 1:1.2:1 for the Savonius cluster and 1:1.1:1 for the Darrieus cluster**

- **The efficient three turbine clusters are used to build efficient patterned Vertical axis wind turbine farms having the same geometric topology of the cluster and the same power ratio enhancement**

- **The pattern is confirmed by solving 9 and 27 Savonius turbine farms and a 9 turbine Darrieus farm**

- **The developed farms are patterned and have the same power ratios of the three turbine clusters**

- **The power density of the Savonius nine turbine farm is about 7 times a nine isolated turbine farm, and the power density of the twenty-seven turbine farm is 4 times a twenty-seven isolated turbine farm**

- **The power density of the Darrieus nine turbine farm is more than 13 times a nine isolated turbine farm**

- **The advantage of the patterned farm appears is the power ratio achieved by the clusters and confirmed by the farms**

- **This power ratio is used to predict the performance of larger farms with the same topology to save processing time and man power**

- **The developed farms have smaller structure size, wind farm signature, material and manufacturing costs than conventional HAWTs**

- **The developed farms are simpler in logistics of installation, operation and maintenance**

- **The developed farms are safer for birds, produce lower noise, and have a lower impact on radar signals**

- **A preliminary analysis of the mean velocity field around the turbine blades at different tip speed ratios shows a velocity distribution close to the structure of a Rankine vortex**

- **A future work will be considered for numerical modeling of the Darrieus turbine as a combination of the free stream with a Rankine vortex.**

- **The solution of adjacent vortices can be used to determine the performance of closely oriented Darrieus turbines and represented a farm by a group of vortices**


Thank you!
Questions

Publications

Published Journal Papers:

- M. Shaheen , M. El-Sayed, and Shaaban Abdallah, "**Numerical Study of Two-Bucket Savonius Wind Turbine Cluster**" Journal of Wind Engineering & Industrial Aerodynamics.

Reviewers Comments:

In fact, the reviewer acknowledges the authors for doing very well in the manuscript.

Without any doubt, the authors tackle a highly interesting problem in the field of VAWTs and the numerical approach sounds extremely inviting.

It is my impression that this is a well written paper and is of a quality/standard worth publishing

Bending Journal and Conference Papers

- M. Shaheen and Shaaban Abdallah, “Efficient Clusters and Patterned Farms for Darrieus Wind Turbines ,” Journal of Renewable Energy
- M. Shaheen and Shaaban Abdallah, “ Development of Efficient Savonius Vertical Axis Wind Turbine Clustered Farms ,” Journal of Sustainable Energy
- M. Shaheen and Shaaban Abdallah, “A Numerical Comparison Study between Co-Rotating and Counter-Rotating Savonius Wind Turbine Clusters ” 3rd International Conference and Exhibition on Mechanical & Aerospace Engineering 2015, US, Los Angeles

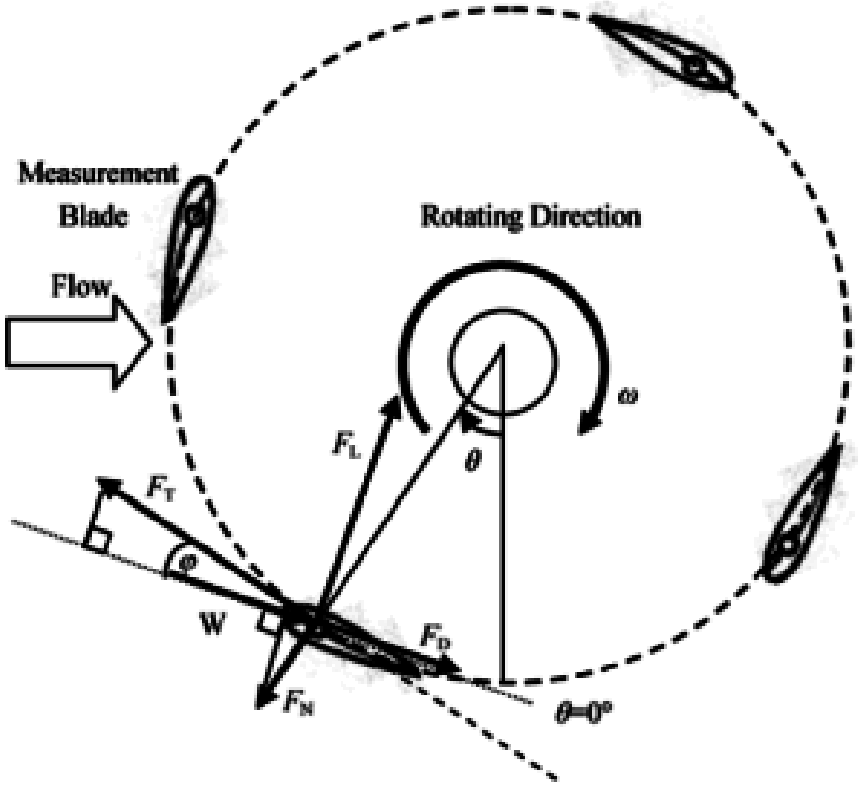
Poster Presentation:

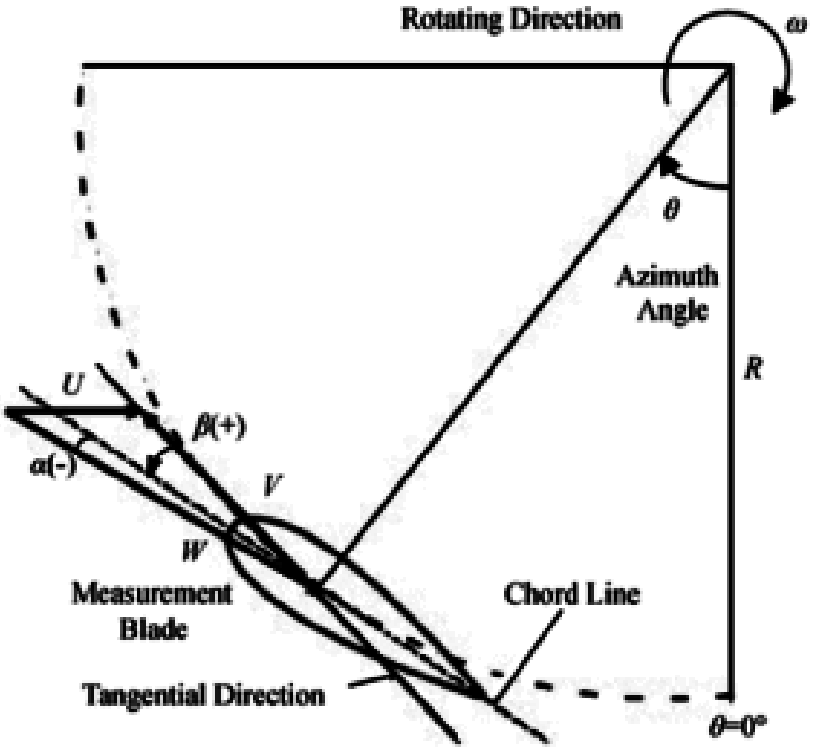
- M. Shaheen , M. El-Sayed, and Shaaban Abdallah, “**Numerical Study of Two-Bucket Savonius Wind Turbine Cluster**,” 2nd International Conference and Exhibition on Mechanical & Aerospace Engineering. September 08-10, 2014 Philadelphia, USA
- M. Shaheen , and Shaaban Abdallah, “ **A Novel Clustered and Patterned Vertical axis Wind Turbine Farm** ,” Graduate Student Expo & Poster Forum 2015, University of Cincinnati.

Under Construction

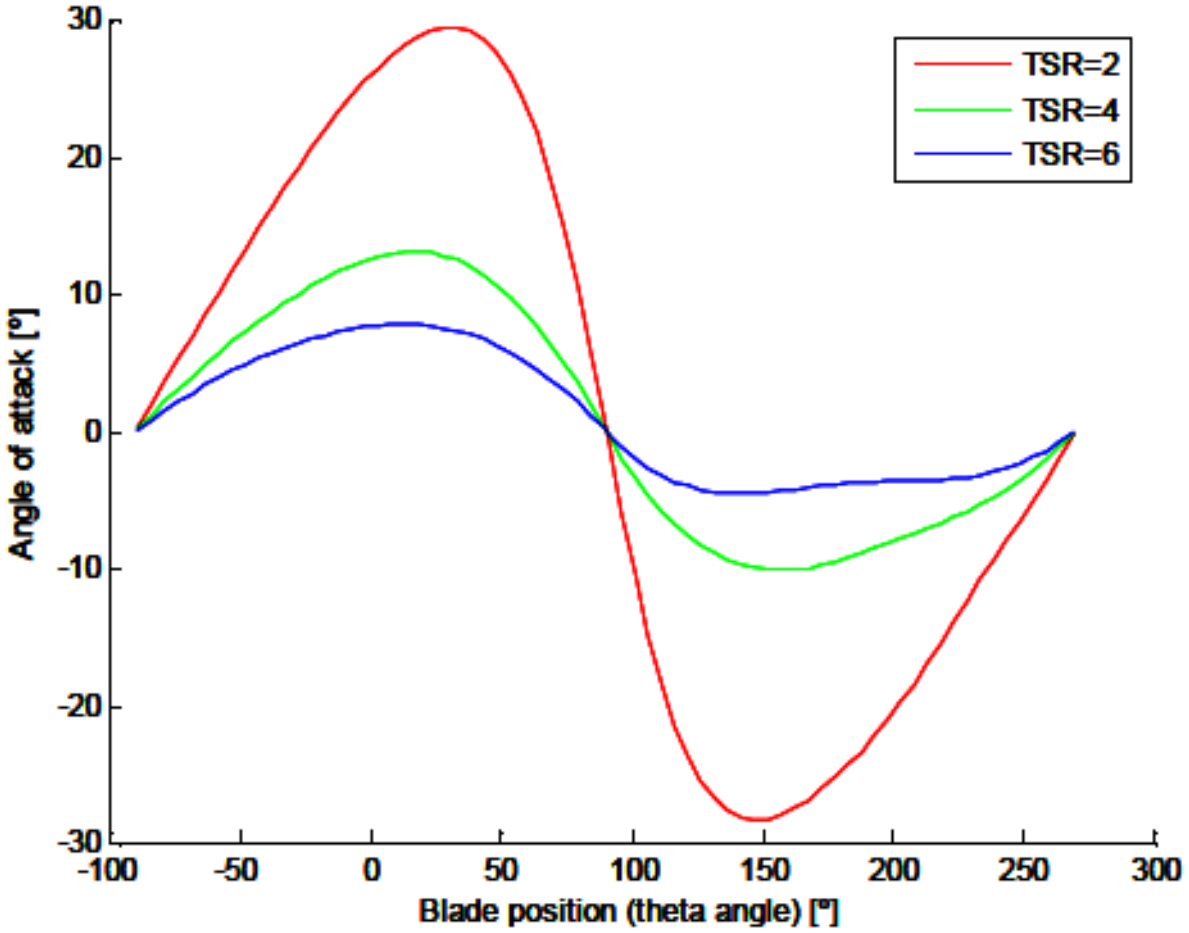
- “ **Physical Insights for vortex modeling of Darrieus Vertical Axis Wind Turbines**”

Force Analysis on Darrieus Turbine

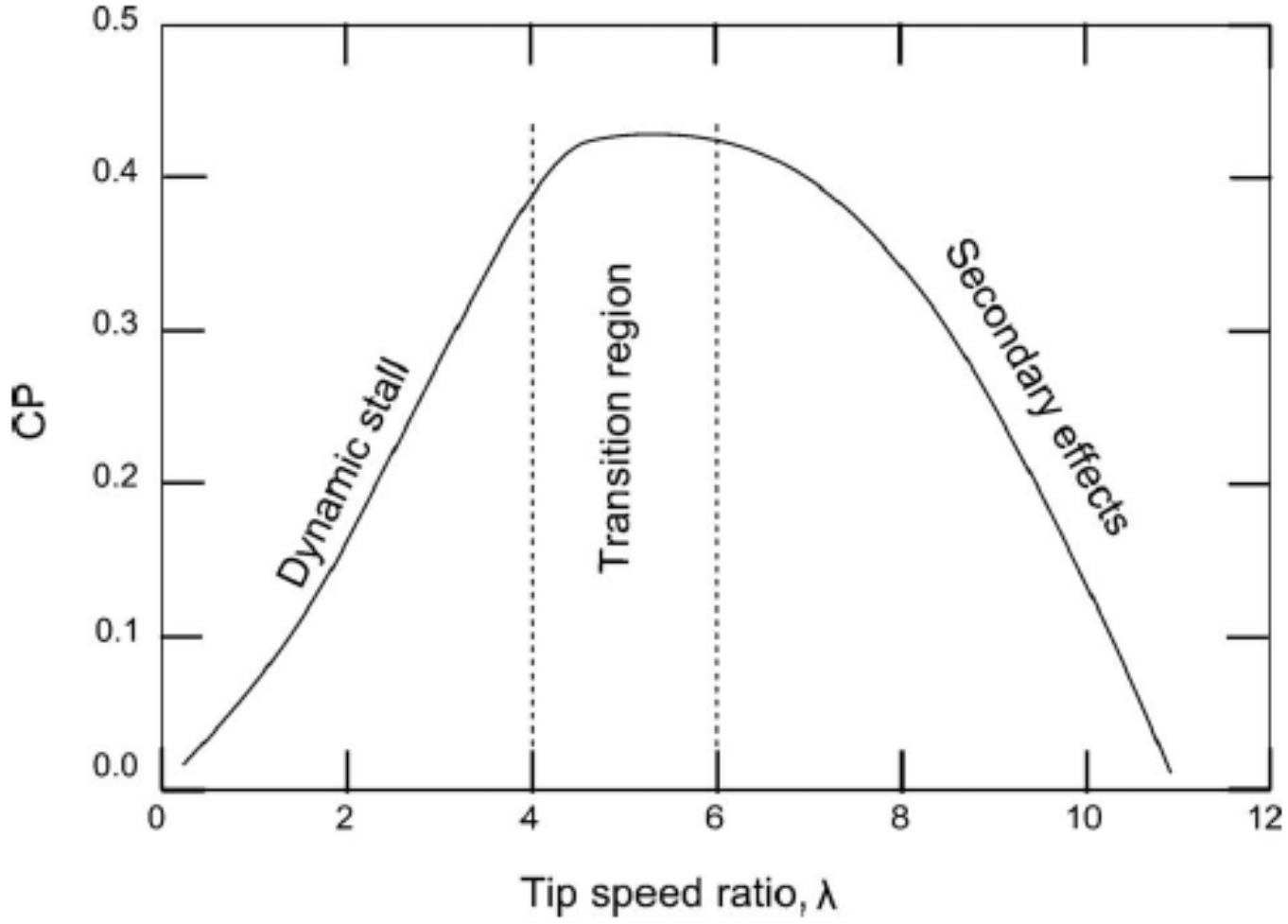




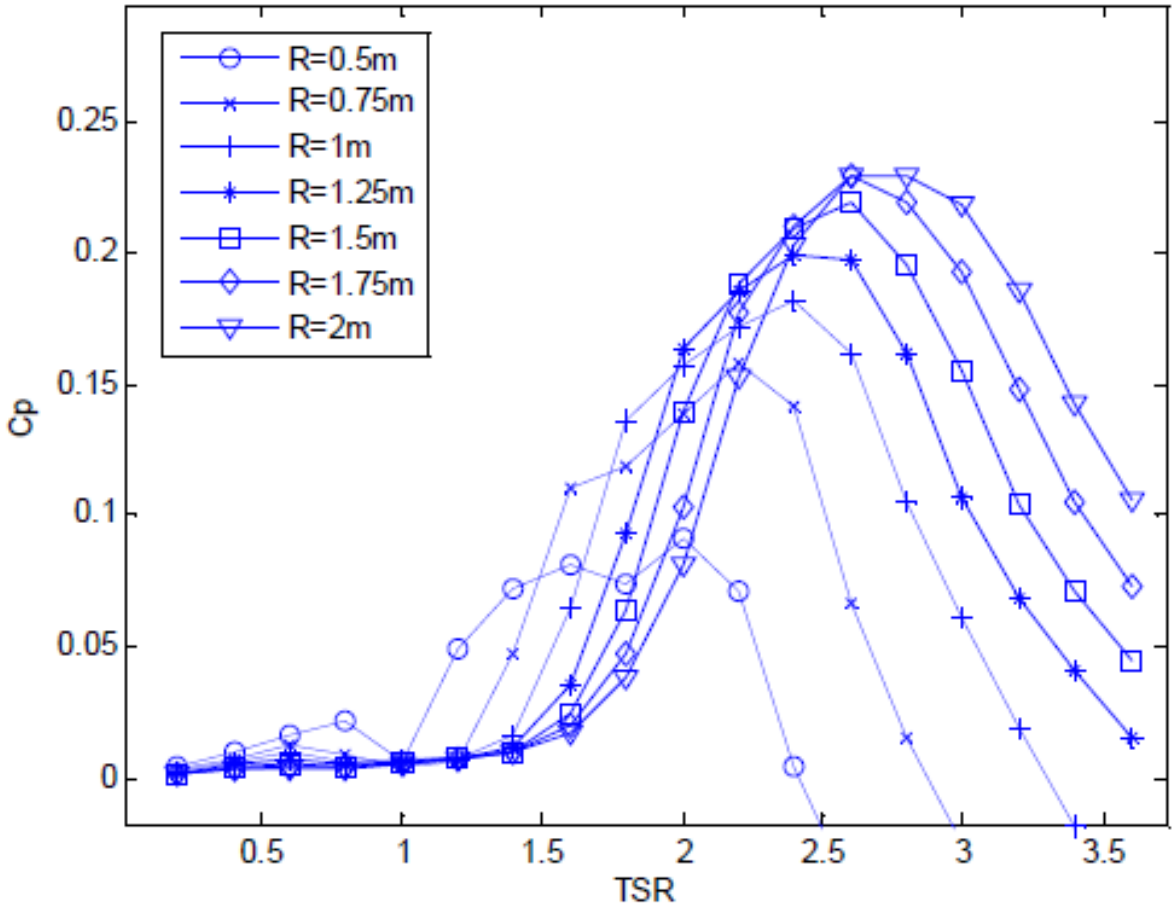
Variation in Angle of Attack Vs Tip Speed Ratio



Transition in VAWTs

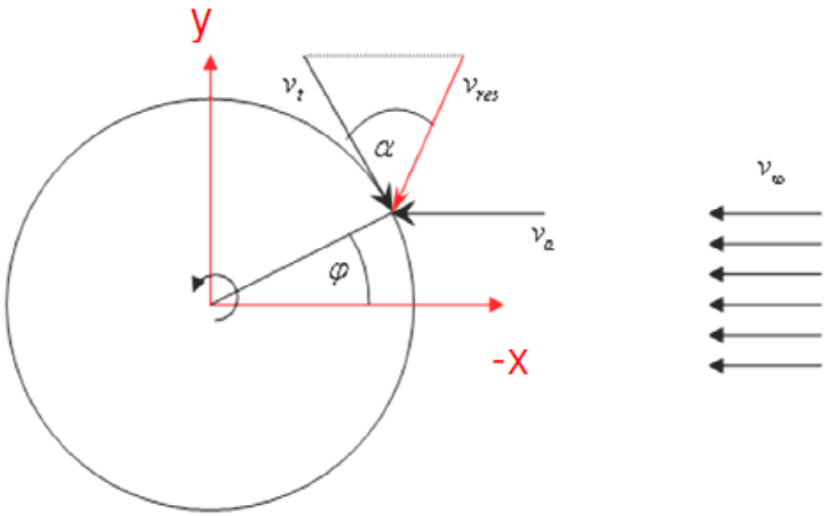


Effect of Turbine Radius on The Power Coefficient



At low tip speed ratios there is no effect for the turbine radius on the Power Coefficient

Induced Speed Vs Azimuth Angle



The induced wind speed v_a is given by

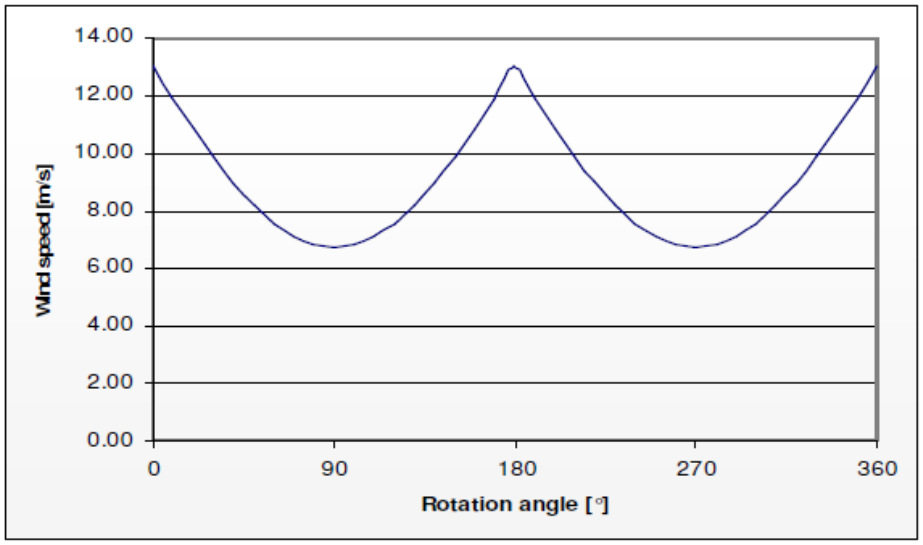
$$v_a = v_\infty (1 - a)$$

with the reduction factor

$$a = X \cdot \frac{r \cdot \omega_{rated}}{v_\infty} |\sin(\varphi)|$$

and the Wilson-Factor

$$X = \frac{B \cdot c}{2r}$$



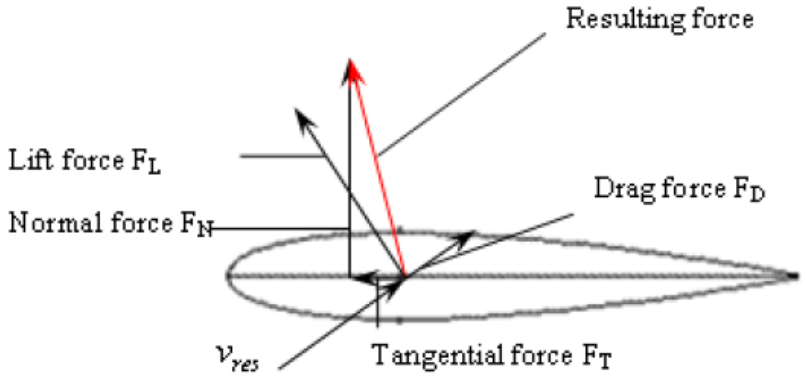
The lift (F_L) and the drag (F_D) force are given by:

$$F_L = C_L \cdot \frac{\rho}{2} \cdot v_{res}^{\ 2} \cdot A_{bl}$$

$$F_D = C_D \cdot \frac{\rho}{2} \cdot v_{res}^{\ 2} \cdot A_{bl}$$

$$F_N = F_L \cdot \cos(\alpha) + F_D \cdot \sin(\alpha)$$

$$F_T = F_L \cdot \sin(\alpha) - F_D \cdot \cos(\alpha)$$



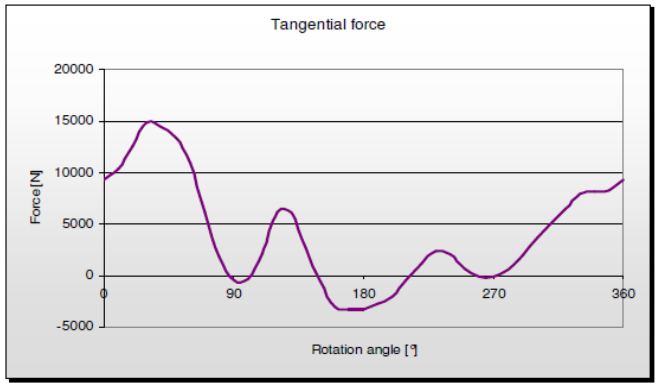


Fig 4: Tangential force vs. rotation angle

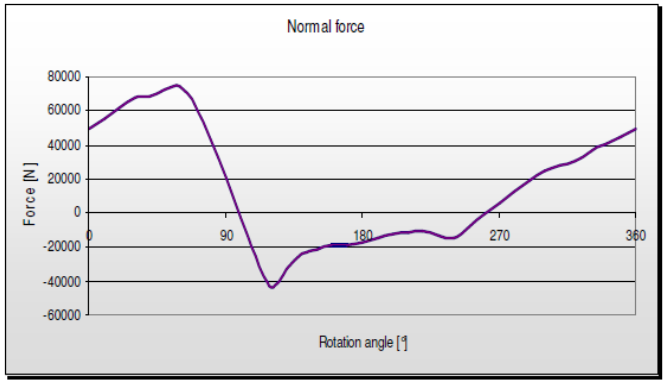


Fig 5: Normal force vs. rotation angle

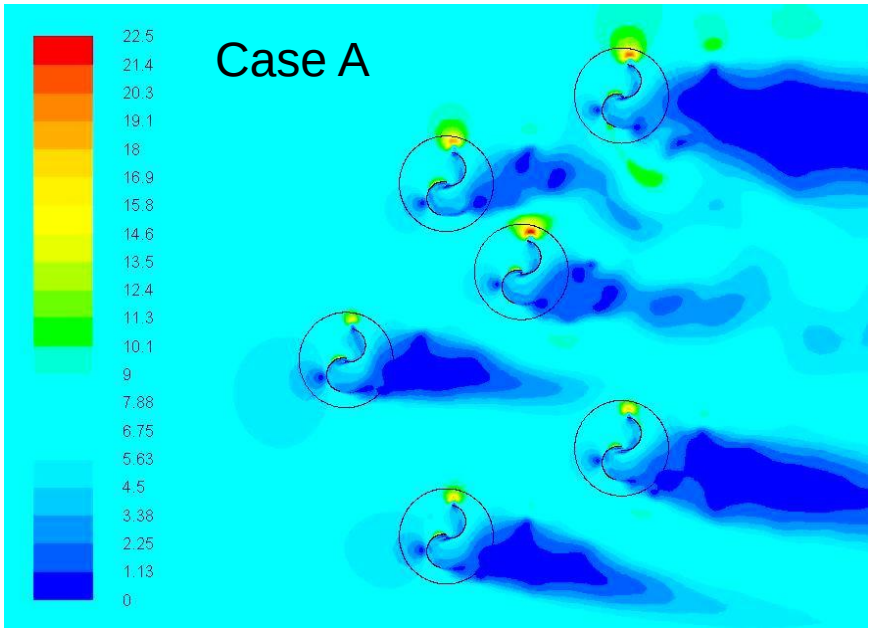
Why the Savonius turbine cannot be modeled with simple momentum theory

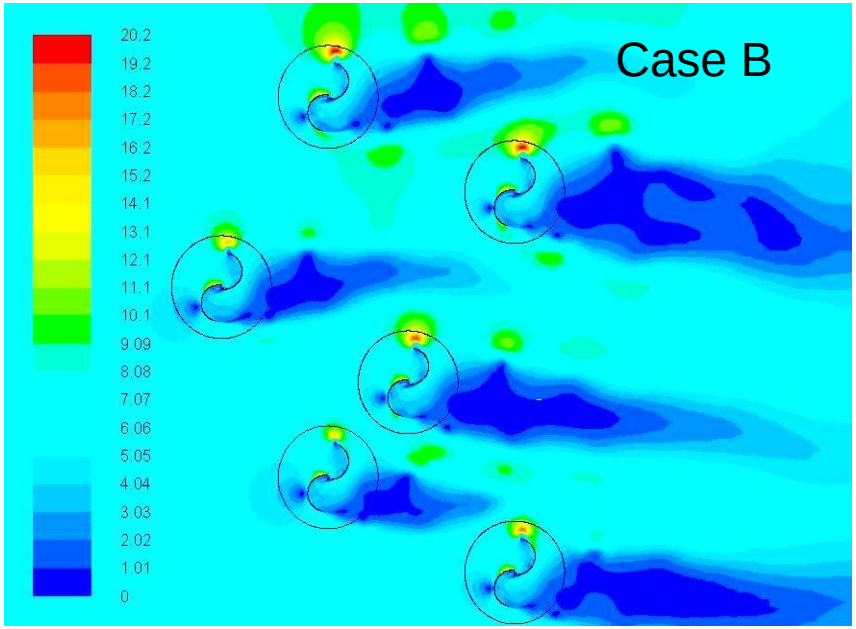
The performance of a single Savonius turbine utilizes the interactive flow between the two blades:

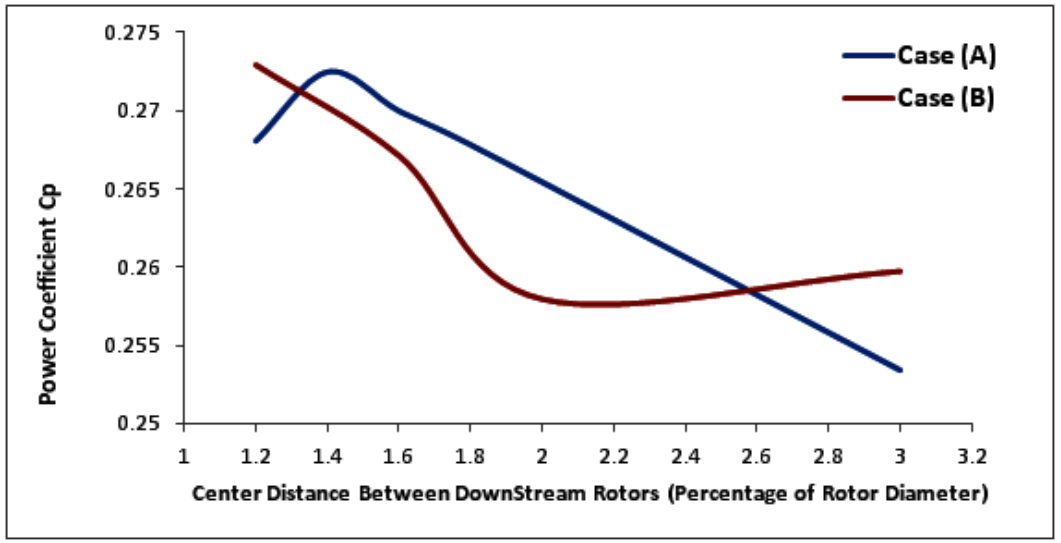
1) The flow attachment to the convex surface of the advancing blade produces a low-pressure region above it to pull the blade in torque-adding direction, i.e. the lift effect at a low tip-speed ratio

3) A large vortex is slowly shed behind the returning blade, which produces low-pressure downstream of the advancing blade.

Second Row


Case A
22.5
21.4
20.3
19.1
18
16.9
15.8
14.6
13.5
12.4
11.3
10.1
9
7.88
6.75
5.63
4.5
3.38
2.25
1.13
0


Case B
20.2
19.2
18.2
17.2
16.2
15.2
14.1
13.1
12.1
11.1
10.1
9.09
8.08
7.07
6.06
5.05
4.04
3.03
2.02
1.01
0


Case (A)
Case (B)
Power Coefficient Cp
0.275
0.27
0.265
0.26
0.255
0.25
1
1.2
1.4
1.6
1.8
2
2.2
2.4
2.6
2.8
3
3.2
Center Distance Between DownStream Rotors (Percentage of Rotor Diameter)

Vorticity equation

$$\frac{D\vec{\omega}}{Dt} = \frac{\partial\vec{\omega}}{\partial t} + (\vec{u}\cdot\nabla)\vec{\omega}$$

The circulation around a closed contour is given by

$$\Gamma = \oint_C \vec{U} \cdot \vec{dl} \, .$$

The lift per unit span is related to the circulation by the Kutta-Joukowski theorem of lift,

$$L = \rho U_\infty \Gamma \, ,$$

2.2 Prandtl's Lifting Line Theory

According to the Prandtl lifting line theory [Von Mises, 1959], a finite wing may be represented by a single equivalent line of vorticity known as the "bound vortex," since it is in a sense bound to the wing. The strength of this vortex, $\Gamma(y)$, is related to the lift distribution along the wing by the Kutta-Joukowski relationship:

$$L(y) = \rho U \Gamma(y) \, . \qquad (2.3)$$

Two-dimensional flow equation

$$\frac{\partial u}{\partial t} + u\frac{\partial u}{\partial x} + v\frac{\partial u}{\partial y} = -\frac{1}{\rho}\frac{\partial p}{\partial x} + \nu\left(\frac{\partial^2 u}{\partial x^2} + \frac{\partial^2 u}{\partial y^2}\right),$$

$$\frac{\partial v}{\partial t} + u\frac{\partial v}{\partial x} + v\frac{\partial v}{\partial y} = -\frac{1}{\rho}\frac{\partial p}{\partial y} + \nu\left(\frac{\partial^2 v}{\partial x^2} + \frac{\partial^2 v}{\partial y^2}\right),$$

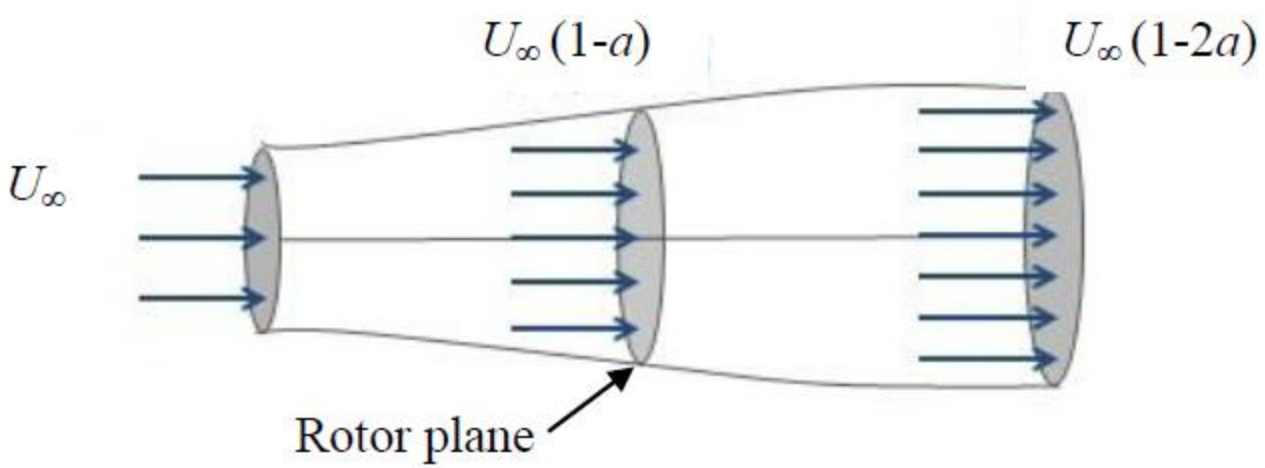
$$\frac{\partial u}{\partial x} + \frac{\partial v}{\partial y} = 0,$$

Axial Induction Factor

The fraction by which the axial component of velocity is reduced is known as the axial induction factor (a*).*

If the free stream velocity is U_∞ and the axial velocity at the rotor plane is U_1 , then the axial induction factor is,

$$a = \frac{U_\infty - U_1}{U_\infty}.$$



The power W extracted by the wind turbine is related to the axial induction factor (a):

$$\dot{W} = \frac{1}{2}\rho A U_\infty^{\,3} 4a(1-a)$$

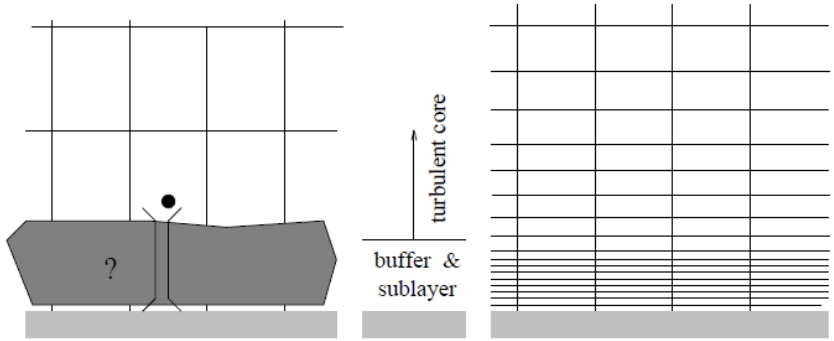
Tangential induction factor

The tangential induction factor (*a') which is due to rotation of the flow in the wake.*

$$a' = \frac{\omega}{2\Omega},$$

where *Ω is the angular speed of the rotor and ω is the angular velocity at which the wake rotates.*

Wall Functions vs. Near-Wall Model



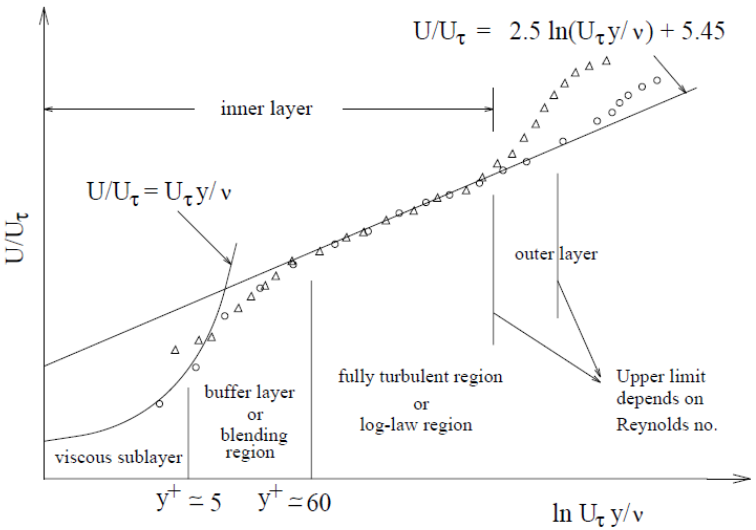
Wall Function Approach

- The viscosity-affected region is not resolved, instead is bridged by the wall functions.
- High-Re turbulence models can be used.

Near-Wall Model Approach

- The near-wall region is resolved all the way down to the wall.
- The turbulence models ought to be valid throughout the near-wall region.

$$y^+ \ (\equiv \rho u_\tau y/\mu)$$



Numerous experiments have shown that the near-wall region can be largely subdivided into three layers. In the innermost layer, called the “viscous sub-layer”, the flow is almost laminar, and the (molecular) viscosity plays a dominant role in momentum

“wall functions” are used to bridge the viscosity-affected region between the wall and the fully-turbulent region.

It is known that the log-law is valid for $y^+ > 30$ to 60.

Dimensionless wall distance (y plus)

$$y^+ \equiv \frac{u_* \, y}{\nu}$$

u_* friction velocity at the nearest wall

y the distance to the nearest wall

ν the local kinematic viscosity of the fluid

$$\mathrm{Re_x} = \frac{\rho U_\infty L}{\mu}$$

$$C_\mathrm{f} = \frac{0.026}{\mathrm{Re}_x{}^{1/7}}$$

$$\tau_\mathrm{wall} = \frac{C_f \rho {U_\infty}^2}{2}$$

$$U_\mathrm{fric} = \sqrt{\frac{\tau_\mathrm{wall}}{\rho}}$$

wall spacing $$\Delta s = \frac{y^+ \mu}{U_\mathrm{fric} \rho}$$

http://www.pointwise.com/yplus/

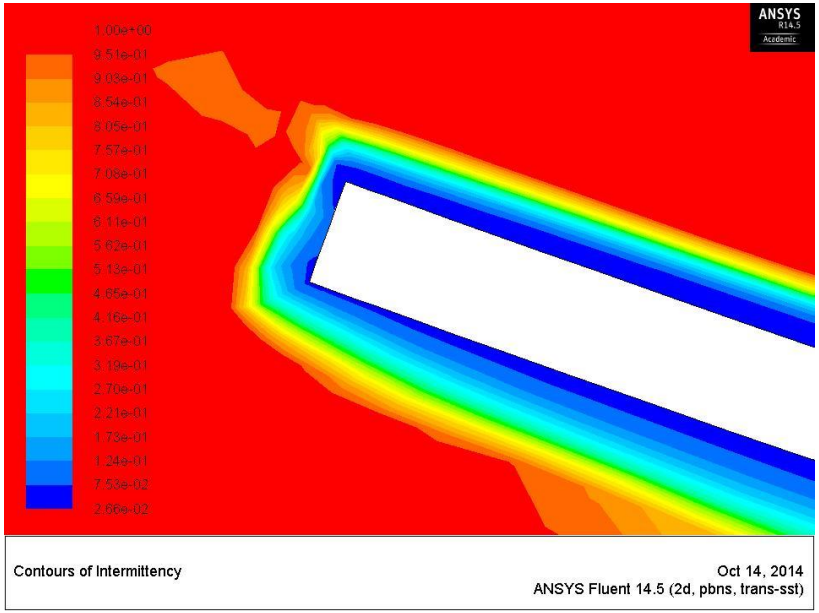
Intermittency Contours

For point surfaces, the value is interpolated from all the mesh nodes of the cell containing the point

$$t = \frac{500\,\mu}{\rho U^2}$$

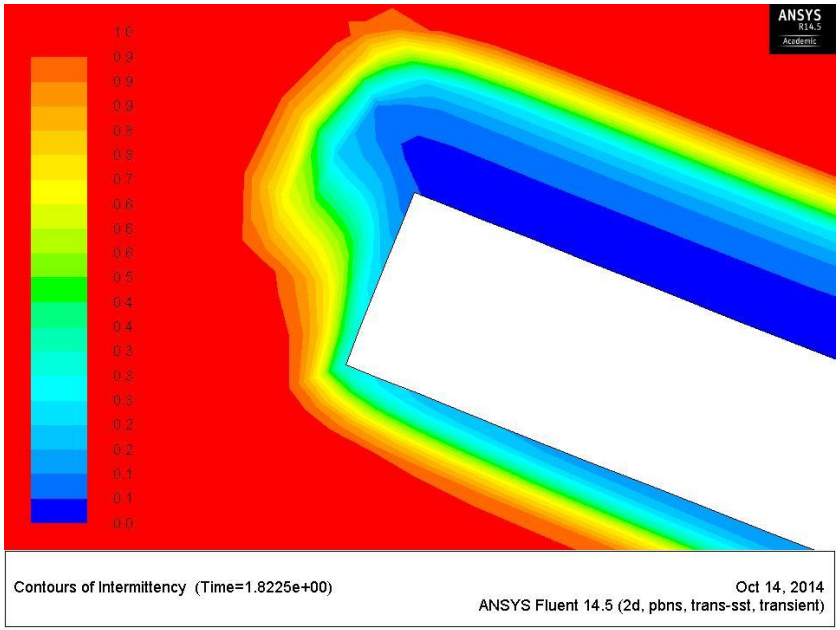
ANSYS Model based on Intermittency

- Intermittency: $\gamma = \dfrac{t_{turb}}{t_{lam} + t_{turb}}$
- Laminar flow: $\gamma = 0$
- Turbulent flow $\gamma = 1$
- Transition $0 < \gamma < 1$



static

Average Intermittency on the blades 0.9

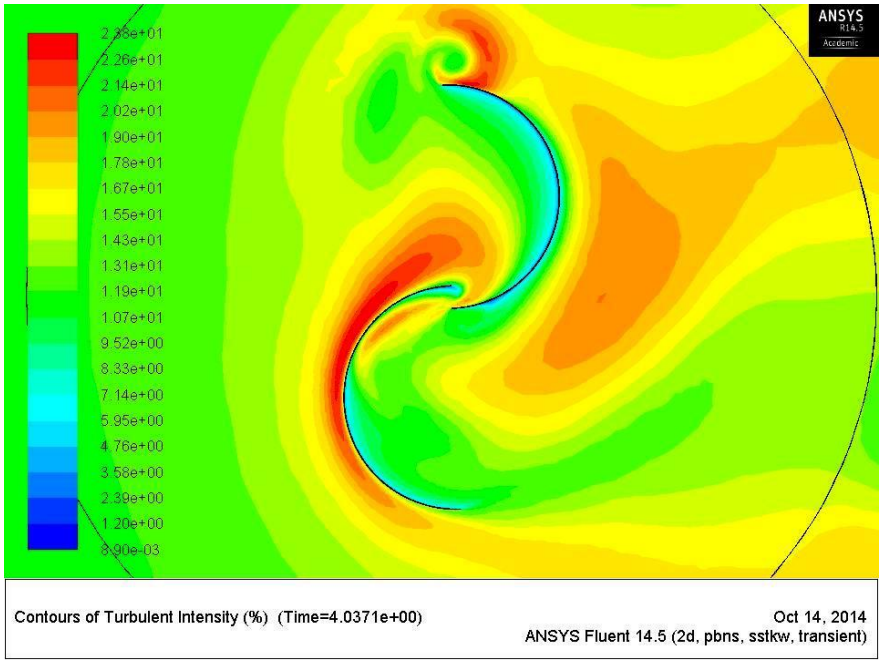


Rotating

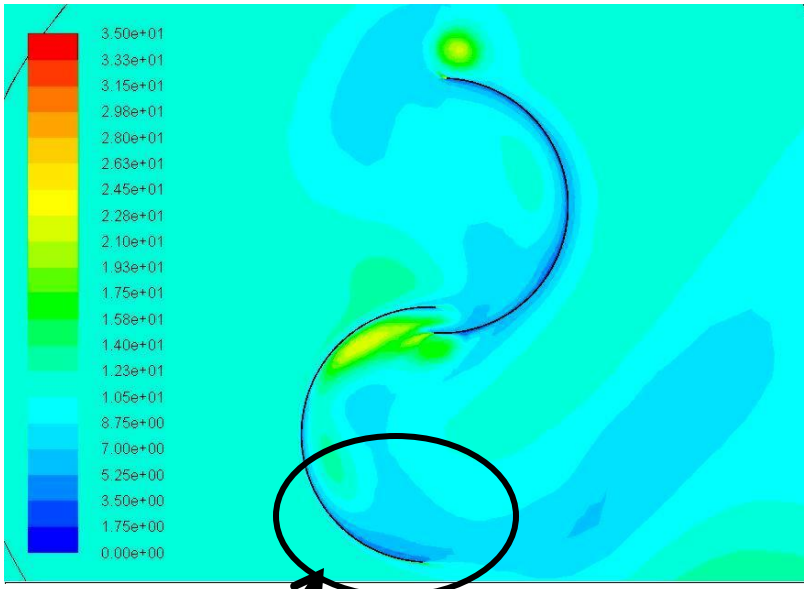
Average Intermittency on the blades 0.4

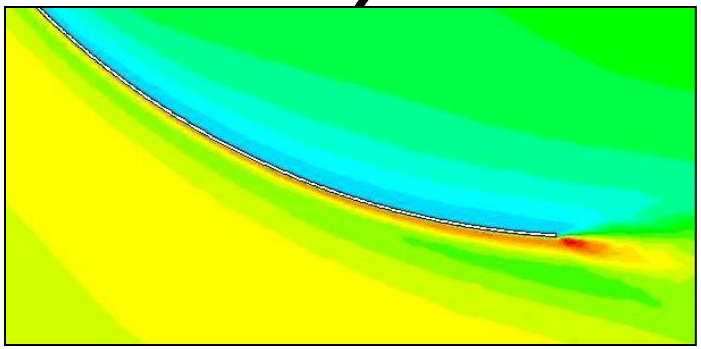
Contours of Turbulence Intensity

K-w (SST model) full turbulent



K-w (Trans SST model)

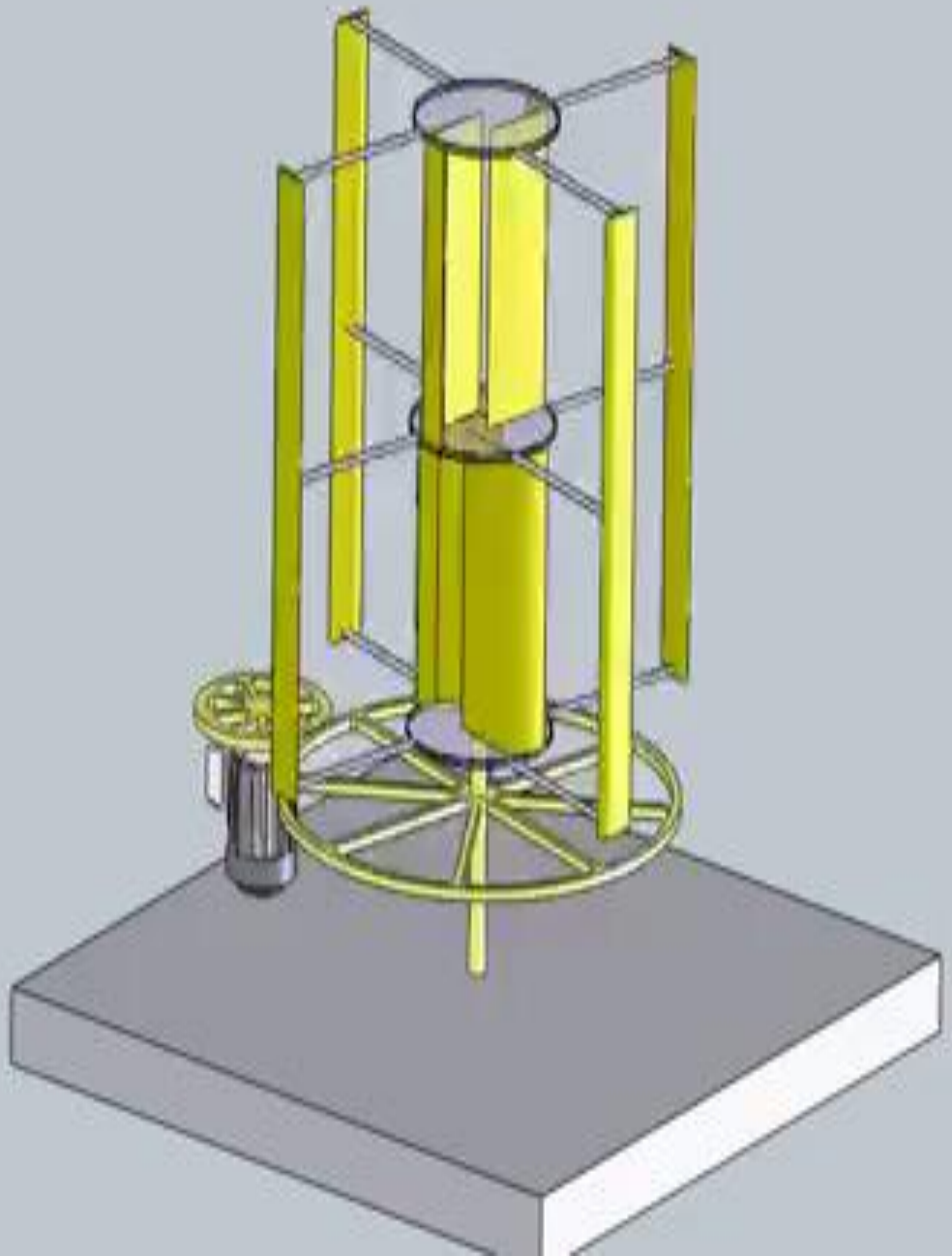




Magnification of Transition Position

WWW.TONCHEV.ORG

ROTOJET™




Power is generated from the wind or from the current, or from both.
Adaptable to meet varying metocean conditions.
3
2
A gearbox transmits the increased rotation to the Darrieus Wind Turbine.
No External power is required for startup.
The Savonius Current Turbine harnesses the energy produced by the ocean currents.
1

Experimental Data Correction

An object placed in a wind tunnel produces some "tunnel blockage"

This causes the local wind velocity in the test section to increase.

This increase has to be accounted for by determining a tunnel blockage factor (ε)

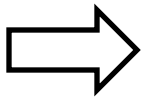
The total tunnel blockage correction be determined by applying the following equation:

$$\epsilon = \frac{1}{4} \frac{\text{Model frontal area}}{\text{Test section area}}$$

Pope, A. and Harper, J.J., *Low Speed Wind Tunnel Testing,* John Wiley, New York, 1966.

$$V_\infty = V_{\infty_u} (1 + \epsilon)$$

$$q_\infty = q_{\infty_u} (1 + \epsilon)^2$$



Tip speed ratio

$$X_\infty = R\Omega / V_\infty$$

Torque coefficient

$$C_Q = (Q + Q_f) / \tfrac{1}{2}\rho_\infty V_\infty^2 R A_s$$

Power coefficient

$$C_P = (Q + Q_f)\Omega / \tfrac{1}{2}\rho_\infty V_\infty^3 A_s$$

My Status

- Arrived at USA on 23 September 2012
- Did written qualifier exam on November 2013
- Finished courses on December 2013, with GPA: 3.833
- Did oral qualifying exam on January 2014
- Did proposal defense on October 2014

UNIVERSITY OF Cincinnati